ASSESSING THE IMPACT OF LANDUSE/LANDCOVER CHANGE ON THE HYDROLOGICAL RESPONSE OF KOLA RIVER WATERSHED, SIDAMA REGION, ETHIOPIA

M.Sc. THESIS.

NIGUSU MULETA ETANA

HAWASSA UNIVERSITY, HAWASSA, ETHIOPIA

JULY, 2021

ASSESSING THE E IMPACT OF LANDUSE/LANDCOVER CHANGE ON THE HYDROLOGICAL RESPONSE OF KOLA RIVER WATERSHED, SIDAMA REGION, ETHIOPIA

NIGUSU MULETA ETANA

A THESIS SUBMITTED TO THE FACULTY OF BIO-SYSTEMS AND WATER RESOURCE ENGINEERING DEPARTMENT OF WATER RESOURCE AND IRRIGATION ENGINEERING

HAWASSA UNIVERSITY INSTITUTE OF TECHNOLOGY
SCHOOL OF GRADUATE STUDIES
HAWASSA UNIVERSITY
HAWASSA, ETHIOPIA

IN PARTIAL FULFILLMENT OF THE REQUIREMENTS FOR THE DEGREE OF MASTERS OF SCIENCE IN WATER RESOURCE AND IRRIGATION ENGINEERING (SPECIALIZATION: WATER RESOURCE ENGINEERING AND MANAGEMENT)

JULY, 2021

ADVISORS' APPROVAL SHEET

SCHOOL OF GRADUATE STUDIES

HAWASSA UNIVERSITY ADVISORS APPROVAL SHEET

This is to certify that the thesis entitled "Assessing the Impact of landuse/land cover change on the hydrological response of Kola River Watershed Sidama Region, Ethiopia" submitted in partial fulfillment of the requirements for the degree of masters with specialization in Water Resource Engineering and Management, Department of Water Resource and Irrigation Engineering, and has been carried out by Nigusu Muleta ID NO. PGWREMR/0013/11, under our supervision. Therefore, we recommend that the student has fulfilled the requirements and hence hereby can submit the thesis to the department.

Tewodros Assefa (Ph.D.)	……	…….
Name of Major Advisor	Signature	Date
Teshale Tadesse (MSC)	……	……
Name of Co-Advisor	Signature	Date

EXAMINER'S APPROVAL SHEET

SCHOOL OF GRADUATE STUDIES

HAWASSA UNIVERSITY EXAMINERS' APPROVAL SHEET-1

We, the undersigned, members of the Board of Examiners of the final open defense by Nigusu Muleta Etana have read and evaluated his thesis entitled "Assessing the Impact of Landuse/landcover Change on the Hydrological Response of Kola River Watershed, Sidama Region, Ethiopia", and examined the candidate. This is, therefore, to certify that the thesis has been accepted in partial fulfillment of the requirements for the degree of master's science.

Tewodros Assefa (Ph.D.)	_____	_____
Name of Major Advisor	Signature	Date
Tewodros Melese (Ph.D.)		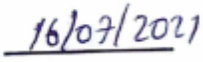
Name of Internal Examiner-I	Signature	Date
Mulugeta Dadi (Ph.D.)	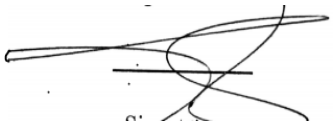	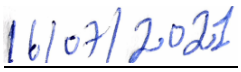
Name of Internal Examiner-II	Signature	Date
Michael Mehari (Ph.D.)	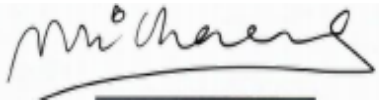	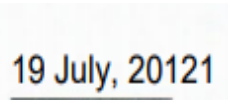
Name of External examiner	Signature	Date

_____	_____	_____
SGS Approval	Signature	Date

DECLARATION

I declare and confirm by my signature that this thesis entitled “Assessing the Impact of landuse/land cover change on the hydrological response of Kola River Watershed Sidama Region, Ethiopia” is my original work that has not been submitted to any other institution anywhere for the award of degree, diploma or certificate. Data analysis and preparation of this paper and that all the sources that I have used or quoted have been indicated and acknowledged.

Name: Nigusu Muleta Etana

Signature: ……

Date: ……

ACKNOLOGIMENT

I would like to express my greatest gratitude to Almighty God for blessing me in all so that I complete my M.SC thesis. I also express my thankfulness to Dilla University for allowing me to study for my M.SC and sponsoring me. I also delighted my gratitude to my major advisor Tewodros Assefa (Ph.D.) for his valuable and critical comment, tremendous support and hard questions were beneficial and improved the quality of my research. I sincerely gratitude my Co_Advisor (M.Sc.), Teshale Teddesse, for his great guiding giving constructive comments during doing my research.

Last but not least, to my family. I want to express my deep gratitude to my, father who sends me to school and helping me in all things during he was in life but hasn't got the chance to see my success, besides, I would like to express my gratitude to my mother, sisters, and brothers for their unconditional love, patience, and encouragement throughout my study. They have been a source of my inspiration, and without them, this accomplishment would not have been possible.

LIST OF ABBREVIATIONS

Arc SWAT	SWAT integrated with ArcGIS
BoARD	Bureau of Agricultural and Rural development
BoFED	Bureau of financial and economic development
CA	Cellular Automata
CN	Curve Number
CRV	Central Rift Valley
CSA	Central Statistical Agency
DEM	Digital Elevation Model
ERDAS	Earth Resource Data Analysis System
ET	Evapotranspiration
ETM^{+}	Enhanced Thematic Mapper
FAO	Food and Agricultural Organization
GCP	Ground Control Point
GIS	Geographic Information Systems
HRU	Hydrologic Response Unit
ISO DAT	Iterative Self-Organized Data Analysis Technique
Klocation	Kappa for Location
KlocationStrata	Kappa for Stratum-Level Location
Kno	Kappa for no Information
Kstandard	Kappa for Standard
LCM	Land Change Modular
LUCHEM	Landuse Change on Hydrology by Ensemble Modeling
LULC	Landuse/land cover
LULCC	Landuse/land Cover Change
masl	Meter above sea level
MoWIE	Ministry of Water Irrigation and Energy
MSS	Multispectral Scanner
NSE	Nash-Sutcliffe Efficiency
OBIA	Object-Based Image Analysis

OLI	Operational Landsat Imagery
PBIAS	Percent Bias
SCS	Soil Conservation System
SUFI2	Sequential Uncertainty Fitting two
SWAT	Soil and Water Assessment Tool
SWAT_CUP	Soil and Water Assessment Tool, Calibration and Uncertainty Program
TM	Thematic Map
USDA	United States Department of Agriculture
USGS	United States Geological Survey
UTM	Universal Transverse Mercator
WGS	World Geodetic System

TABLE OF CONTENT

DECLARATION i
ACKNOLOGIMENT ii
LIST OF ABBREVIATIONS iii
TABLE OF CONTENT v
LIST OF THE TABLES. viii
LIST OF THE FIGURES. ix
LIST OF APPENDIXES x
ABSTRACT xi
1 INTRODUCTION 1
1.1 Background of the Study 1
1.2 Statement of the Problem 3
1.3 Objectives 4
1.3.1 General objective 4
1.3.2 Specific objectives 4
1.4 Research Questions 4
1.5 Scope of the Study 5
1.6 Significance of the Research 5
2. LITERATURE REVIEW 6
2.1 General Overview of Landuse/land Cover Change 6
2.1.1 Landuse/land cover change studies in Ethiopia 7
2.1.2 Assessment of LULC change 7
2.2 Predicting Landuse/land cover Change 8
2.3 Impact of Landuse/land cover change on Hydrological Response 9
2.3.1 Previous studies on LULC change impact on hydrological responses in Ethiopia. 10
2.3.2 Hydrologic Models 11
2.3.2.1 SWAT model 12
2.3.2.2 Model selection 16
3. MATERIAL AND METHODS 17
3.1 Description of the Study Area. 17
3.1.1 Location 17

3.1.2 Climate 18
3.1.3 Topography 18
3.1.4 Demography of study area 18
3.2 Data Collection and Analyses 19
3.2.1. Data Collection and Analyses for landuse/land cover change investigation 19
3.2.1.1. Preprocessing of satellite image 20
3.2.1.2. Image Classification 21
3.2.1.7. Accuracy assessment 22
3.2.1.8. LUCC Identification and Quantification. 23
3.2.3. Landuse/land cover Prediction 25
3.2.3.1. IDRISI model validation 26
3.2.4. SWAT Model Input Data Collection and processing 27
3.2.4.1. Spatial data collection and analysis 28
3.2.4.2. Meteorological data 31
3.2.4.4. Meteorological data analysis 34
3.2.4.5. Filling missing data for the selected stations 35
3.2.4.6. Homogeneity Test of Rainfall Data. 35
3.2.4.7. Consistency test of selected stations by using Double mass curve. 36
3.2.4. 8. SWAT Model set up, and hydrological response analysis. 37
3.2.4.9. Watershed delineation 38
3.2.4.10. Hydrological response units (HRU) 39
3.2.4.11. Weather Generator` 40
3.2.4.12. Sensitivity analysis 40
3.2.4.13. Calibration and Validation 41
3.2.4.14. Model performance evaluation 42
3.2.4.15. Analyzing the effects of LULCC on the hydrological response of the study watershed 43
4 RESULTS AND DISCUSSION 46
4.1. Landuse/Land cover change detection and accuracy assessment 46
4.1.1 Landuse/Land cover map for 1988. 46
4.1.2 Landuse/land Cover for 1998. 48
4.1.3 Landuse/Land Cover for 2008. 50

4.1.5. Analysis of landuse/land cover change. 56
4.2 Predicting of the Future LULCC with IDRISI (CA- Markov Method) 60
4.3 Modeling of the hydrological response of kola River watershed 64
4.3.1 SWAT model sensitivity analysis 64
4.3.2 Calibration and validation 65
4.3.3 Evaluation the effect of landuse/land Cover Change on hydrological components 67
5. SUMMARY AND CONCLUSIONS 75
5.1. Summary 75
5.2. Conclusion 77
6. REFERENCES 79
7. APPENDIXES 88

LIST OF THE TABLES.

Table 3. 1 Satellite images with their dates of acquisition, path/row, and resolution 19
Table 3. 2 Table Kappa statics recommended Range. 23
Table 3. 3 Classes and description of LULC of the study area based on FAO classification.. 24
Table 3. 4 Soil types of Kola River watershed..... 29
Table 3. 5 Slope classes and area coverage of kola watershed 30
Table 3. 6 Meteorological station locations and length of data series. 31
Table 3. 7 Percentage of missing data for precipitation in all stations..... 34
Table 3. 8 General performance ratings for recommended statistics for a monthly time step. 43
Table 4. 1 Accuracy assessment of LULC Map of 1988 48
Table 4. 2 Accuracy assessment of LULC Map of 1998 50
Table 4. 3 Accuracy assessment of LULC Map of 2008. 52
Table 4. 4 Accuracy assessment of LULC Map of 2018 54
Table 4. 5 Areal coverage of LULC of the study area 1988_2018 54
Table 4. 6 Transition Matrix of Landuse land cover between 1988and 2018..... 57
Table 4. 7 Landuse land cover change in the study area..... 57
Table 4. 8 Annual changes between each consecutive and the begging and last year..... 59
Table 4. 9 Actual and predicted LULC (2018) 60
Table 4. 10 Results of validation analysis of 2018 simulated and actual classified image..... 61
Table 4. 11 Results of validation kappa index for 2018 simulated and actual classified image 62
Table 4. 12 Comparison of actual (2018) and projected LULC (2048)..... 62
Table 4. 13 Sensitivity parameters 65
Table 4. 14 Model performance statistics for the calibration and validation period..... 67
Table 4. 15 Seasonal variability Hydrological component due to LULCC 1988_2048 70
Table 4. 16 Seasonal change of hydrological components from 1988 to 2048 72
Table 4. 17 Mean annual streamflow changes from 1988 to 2048 73
Table 4. 18 Annual hydrological component values for different LULC from 1988 to 2048 in the study area..... 74

LIST OF THE FIGURES.

Figure 2. 1 Hydrological cycle)..... 15
Figure 3. 1 Location map of the Kola River watershed 17
Figure 3. 2 Schematic representation of Landuse land covers analysis procedure 27
Figure 3. 3 Maps of spatial data of Kola River Watershed: DEM (A), Slope map (B), Landuse map (C) Soil map (D) of 1988. 30
Figure 3. 4 Average Annual Precipitation of the Meteorological Stations (1988-2018). 32
Figure 3. 5 Mean monthly rainfall graph selected meteorological stations in Kola watershed (1988-2018). 32
Figure 3. 6 Long-term mean monthly variations of minimum and maximum air temperature (1988-2018) 33
Figure 3. 7 Long-term mean annual air temperature of the study watershed 33
Figure 3. 8 Homogeneity tests for selected weather station at Kola watershed 36
Figure 3. 9 Double mass analysis representing data consistency of stations on the Kola watershed. 37
Figure 3. 10 Delineated Watershed of the study area 39
Figure 3. 11 Arc SWAT processing procedures flowchart. 44
Figure 3. 12 Methodological flow chart 45
Figure 4. 1 LULC map of the study area in 1988 47
Figure 4. 2 LULC map of the study area in 1998 49
Figure 4. 3 LULC map of the study area in 2008 51
Figure 4. 4 LULC map of the study area in 2018 53
Figure 4. 5 Summary of LULC change in the Kola watershed (1988_2018) 55
Figure 4. 6 Gains and losses, and net change for 1988-1998, 1998-2008, 2008-2018, and 1988 –2018. 58
Figure 4. 7 Relationships between area statistics of predicted LULC of 2018 using 1988 and 1998LULC image (a), 1988 and 2008 (b). 61
Figure 4. 8 Actual, simulated, and projected map of the study area 63
Figure 4. 9 Predicted 2048 LULC map of kola watershed. 64
Figure 4. 10 Monthly calibrations (a) and validation (b) of the SWAT model. 66

Figure 4. 11 Scatter plot of the observed and simulated monthly average flow (m3 /s) in the calibration (a) and validation (b) period. 67
Figure 4. 12 Monthly average (1988-2048) streamflow, surface runoff, lateral flow, water yield, and ET response to the LULC changes in the Kola watershed. 69

LIST OF APPENDIXES

Appendix Table 1 LULCC matrix of 1988-1998(a), 1998-2008(b), 2008-2018(c), and 1988-2018(d) 89
Appendix Table 2: Transition matrix of Markov prediction to 2048 based on LULC 2018 map. 92
Appendix Table 3: Annual rainfall of stations around kola watershed in (mm) 93
Appendix Table 4: Mean monthly rainfall (mm) data for stations around the study area 94
Appendix Table 5: Maximum, minimum and mean monthly temperature (^{o}C) records of the stations in and around the study area. 94
Appendix Table 6: Long term mean monthly discharge of Kola River (1988_2013) 95
Appendix Table 7: Sensitivity parameters and their definition. 96
Appendix Table 8: Average monthly basin values 96
Appendix Figure 1: Satellite Data for 1988, 1998, 2008, and 2018. 88
Appendix Figure 2: Validation of simulated 2018LULC by 2018clasified image. 91
Appendix Figure 3: projected 2018(a) 2048(b) LULC by CA_ Marcove 92

ABSTRACT

Landuse/land cover change is one of the major factors that affect the hydrological response of watersheds. Hence studying the impacts of past and future landuse/land cover changes on the hydrology of Watershed is very important for proper watershed management. This study investigated the past and potential future land cover changes and their impact on the hydrological response of the Kola River Watershed by using the Soil Water Assessment Tool (SWAT).To detect and analyze the change that had taken place in the study area, satellite images were downloaded for 1988, 1998, 2008, and 2018 years and processed using ERDAS Imagine 2014. Then by using the supervised image classification technique, the satellite images were classified to agriculture, agroforestry, built up pasture, land, and forest landuse the land cover types. Then accuracy assessment was done, and overall accuracy of 87.83%, 88.41%, 89.15%, and 91.76%, was achieved for the classified images of 1988, 1998, 2008, and 2018 respectively. The changes of landuse/land cover of the study area from 1988 to2018 indicated that Pastureland, Forest, and Agroforestry decreased by 69.55%, 40.86%, and 15.77%, while Agriculture, and Built-up, increased by 24.67%, and 23.9%, respectively. The future LULC of 2048 was projected by IDRISI (CA-Markov method) and the result indicated a continuous increase of Agriculture and Built-up areas as the other landuse land cover such as forest, pastureland and Agroforestry decreased. Model sensitivity analysis was made to choose the most sensitive parameters. Then, R^2 and ENS achieved 0.87, 0.77 during calibration and 0.85, 0.74 for validation respectively. The model performance evaluation indicated that SWAT can be used for modeling the impact of historical and projected LULCC on the hydrological response of the study Watershed. As the investigation of 1988 to2018 shows, due to LULCC, the seasonal flow increased by 25.71%, 23.73%, and 19.96%in the first and, second rainy seasons, and short rainy season, while it decreased by 22.21% in the dry season respectively. The annual surface runoff and water yield increased and by 22.21%, and 3%, whereas evapotranspiration and lateral flow, decreased by, 6.21%, and 14.61% respectively. The future LULCC prediction of 2048 showed that seasonal flow increased by 29.03%, and 28.08%, 14.6% in the first and second rainy season, and short rainy season and decreased by 19.3 in dry seasons. Generally, the investigation of hydrological response to LULCC by taking other data constantly at different predefined study years indicates LULCC has significant impacts on the hydrological response of the study watershed. Therefore to overcome the impact of LULCC, local and national policymakers should be invited to prepare and apply scientific and appropriate watershed planning and management, strategies in the Kola River Watershed.

Keywords: LULCC, LULCC Prediction IDRISI, SWAT, Hydrological Responses.

1 INTRODUCTION

1.1 Background of the Stud

The world is a combination of complex systems, involving a variety of spatial and temporal scales in which different natural environmental factors and humans are thoroughly interwoven (Oliver and Morecroft, 2014). Land and water are crucial natural resources for human beings in this world, so understanding the interaction of these resources is not an optional thing at the moment time (FAO, 2011), Water is a vital natural resource for living things. Since the accessible amount of water is limited, and not spatially distributed to the users, so proper, management of water resources is essential to satisfy the current demands as well as to future sustainability (Guo et al., 2008).

When we compare the terms landuse and land cover; landuse states the utilization of land for diverse purposes, whereas land cover specifies the regular and irregular cover on the land surface such as natural vegetation, agriculture, bare earth, water bodies, and man-made structures (Skaggs et al., 2006). Landuse/land cover change (LULCC) is a term used for the modification of the earth's terrestrial surface by humans, mostly as the result of an interaction between natural and anthropogenic processes (Rawat and Kumer, 2015).

The strong relationship between landuse and water has contributed to the prominent concern to the basic earth characteristics and processes such as the productivity of land, biodiversity, and hydrological process (Oliver and Morecroft, 2014). Considering the effects of landuse/land cover change on water resources are critical for an understanding of the hydrological process, and computing their respective influence has great significance for water resources management and socio-economic activities, as well as policy-making and planning for sustainable development (Yang et al.,2017), and so all by altering the geomorphological and physiological of the landscape. Landuse/land cover change can affect the hydrological components such as infiltration, interception, surface runoff, groundwater recharge, streamflow indirectly modifying soil properties and atmospheric boundary layer (Cuo, 2016). Hence, the availability of data on LULC changes can provide a critical impute on the decision-making of environmental planning and management (Fan, et al., 2007).

There were different approaches such as modeling, statistical analysis (Elfert and Bormann, 2010), and experimental catchments, comparative analysis (Gebresamuel et al., 2010) were

used to investigate the effects of LULC changes on hydrological response. The choice of which approach is used in a particular study depends on the scope in terms of scale, geographic location, and resources available. Among them, Models are generally used in various areas of water resource development, in studying the impact of human interference in an area such as landuse/land cover change, and watershed management (intervention of watershed conservation practices) (Dareje, 2010).

Though landuse/land cover change modeling approach has recently been considered by the scientific community to observe environmental changes at a different level, such as local, regional, national, and global, to achieve Sustainable Development worldwide (Biswajit, et al., 2020). The landuse/land cover change models (LUCCM) are considered crucial tools to evaluate the causes and consequences of landuse/land cover change. Additionally, the LULC model is found to be effective when predicting the future state and spatial distribution of LULC using the gained knowledge from past years (Islam et al., 2018).

Ethiopia is granted a variety of agro-ecological conditions ranging from desert to rainforest and from 200 m below sea level to highlands with altitudes of over 4500 meters above sea level (masl) (Kahsay, 2004). Landuse/land cover (LULC) change in Ethiopia is caused by the interaction of various demographic, socioeconomic, institutional, and biophysical factors (Birhanu et al., 2019). As different previous Studies have shown that the country was also known by hurried population growth, widespread agricultural expansion (Ariti et al., 2015) expansion of settlement, climate change, and the associated changes in landuse/land cover (LULC) (Eyasu et al., 2019) were recognized as the major drivers of landuse/land cover change in the country. As the majority of the rural population of the country depends on agriculture, landuse/land cover changes during the past couple of decades are mostly linked to agricultural development (Gassman, 2007).

Kola River Watershed is an agriculturally very productive area. Headstream of the study area is specifically known for agroforestry (coffee, enset, chat) production, additionally, the Watershed has experienced intensively cultivated landuse, and the rapid population growth has forced farming families of the study area to expand their agricultural fields (Paul, 2015).

1.2 Statement of the Problem

Landuse/land cover change is one of the major factors that affect hydrology cycle elements. These changes caused severe stress on water resources at a different scale. So at this time investigating the impact of landuse/land cover on the hydrological response of watersheds is a very interesting issue worldwide (Sertel et al., 2019).

In Ethiopia, the different study shows there are significant LULCC in different parts of the country (Girmay et al., 2010). These changes have energetic environmental concerns at local and universal scales (Woldeamlak and Solomon, 2013). At the local scale, landuse changes affect the hydrological components of the watershed such as; surface runoff, groundwater recharge, infiltration, interception, and evapotranspiration (ET), and streamflow (Gashaw et al., 2018), this creates serious challenges for water resource project planning and management (Sertel et al., 2019), and responsible for altering the hydrologic response of the Watersheds (Melese, 2012). Hence water resource sensitivity studies were required to simplify the debts of how the hydrological component will respond to prescribed landuse/land cover changes and used to suggest what remade action should be taken to overcome the problem (Taye, 2009).

The different models are used in the world to investigate the impact of landuse/land cover change on watershed hydrology. However, only a few models available outside of the model developing institutions, so depending on the accessibility and compatibility with available data among the freely available models such as ERDAS imagine 2014 which used in image processing, classification, and mapping of landuse/land cover change, IDRISI (Clark labs) this model is useful to project the future landuse/land cover (Verburg and Overmars 2009) and hydrological model is SWAT model is used in this study. SWAT model is a semi-distributed physically-based simulation model and can predict the impacts of landuse change and management practices on hydrological regimes in watersheds with varying soils, landuse, and management conditions over long periods and primarily as a strategic planning tool (Neitsch, 2005). Though modeling the impact of landuse/land cover change are powerful to understand and analyze Water resource management strategies and how LULC changes affect the function of hydrological environments.

Kola River Watershed is an agriculturally very productive area (Paul, 2015). Headstream of Kola River is specifically known for agroforestry (coffee, enset, chat) production, however, the

rapid population growth has forced farming families of the study area to expand their agricultural fields and the catchment has experienced intensively cultivated landuse/land cover following, expansion of agriculture, there is high seasonal yield fluctuation and dry season flow is highly decreasing in the study area (Mechael, 2016). This indicates that the area requires a detailed investigation of the effect of LULCC at the watershed level in the future. However, as tried to have information, there were no complete studies that investigate the impact of historical and future LULC changes on the hydrologic response at the watershed level in the study area. Hence, predicting landuse/land cover change and evaluating its impact on the hydrological response at a local scale is essential for watershed management (Yesuph and Dagnew, 2019). Therefore, this research initiated to project the landuse/land cover change by considering historical landuse/land cover change conditions and examine its impacts on the hydrological response of the Kola River watershed.

1.3 Objectives

1.3.1 General objective

The general objective of the study was to investigate the past and future LULC change and its impact on the hydrological response of the Kola River Watershed in Sidama Region, Ethiopia.

1.3.2 Specific objectives

The Specific objectives of this study were:

- To identify the landuse /land cover change in the kola River Watershed in the last 30 years from 1988 to 2018
- To predict the future landuse/land cover of the study area, using the IDRISI (CA_ Marcove method) for the future 30 years from 2018 to 2048
- To investigate the effect of landuse/land cover change on the hydrological response of the study watershed using the Soil and Water Assessment Tool (SWAT) hydrologic Model.

1.4 Research Questions

1. What is the general trend of landuse/land cover change in the kola River watershed over the past 30 years?

2. What is the future landuse/land cover condition of the study area in 2048?
3. To what extent the landuse/land cover changes affect the hydrologic response of the study watershed?

1.5 Scope of the Study

The study was limited to the Kola river watershed which covers an area of 205.65 km^2. The time considered during the investigation of historical LULCC impact on the hydrological response of the study watershed was 1988 to 2018. In addition to this depending on the result of historical landuse/land cover change analysis, the future landuse/land cover was predicted for the future (2048). Finally, the impact of landuse/land cover change on hydrology was investigated by using the landuse/land cover map of a different time. ERDAS imagine 2014software was used for image classification and preparation of landuse/land cover map and the IDRISI software used for prediction of the future landuse land cover maps, finally, SWAT model was used to investigate the effect of landuse land cover change on hydrological components of the study area.

1.6 Significance of the Research

Understanding how LULCC influences watershed hydrology will enable local Governments, and policymakers of the study area, to formulate and implement effective, and appropriate response strategies to minimize the adverse effects of future LULCC or modifications. To envisage the future effects of landuse change on the watershed, it is important to have an understanding of the effects of historic landuse land cover changes have on the watershed hydrological system. In general, this study is expected to help concerned sectors in planning, developing, and managing water resource projects in the study area. Besides, it will be taken as input for those who are interested in further research for related fields of study in the watershed. Modeling spatially the dynamic change is important for innovative planning strategies (Hatem and Prasanna, 2017).

2. LITERATURE REVIEW

2.1 General Overview of Landuse/land Cover Change

Landuse/land cover is often misunderstood as two identical or interchangeable entities. However, there are significant differences between these terms. Land cover is a representation of biophysical attributes of the earth's terrestrial surface and immediate subsurface, while landuse is the objective for which attributes of land cover have been modified (Lambin and Geist, 2006). LULC change has been perceived as a factor that can produce multiple impacts, ranging from water resources to food security. Specific to water resources, impacts of LULC change have been linked to varying entities such as groundwater, stream water, surface runoff, evapotranspiration, as well as sediment and nutrient yields (Ike, 2017).

Deferent methods were developed to investigate LULC change and its impact. Advancement in science and technologies has refined the understanding of LULC and diversified methodologies (Ike, 2017) landuse is the term that is used to describe human uses of land, or immediate actions modifying or converting land cover (Gebrehewet, 2004). On the other hand, land cover refers to the natural vegetative cover types that characterize a particular area. Landuse change is the proximate cause of land cover change. The driving forces to this activity could be economic, technological, demographic, and other factors. Hence, landuse/land Cover dynamics are a result of complex interactions between several biophysical and socio-economic conditions which may occur at various temporal and spatial scales (Reid et al., 2000).

In the past two centuries, the impact of human activities on land has grown enormously because of population increase, technological development (de Sherbinin, 2004). Landuse/land Cover Changes (LUCC) are the shift in intent and/or management that constitute landuse/land covers (Lambin, 2003). Conversion refers to change from one cover or use type to another, as the case in agricultural expansion, deforestation, or change in urban extent.

Landuse/land cover modification involves the maintenance of broad cover or use type in the face of change in its attributes. Landuse/land cover modification, on the other hand, involves the maintenance of broad cover or use type in the face of change in its attributes (Verburg et al., 2006). Both conversion and modifications of landuse/land cover have important environmental consequences through their impacts on soil and water, biodiversity, and microclimate, hence, contribute to watershed degradation (Lambin, 2003).

2.1.1 Landuse/land cover change studies in Ethiopia

Much of our understanding of LULCC has built up from individual case studies, using both remote sensing and ground-based data, and we will continue to rely on case studies as a means to gain the required knowledge (Kassa, 2009). Studies that have been carried out at different parts of Ethiopia indicated that croplands have expanded at the expense of natural vegetation, including forests and shrublands, similarly, an increasing agricultural land at the expense of natural vegetation in central highlands (Amsalu, 2007). The primary cause for affecting vegetation cover in the Abaya-Chamo basin is underlined that as faster population growth and the resulting pressure on the landuse ecosystems by an expansion of settlements, clear-cutting, expansion of tillage areas (Gericke, 2004).

Many recent studies indicate substantial and speedy LULC change in Ethiopia manifested in environmental and economic impacts (Gashaw et al., 2018). Similarly, in Ethiopia's CRV LULC changes are overseen by a combination of geographical, environmental, and socioeconomic factors. In the CRV area, population pressure is found as one of the major underlying causes of landuse/land cover changes which contribute more to resource degradation through cutting natural plants for fuel consumption and charcoal production (Kabba and Li,2011).

2.1.2 Assessment of LULC change

There are many ways to obtain information on LULC; these can include ground surveys, the use of GPS, air photo, and satellite images through remote sensing. LULC changed studies became routine with the launch of LANDSAT providing global coverage of the earth's surface in 1972. Since then, LULC mapping techniques have advanced significantly. Methods used to extract LULC information are broadly divided into unsupervised classification techniques and supervised techniques (Jensen et al, 1996). The unsupervised technique can be applied without any prior knowledge about the study area and involve clustering with various algorithms such as chain method, Iterative Self-Organizing data analysis technique (ISODATA) iterations, and cluster busting (Jensen, 2007). The supervised method requires a deep knowledge of the study area, field data, and the development of a training dataset involving pixels extracted from the image representing every LULC class (Jensen, 2007). Quite frequently a hybrid method is used which is a blend of the two methods.

The object-Based Image Analysis (OBIA) approach offers new ways of classification by developing segments instead of pixels as the unit of analysis, and combining spectral, textural, and spatial attributes of segments for building supervised classifiers or rules-based classifiers (Lyons et al., 2012). Monitoring changes over time requires consistency among maps both in terms of real-world representation and statistical performance of the maps. Often, studies employing a remote sensing approach for landuse mapping use different sensors to produce a longer temporal coverage. To examine the LULC change using remote sensing, the images have to be acquired at different dates. There have been several methods developed for assessing LULC changes. In mapping LULC, two properties of satellite images namely spatial and temporal resolution should be considered. Images with high temporal resolution can capture highly dynamic changes, but often poor in spatial resolution, which makes them unable to reveal high spatial variability of land cover (Jensen, 2007). Medium spatial resolution Landsat data have been used by studies to map LULC changes with different periods ranging from 2 years, 5 years (Tran et al., 2017), 10 years (Thakkar et al., 2016).

2.2 Predicting Landuse/land cover Change

Prediction of future landuse land cover image is the latest research that will be very much useful to natural resources management (Prakasam, 2010). Landuse/land cover change modeling is growing rapidly in the scientific field. There are many modeling tools in use but the performance of different modeling tools is difficult to compare because LULC change models can be fundamentally different in a variety of ways (Prakasam, 2010). Among the number of landuse/land cover modeling tools and techniques that are most commonly used for predicting the future landuse/land cover are the modeling techniques embedded in Terrasat. Are mostly used in this time, these model includes, Land Change Modeler (LCM), Cellular Automata (CA), Markov Chain, CA Markov (Eastman, 2006).

I Markov model

The Markov model has been widely used in ecological modeling (Brown et al., 2000). Markov's model takes into account past states to predict how a particular variable changes over time. The applicability of the Markov model in landuse change modeling is promising because of its ability to quantify not only the states of conversion between landuse types but also the rate of conversion among the landuse types (Sang et al., 2011).

II CA-Markov model

CA-Markov model combines cellular automata, Markov chain, and multi-criteria, and multi-objective land allocation to predict land cover change over time (Sang et al., 2011). It adds to the Markov model not only spatial contiguity but also the probable spatial transitions occurring in a particular area over time. MARKOV and CA_MARKOV modules in IDRISI were used to create transition probability and transition area matrix. A transition probability matrix is obtained by cross-tabulation of two images of a different time and it determines the probability of a pixel in a landuse class to change into another class during that time. The CA_MARKOV module in IDRISI uses a hybrid Markov- CA model that iterates the land-use allocation until the areas that are predicted by the Markov model are identified. Also, the number of iteration is dependent upon the number of years a projection is made (Praveen et al., 2013).

III Land change modeler

Land Change Modeler for ecological sustainability is integrated software developed by Terrasat for analyzing land cover changes. Land cover change model tools support the analysis of the landuse changes. The use of such a model also gives a better understanding of the functions of the landuse systems and the support needed for planning and policymaking. Such models can also predict the possible future change and use of the land cover under different scenarios (Ahmed, 2012).

2.3 Impact of Landuse/land cover change on Hydrological Response

The relationship between landuse and hydrology is greater interest worldwide as it can provide advice for management actions to avoid or minimize the negative effects of specific landuse activities on the hydrology of a certain region. However, there are still uncertainties on the impact of specific landuse practices on different processes of the hydrological cycle (Defries and Eshleman, 2004) mentioned, land cover can affect both the degree of infiltration and runoff following rainfall events, while the degree of land cover can affect rates of evaporation (Kashay, 2004). Land cover has various properties that help to regulate water flows both above and below ground. For example, tree canopy and leaf litter can help reduce the impact of raindrops on the ground, hence reduce soil erosion, while roots hold the soil in place and also absorb water. In the absence of vegetative cover, soil erosion will result and the effects of this phenomenon.

Landuse/land cover change is highly affected by human-induced activities rather than natural events. The driving forces to this activity could be economic, technological, demographic, and other factors. Hence, Landuse/Land Cover dynamics are a result of complex interactions between several biophysical and socio-economic conditions which may occur at various temporal and spatial scales (Reid et al., 2000).

2.3.1 Previous studies on LULC change impact on hydrological responses in Ethiopia.

Hydrological processes are affected by many factors such as landuse/land cover, climate, soil properties, the geology of the land, and topography. Landuse/land cover change mainly caused by anthropogenic interference alters watershed hydrological processes by fluctuating the balance between hydrological components (Chimdessa et al., 2018).LULC change contributes to the change in the hydrological system in Ethiopia. Quantifying the effects of LULC change on watershed hydrological response has recently been given attention by researchers, and previous studies in the country have quantified watershed hydrological responses as a result of the change in landuse/land cover.

A study in Gilgel Tekeze Catchment, Northern Highlands of Ethiopia, by (Haregeweyn et al., 2015) Found that the increment of cultivated land by 15.4% and settlements by 9.9% at the expense of shrubland and grazing lands triggered the increment of annual surface runoff by 101 mm, reduction of groundwater recharge by 39 mm, and reduction of annual evapotranspiration by 91 mm over the period between 1976 and 2003. Similarly, (Gashaw et al., 2018) reported the continuous expansion of cultivated land and built-up area and diminishing of forestland, shrubland, and grassland, which have occurred from 1985 to 2015, had increased the annual flow by 2.2%, wet seasonal flow by 4.6%, surface runoff by 9.3%, and water yield by 2.4%. On the other hand, the observed changes had reduced dry season flow by 2.8%, lateral flow by 5.7%, groundwater flow by 7.8%, and evaporation and transpiration (ET) by 0.3% in the Andassa Watershed, Blue Nile Basin of Ethiopia. Another study by (Choto and Fetene, 2019) on Gojeb Watershed, Omo-Gibe basin of Ethiopia, found that an increase of cultivated land by 14.97% at the expense of forest land and shrubland between 1985 and 2015 resulted in an increase of streamflow by 8.6 m3 /s. The other study conducted in ketat catchment in the rift valley of Ethiopia, by (Fufa and Abbulu, 2015) Found that the increment cropland 27.7%

whereas Forest loss by 53%, grassland decreased by 33.7%, triggered the increment of Mean wet monthly flow 3.6%, reduction Dry average monthly flow 12.3% 1986 and 2010.

2.3.2 Hydrologic Models

Models are used in decision-making applications to select an optimal course of action and are often constructed to enable reasoning within an idealized logical framework about the processes (Narayan, 2011). Watershed models are essential for studying hydrologic processes and their responses to both natural and anthropogenic factors, but due to model limitations in the representation of complex natural processes and conditions, models usually must be calibrated before application to closely match reality (Bastidas, 2002).

There have been several methods developed to assess water resources, among these hydrologic models, examine water distribution patterns and constituents specification (deterministic or stochastic), and spatial representation (lumped or distributed) (Melone et al., 2005). The empirical watershed hydrology model is an assemblage of mathematical descriptions of components of the hydrologic cycle (Singh, 2002). The model structure and architecture are determined by the objective for which the model is built and they are increasingly used in hydrology to simulate changes in watershed management, to investigate the impacts of external influences (such as landuse/land cover changes), and also to extend data sets (Singh, 2002).

Hydrological modeling involves the application of mathematical expressions that define quantitative relationships between inputs and outputs. The scope of hydrologic modeling and its applications has broadened dramatically over the past decades. Hydrologic modeling is related to the spatial processes of the hydrologic cycle and is often used to estimate basin water resources as well as for impact assessment or more precisely water resources management. Many hydrologic models have been developed in the past and more are being developed and they are used to determine the performance of watersheds under inevitable land-use change (Melone et al., 2005). The following are some of the hydrological models which are used to analyze the hydrological response of the watershed.

TOP model: This model is one of the hydrologic models that bases its distributed predictions on an analysis of basin topography. The model allows basins to be divided into a set of sub-basins. Evaporation is estimated by using the Penman-Monteith method. Surface runoff is computed based on variably saturated areas (Abdrhman, 2011). The subsurface flow is

calculated using an exponential function of water content in the saturated zone. Channel routing and infiltration excess are calculated using the Beven and Kirk method. This model requires a spatial component of high-quality DEM without a sink (Beven, 1997).

HEC-HMS model: The HEC-HMS model is a physically-based and conceptually semi-distributed event-based model designed to simulate rainfall-runoff processes in a wide range of geographic areas, from large river basin water supplies and flood hydrology to small urban and natural watershed runoffs. (Feldman, 2000). HEC-GeoHMS was used to create a basic model and a meteorological model, and to control specifications before running the model. The basin model and the basin features were taken as the background map file and imported to HEC-HMS. Since we do not have observation stations in each sub-basin, the precipitation values were estimated by the most commonly used Thiessen Polygon method, and weights were worked out in HEC-GeoHMS software. During calibration, a daily simulation time step was used in estimating the parameters of the selected methods (Bajwa and Tim, 2002). The Soil Conservation Service Curve Number, SCS Unit hydrograph, and Muskingum routing methods were selected for each component of the runoff process as runoff depth, direct runoff, and channel routing respectively (Jin, 2015).

2.3.2.1 SWAT model

The Soil and Water Assessment Tool (SWAT) model was developed by the USDA Agricultural Research Service. This model is a watershed scale model that can predict the impact of changes in land management on water and sediment. It is physically based requiring specific information about soil, topography, weather, and land management practices within the watershed (Arnold et al., 1998). SWAT is a useful tool because watersheds that do not have any monitoring data can be modeled

SWAT is a physically-based, computationally efficient model that is well-suited for studying the large-scale impacts of land-use changes as described in a series of papers based on the LUCHEM (Landuse Change on Hydrology by Ensemble Modeling) project (Breuer, 2009). SWAT has gained international acceptance as a robust watershed model as evidenced by hundreds of peer-reviewed and conference publications. Besides, the model has been widely used by federal and state agencies (Gassman, 2007). SWAT was developed to predict the impact of land management practices on water, sediment, and agricultural chemical yields in large,

complex watersheds with varying soils, landuse, and management conditions over long periods (Neitsch, 2005). Components of the model include weather, hydrology, soil characteristics, plant growth, nutrients, pesticides, and land management (Gassman, 2007). In SWAT, a watershed is divided into sub-basins, which are further divided into hydrologic response units (HRUs) based on similar landuse, soil distribution, and slope. Hydrology components of SWAT include canopy storage, infiltration, evapotranspiration, lateral subsurface flow, surface runoff, ponds, tributary channels, and return flow. Based on daily precipitation, runoff, evapotranspiration, percolation, subsurface return flow, groundwater flow, and changes in water storage, a daily water budget in each HRU is calculated. The water budget components in the SWAT model are:

Surface Runoff: Two methods for estimating surface runoff are provided in SWAT: The SCS curve number procedure (SCS, 1972) and the Green & Ampt infiltration method (1911). In this study, the SCS method was used. Also, the peak runoff rate is calculated with a modified rational method. The SCS curve number method estimates surface runoff from daily rainfall using initial abstractions (surface storage, interception, and infiltration before runoff) and a retention parameter (varies based on changes in soil, landuse, management, and slope as well as temporarily due to changes in soil water content) (Andreassian, 2004).

Evapotranspiration: Potential evapotranspiration (PET) is the volume of water that can be evaporated and transpired if enough water is available. SWAT estimates daily PET using one of three methods requiring varying inputs: Penman-Monteith, Hargreaves, or Priestly-Taylor. Daily PET values obtained from monitoring can also be incorporated into the model. In SWAT model after the PET is determined, actual evaporation is calculated. Rainfall intercepted by the plant canopy is evaporated first then the maximum amount of transpiration and sublimation/soil evaporation will be estimated, next the actual amount of sublimation and evaporation from the soil is then calculated. Sublimation occurs if snow is present in an HRU, although no snow conditions must be in effect for evaporation from the soil to occur (Neitsch S. A., 2009).

Soil Water Relationship: Water that enters the soil may move along various pathways, including removal from soil by plant uptake or evaporation, percolation past the soil profile to become aquifer recharge, or lateral movement in the profile and contribute to streamflow. SWAT uses a kinematic storage model developed by Sloan et al. (1983) to estimate lateral subsurface flow. This model simulates subsurface flow in a two-dimensional cross-section

along a flow path down a steep hill slope. SWAT uses a storage routing methodology to calculate percolation for each soil layer in the profile. If the soil is frozen during the simulation period, percolation in the soil layer is equal to zero (Neitsch, 2005).

Groundwater: The groundwater system in SWAT consists of shallow and deep aquifers. Shallow aquifer water balance consists of recharge entering the aquifer, groundwater flow, or base flow Into the main channel, the amount of water moving into the soil zone in response to water deficiencies, and the amount of water removed from the shallow aquifer due to pumping. The deep aquifer water balance consists of percolation from the shallow aquifer to the deep aquifer and the amount of water removed from the deep aquifer due to pumping. SWAT uses empirical and analytical techniques to account for the above components (Neitsch, 2005). In SWAT, water is routed through the channel network using the variable storage routing method or the Muskingum River routing method (Rohshare et al., 2008). Each routing method is a variation of the kinematic wave model. In SWAT, the impacts of spatial variations in topography, landuse, soil, and other watershed characteristics on hydrology are considered in subdivisions. There are two-level scales of subdivisions: (1) a basin is divided into several sub-basins based upon drainage areas of the tributaries, and (2) each sub-basin is further divided into many hydrologic response units (HRUs) based on land cover and soil type. Each HRU is assumed to be spatially uniform in terms of landuse, soil, topography, and climate (Alamirew, 2006). No matter what type of problem is studied with SWAT, water balance is the driving force behind everything that happens in the watershed. To accurately predict the movement of pesticides, sediments, or nutrients, the hydrologic cycle as simulated by the model must match what happens in the watershed. The simulation of the hydrology of a watershed can be separated into two major divisions. The first division is the land phase of the hydrologic cycle (Arnold et al., 1998). The land phase of the hydrologic cycle controls the amount of water, sediment, nutrient, and pesticide loadings to the main channel in each sub-basin. The second division is the water or routing phase of the hydrologic cycle which can be defined as the movement of water, sediments, etc. through the channel network of the watershed to the outlet (Arnold et al., 1998).

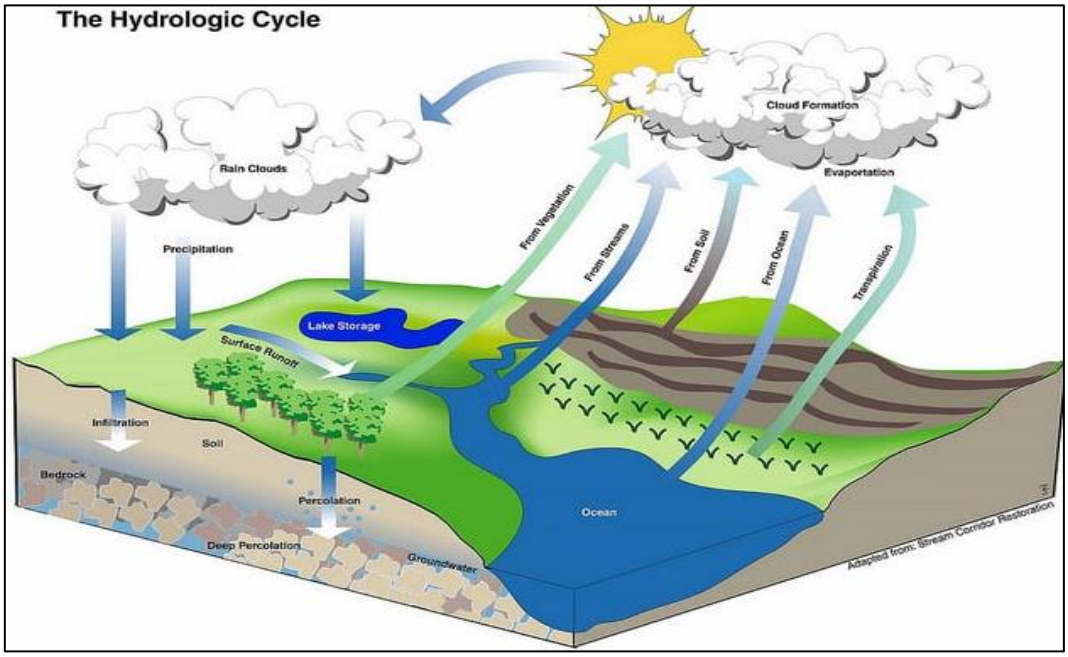

Figure 2. 1 Hydrological cycle (Source:https://www.conserve-energy-future.com/wp-content/uploads/2016/05/hydrologic-cycle.jpg).

SWAT simulates the hydrological cycle based on the water balance equation as shown in Equation (2.1) (Neitsch S. A., 2009)

$$SWT = SWo + \sum_{i=1}^{t}(Rday - Qsurf - Ea - Wseep - Qgw) \quad \text{..... (2.1)}$$

Where: SWt = is the final soil water content (mm);

SWo = is the initial water content (mm)

t =is the time (days)

Rday =is the amount of precipitation on a day i (mm)

Qsurf= is the amount of surface runoff on a day i (mm)

Ea= is the amount of evapotranspiration on a day i (mm)

Wseep= is the amount of water entering the vadose zone from the soil profile on the day i (mm)

Qgw= is the amount of return flow on a day i (mm).

Surface runoff volumes and peak runoff rates for each HRU. The SCS curve number method was used to estimate surface runoff by equation (2.2). The SCS curve number equation is:

$$Q\ Surf = \frac{(Rday - 0.2S)2}{(Rday + 0.8S)} \quad \text{..... (2.2)}$$

Where: Qsurf is the accumulated runoff or rainfall excess (mm), Rday is the rainfall depth for the day (mm), S is the retention parameter (mm).

The retention parameter S can be calculated by using equation (2.3)

$$S = 2.54 * \left(\frac{1000}{CN} - 10\right) \quad \text{(2.3)}$$

Where, CN is the curve number for the day and its value is the function of landuse practice, soil permeability, and soil hydrologic group.

2.3.2.2 Model selection

To get the required result for the proposed research objective, the selection of the appropriate model which is more efficient in analyzing the outlined problem is the crucial task in carrying out the best researches. At present, numerous hydrological models are used to simulating the hydrological process at different spatial and temporal scales. The criteria for selecting appropriate models are project-dependent since every project has its objectives. Further, more some criteria are also user interest and experience, and resource availability, such as the personal preference for the graphical user interface, computer operating system. Some of the criteria that have to consider during mode selection are as follows.

Consider models that are readily available and whose investment of time and money appeared worthwhile.

Decide whether the model under consideration will produce the outputs needed to meet the aims of a particular objective.

Make a list of the inputs required by the model and decide whether all the information required by the model is provided within the time and cost constraints of the objective.

The SWAT model is selected rather than the other model for determining the impact of landuse land cover on the hydrological response of the kola river catchment for the following reasons: The model uses readily available inputs for weather, soil, and land, and topography. It allows considerable spatial detail for basin-scale modeling. It is capable of simulating the change in watershed characteristics using different scenarios and it has the capability to interface with a geographical information system (GIS).

3. MATERIAL AND METHODS

3.1 Description of the Study Area.

3.1.1 Location

Kola River Watershed is located in the Central Main Ethiopia Rift valley (MER), in the Sidama Regional State of Ethiopia. The watershed is located in the south-central part of Sidama Region at a distance of around 64 km from the capital city of, Hawassa, and 337 Kilometers (km) southeast of Addis Ababa. Geographically it is situated in the coordinates of 6˚ 25′ to 6˚ 40′ North latitude and 38˚ 15′ to 38˚ 37′ East longitudes. The total area of the watershed is 205.65 square kilometers. The figure below (figure 3.1) indicates the location of the study area Watershed starting from the Ethiopian main basin to Gidabo Sub-basin and the Kola Watershed respectively.

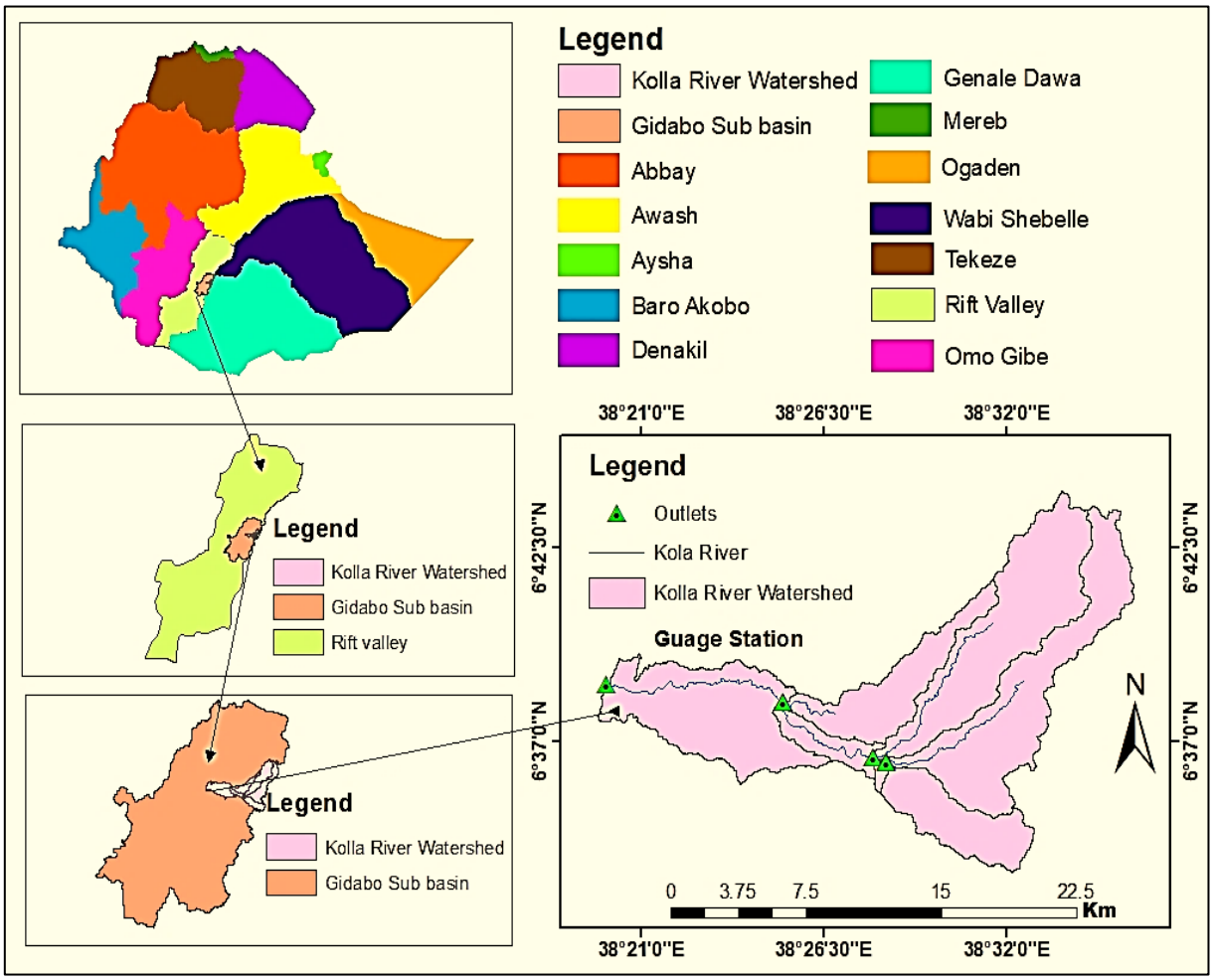

Figure 3. 1 Location map of the Kola River watershed

3.1.2 Climate

The climate pattern of Ethiopia is mainly determined by ITCZ (Inter Tropical Convergence Zone) and the influence of the Indian Monsoon throughout the year (Kassa, 2009). According to (Esayas, 2010) the climatic classification map of Ethiopia, the climate of the Kola River watershed is dominated by Tropical Climate with distinct dry winter in the western, Warm Temperate Rainy Climate in the eastern part. Based on the Moisture Index Classification of climate, the climate of the watershed, in general, knows by dry sub-humid in the northern part of the high lands and moist sub-humid in the eastern and southern part (BoARD, 2016). The agroecology of the district includes 85.1% Weina Dega (Temperate, cool sub-humid) and 14.9% Dega (Cool, humid). The average monthly temperature varies from 21 to 25 °C in the lowlands and < 11.5 to 13.5 °C in the high elevation plateau. The average annual rainfall ranging from 1100mm to 1600mm. In the study area, the annual precipitation follows a bimodal distribution and the annual pattern is commonly distinguished as maximum rainy season April and May and a secondary peak in September and October. The daily variation of temperature in the catchment is more visible than its seasonal variation. (BoARD, 2016).

3.1.3 Topography

The geomorphology of the area is highly variable and it is generally the result of repeated volcanic and tectonic events with the associated erosion of volcanic rocks and deposition processes. The principal feature of the Rift Valley is that it is a grabbed, a block fault geological structure in which the floor of the valley has become vertically displaced concerning the valley sides. The tectonic activity and lithological variation in the area also partly or wholly control the drainage density. Out of the total area of the district, 46.4% is hilly/ mountainous, 35% is sloppy/valleys and the rest 14.6% are flat plains (BoARD, 2016). The altitude of the terrain of the kola watershed drains ranges from about 1702m to 3171 m.a.s.l and the average altitude is about 2436.5m.

3.1.4 Demography of study area

There are around 236070 people in the district who live being clustered in 29 Peasant Associations (PAs), out of which 49.2% (116099) are females and the rest 50.8% (119971) are males, as per the 2016 statistics of Sidama zone Bureau of Finance and Economic Development

(BOFED, 2016). Around 88.2% (208141) of the people are living in rural areas depending on crop production and animal rearing and the rest 11.8% (27929) are dwellers in the urban part of the district. The average population density is estimated to be 651 persons per square kilometer and the average landholding size of the district is 0.5 hectares according to districts' BoARD (2016), which is below the national average (1.2 ha) (CSA, 2010 cited in (Genene and Abiy, 2014).

3.2 Data Collection and Analyses

3.2.1. Data Collection and Analyses for landuse/land cover change investigation

To investigate LULCC in the past 30year (1988 to 2018) the temporal satellite images were captured, from the Website of the United States Geological Survey (USGS), and used for LULCC analysis and mapping. The required images were collected in December and January months to avoid the cloud and haze effects. The satellite image collection years were chosen based on the political change in the country, quality of the available images, and compatibility with the metrological and hydrological available data in the study area. Based on the above criteria, satellite images of 1988, 1998, 2008, and 2018 were collected from the following sources Landsat 5 TM was used for 1988 and 1998 images, Landsat 7 ETM+ was used for 2008 image, and Landsat 8 OLI for 2018 respectively. All the images were downloaded by using 168 paths, and 55-row. Detailed information's about the collected satellite images are indicated in the table below (Table3.1).

Table 3. 1 Satellite images with their dates of acquisition, path/row, and resolution

Satellite ID	Sensor ID	Path/Row	Date of Acquisition	Spatial Resolution
Landsat 5	TM	168/55	Jan/18/1988	30m*30m
Landsat 5	TM	168/55	Jan/30/1998	30m*30m
Landsat 7	ETM+	168/55	Jan/12/2008	30m*30m
Landsat 8	OLI	168/55	Dec/30/2018	30m*30m

In addition to a satellite image, the other data which was crucial for landuse/land cover quality assessments are ground control points. This data can be obtained from different sources such as

georeferenced thematic maps, aerial photographs, and global position system, and Google Earth. Depending on the availability of data, time and cost, google earth was chosen as the source of ground control points for this study.

3.2.1.1. Preprocessing of satellite image

The raw Landsat images have errors and will not be directly used for features identification and any applications, as it needs some correction. Pre-processing is done before the main data analysis and extraction of information. Image preprocessing involves the initial processing of raw image data to correct geometric distortions, radiometrically data calibration, and eliminate the noise present in the data. Pre-image classification processes were conducted before the image classification was carried out. Some of the major preprocess conducted before image classifications are discussed in the following paragraphs.

I Geometric Correction

Information extracted from the remotely sensed image is integrated with map data in a geographical information system. The remotely sensed image enhancement and the transformation were performed into a map with scale and projection properties through georeferencing. The satellite image utilized in this study were Orth-rectified to a Universal Transverse Mercator (UTM) projection system using datum World Geodetic System (WGS) 84, zone 37 N). Then after the collected Landsat data, corrected radiometrically, and geometrically, the area where this research was conducted was subsetted from the acquired satellite images using EARDAS imagine 2014 software.

II Scan line correction

From starting 2003 Landsat 7 have faced a scan line error, so the image downloaded from the satellites by using Landsat 7 had a scan line gap, in the case before image processing this problem should be corrected. The Landsat Enhanced Thematic Mapper (ETM^{+}) with Landsat 7 sensor was used for the acquisition of the 2008 year images. However, the Scan Line Corrector (SLC; and electromechanical device that compensates for the forward motion of the satellite) on Landsat 7's Enhanced Thematic Mapper Plus (ETM+) instrument, failed on 31 May 2003 (Gaohong et al., 2016) So to correct the scan line error there are different method of gap-filling techniques were available, such as focal analysis by using EERDAS, using Landsat toolbox,

etc. among them the Landsat toolbox was chosen for this study to fill the data gap of the 2008 year image before pre-classification process and image classification conducted.

III Haze Reduction Atmospheric correction

Atmospheric correction is the elimination of atmospheric and terrain effects to retrieve physical parameters of the earth's surface, including surface reflectance, ground visibility, and temperature. Such correction is especially important in cases where multi-temporal, multisensory, or multi-condition images are to be compared and analyzed. There are different methods are used to reduce haze among them image enhancement was used in this study.

IV Satellite Images Spectral Band Selection

Satellite imageries may have multiple spectral bands of information. Each band is a set of data file values with a specific portion of the electromagnetic spectrum of reflected light or emitted heat. In this research, the false-color composite image made using Land sat 8 bands 5-4-3 (R-G-B), Land-sat 5TM bands 4-3-2 (R-G-B), and land-sat7 ETM^{+} 4-3-2 (R-G-B) for the identification of major land cover classes in the study area.

3.2.1.2. Image Classification

In the development of landuse/land cover maps, using a supervised image classification technique, the remotely sensed satellite image was used for accurate signature development. This method is used to cluster pixels in a data set into classes corresponding to a user-defined area of interest training classes which are selected as representative areas to be mapped in the output. Historical information has been integrated to minimize complete reliance on spectral information and solve the mystery of spectral similarity of different land cover classes to improve classification accuracy.

Supervised image classification approaches provide a tool for detailed mapping of landuses, considering groups of pixels and the geometric properties of image objects and segmenting the images into homogenous regions based on neighboring pixels' spectral and spatial properties (Mori et al., 2004). In this study, the EARDAS imagine software was used to classify remotely sensed satellite images of the study area. It also supports different methods to train the algorithm and build up the resource and knowledge-based image classification. Then after image classification was done, the LULC mapping was performed by ArcGIS10.4.

3.2.1.7. Accuracy assessment

The accuracy assessment was conducted after image classification to check where the classified map was confined with the reference data taken from different sources. The use of remote sensing products relating to change for scientific, management, or policy support activities all require quantitative accuracy statements to increase the confidence in the information generated and in any subsequent reporting or inferences made (Stehman, 2009). Users with a variety of applications should be able to evaluate whether the accuracy of the map suitable for their objectives or not. In the accuracy assessment process, an error matrix and some accuracy measures derived from it were used. An error matrix is established using some known reference data and corresponding classified data (Hashemian, 2004). The quality evaluation is one of the first steps in making LULC classifications before it is used for a different purpose (Giri and Long, 2014). Thus, to check the accuracy and performance of LULC classification, Ground Control Points (GCP), which were taken from a different source such as Georeferenced thematic map, Aerial photo interpretation, GIS layers, Ground truth with GPS, and Google Earth were used.

In this paper, Google Earth was used as a source of reference control point and a stratified random sample strategy was adopted to assess the accuracy of the classified map. Then, a comparison of classified images and reference data was carried out statistically using the error matrix. Classified map and chance agreement of random classifier compared to reference data, were also calculated and from accuracy assessment. Then of the accuracy of producer accuracy, user accuracy, overall accuracy, and kappa coefficient were checked based on (Food, 2002) recommendations. ERDAS imagine 2014 software and micro excel were used to assess how well a classification worked and Understand how to interpret the usefulness of the classification results. The overall accuracy of the image classifications was computed by the following equation.

$$OA= \left(\frac{X}{Y}\right) * 100 \quad \text{..... (3.1)}$$

Where OA is overall accuracy, X is several correct values in diagonals of matrix and Y is the total number of values taken as a reference point.

Kappa analysis is a discrete multivariate technique used in accuracy assessments. According to (Badura et al., 2011) the acceptable ranges of the kappa coefficient are presented in the table below.

Table 3. 2 Table Kappa statics recommended Range.

SNO	Kappa Statistic	Strength of agreement
1	<0.00	Poor
2	0.00-0.2	Slight
3	0.21-0.4	Fair
4	0.41-0.6	Moderate
5	0.61-0.8	Substantial
6	0.81-1	Almost perfect

The kappa coefficients of the classified images were calculated by equation (3.5) which was recommended by (Congalton., 1991).

$$K=\frac{N\sum_{i=1}^{r} Xii-\sum_{i=1}^{r}(Xi+*X+i)}{N2-\sum_{i=1}^{r}(Xi+*X+i)} \quad \ldots\ldots\ldots\

modified the descriptions of some of the landuse/land cover classes by considering the landuse diversity of the study area. Depending on the above criteria, five landuse/land cover classes, and their respective definitions are mentioned in the table below (Table 3.3).

Table 3. 3 Classes and description of LULC of the study area based on FAO classification.

SNo	Class name	Description
1	Agriculture	Agricultural Land defined as a land cover category encompasses areas allocated for the production of the perennial and seasonal crops
2	Agroforestry	Woody perennials are purposely integrated with crops and/or in the same land management unit.
3	Built-up	Areas comprised of medium residential regions in scattered housing, dense residential areas, and little road infrastructure
4	Pastureland	Grassy areas are used for communal grazing, as well as bare lands, that have very little grass or no grass cover (exposed rocks). It also includes other small seized plant species.
5	Forest	Land spanning > 0.5 ha covered by trees a height of ≥ 2m and a canopy cover of more than 20%

Source: FAO classification and knowledge of the landuse diversity of the area

LULCC finding is the process of identifying differences in the state of an object or phenomenon by observing it at different times. Essentially, LULCC recognition involves the ability to quantify temporal effects using multi-temporal data sets. The general approach of LULCC is based on the post-classification comparison method, which is commonly employed in land cover change detection studies. In this method, after two images from different dates are independently classified, post-classification comparison of independently classified and developed landuse/land cover maps of 1988, 1998, 2008, and 2018 years were conducted, after their accuracy assessment was cheeked.

LULCC detection is the process of finding differences in the state of landuse/land cover by observing it at different times. LULCC detection involves the ability to quantify temporal effects using multi-temporal data sets. In the supervised classification technique, images with different dates were independently classified, to the pre-defined landuse/land cover types, and compared to each other. Landuse/land cover change comparison matrix gives general

information about major changes in the landuse/land cover classes between two periods. To recognize the major land cover gain and loss of cover classes, the conversion matrix for each period was analyzed. The conversion matrix of consecutive years was computed by using intersect functions in the GIS and the intersected area was computed, then the attribute table was exported to excel and the conversion matrixes were determined

The annual rate of change for individually landuse classes was calculated by the difference between a final year to initial year which represents the magnitude of change between corresponding years was divided by the number of study years, i.e. 1988-1998, 1998-2008, 2008-2018 (10 years) and 1988-2018 (30 years) respectively using the following equations.

$$\text{Annual R}\Delta\ (\%) = \frac{\text{Change (\%)}}{\Delta T} \quad \text{.....} \quad (3.3)$$

$$\text{Change (\%)} = \frac{(\text{Final year} - \text{Initial year}) * 100}{\text{Initial year}} \quad \text{.....} \quad (3.4)$$

Where: RΔ = Annual Rate of Change, Change (%) = % change in the area of specific landuse/land cover class, and ΔT = time interval between initial and previous LULC class in years

3.2.3. Landuse/land cover Prediction

Spatial modeling of the future landuse/land cover change processes is carried out by analyzing historical remote sensing data. By comparison of images between two or more years through image classification in which assigning pixels of a continuous raster image to predefined land cover classes (Kumar et al., 2008). LULC change prediction was employed using the CA-Markov model, which is available in IDRISI; Geospatial software for monitoring and modeling of the Earth.

CA-Markov model is a multi-criteria evaluation function that integrates CA and Markov chain. Using the quantity of change that is expected to achieve through Markov chain analysis, principally the transition area matrix, CA-Markov applies a contiguity kernel to grow out a landuse map to a later period through a CA function. The CA-Markov model has been applied in this study for the advantages of the combination of the stochastic spatial Markov technique with the stochastic spatial cellular automata method. The inputs to the model were the earlier image, later image, and the number of years of projection in the future concerning the base year. The previous and the later image provide the trends that were used in projection while the

number of years of projection determines the number of iterations. Markov involves two techniques; the first is to analyze expected LULC based on early and later map of LULC that has enabled us to obtain transition probability matrix records, that is the probability of each land cover category to change to another category. In the second step, a set of conditional probability images one for each land cover class was produced. These maps express the probability that each pixel will belong to the designated class in the next period. They are called conditional probability maps since this probability is conditional on their current state. In this study Landuse/land cover of 1988 and 2018 were used to predict the future landuse land cover of the study area.

3.2.3.1. IDRISI model validation

An important stage in the development of any predictive change model is its validation. Typically, one's understanding of the process, and the power of the model, by using to predict some period when the land cover conditions are known. This is then used as a test for validation. IDRISI supplies a pair of modules to assist in the validation process. The first is called VALIDATE and provides a comparative analysis based on the Kappa Index of Agreement. Kappa is essentially a statement of proportional accuracy, adjusted for chance agreement. However, unlike the traditional Kappa statistic, VALIDATE breaks the validation down into several components, each with a special form of Kappa or associated statistic (Pontius, 2000). The other validation procedure is the ROC (Relative Operating Characteristic). It is used to compare any statement about the probability of an occurrence against a Boolean map that shows the actual occurrences. It can be useful, for example, in validating modifications to the conditional probability maps output from MARKOV.

The prediction capacity of the IDRISI model was validated by comparing the actual classified map at a known point in time with the predicted map at the same time. The validation of the model was done by using the validation tool available in the IDRISI software. To check the performance of the model in the past, measures of the 'goodness of fit' were commonly performed by using a simple percent correct measure or, at best, a multiple-resolution percent of correctness (Costanza, 1989). Spatial measures of 'goodness of fit' have been developed that measures the degree to which a simulated map agrees with a real map concerning both location (Kappa-for-location) and quantity of correct cells (Kappa-for-quantity) (Girirajet al., 2008).

Kappa statistics were used to assess the similarity of the two images. If the value computed by Kappa greater than 0.75, the two images are similar and change slightly (Pontius and Schneider, 2001).

The figure below indicates the general layout, and procedure used to investigate the land-use/land cover changes in the study area, from stating Landsat data collection up to land-use/land cover prediction.

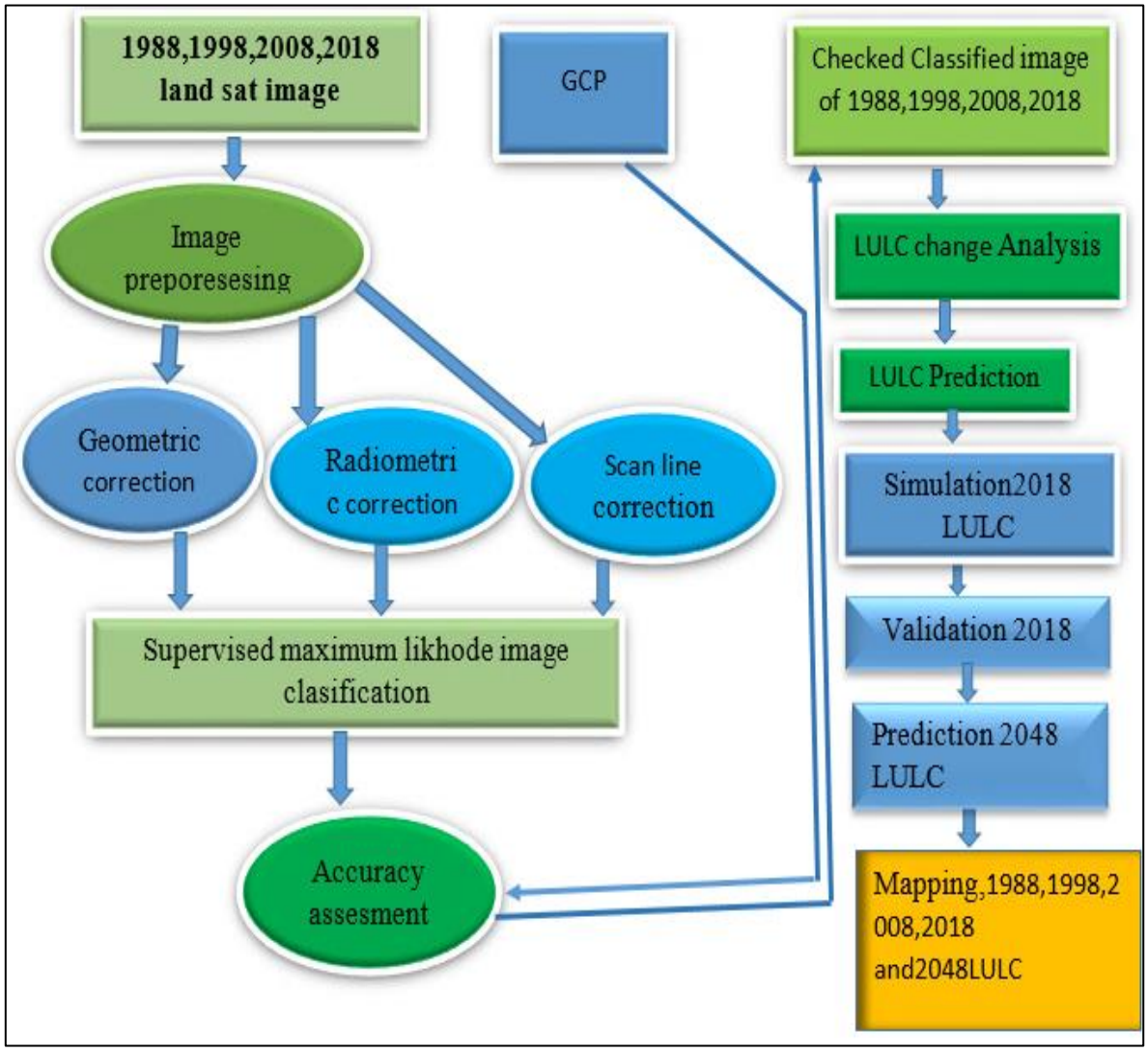

Figure 3. 2 Schematic representation of Landuse land covers analysis procedure

3.2.4. SWAT Model Input Data Collection and processing

Hydrological modeling is a powerful technique of hydrological system investigation for both the researcher and hydrologist practicing in water resources. As it involved planning and

development of an integrated water resources management. Moreover, watershed modeling techniques are useful tools for investigating interactions among the various watershed components and hydrologic response analysis to LULCC and River basin management at various spatial scales (Silberstein, 2006) . The Soil Water Assessment Tool (SWAT) model was used in this study to assess the impact of landuse/land cover on the hydrological response of the study watershed. SWAT Model, requires spatial data such as landuse/land cover, soil, and digital elevation model besides the time serious data such as climatic data and hydrological data. These data were the crucial inputs of the SWAT model, so the required data were collected from different sources and rearranged according to the model impute format. The basic required data to run SWAT model were collected and analyzed as indicated in the paragraph below.

3.2.4.1. Spatial data collection and analysis

The basic spatial data sets required to develop an input database for the SWAT2012 model such as DEM, soil, and landuse/land cover were collected and analyzed, as tried to mention in the following paragraph, the source of the spatial data and their respective collection method and preparation were discussed.

I. Digital elevation model (DEM)

DEM (Digital Elevation Model) of (30x30) resolution was downloaded from the United States Geological Survey (USGS). DEM is used in the SWAT model to delineate the watershed and to further divide the watershed into sub-watersheds and hydrologic response units (HRU). The resolution of the digital elevation model (DEM) is the most critical input parameter when developing a SWAT model (Gassman et al., 2007).

II. Landuse/Land Cover

The satellite image of a 30-meter resolution was downloaded from the USGS Data Server and supervised image classification with maximum likelihood classifier algorism was carried out. Finally, the LULC maps were prepared to use in SWAT. Then the classified landuse/land cover map was clipped in the Kola River watershed. Then, the clipped landuse map was used for SWAT landuse reclassification. The LULC data set was reclassified into five major LULC classes such as: built up, forest, pasture, agriculture, and agroforestry (Figure 3.3).

III. Soil data

Soil data is important for the analysis of the impact of landuse/land cover on the hydrology of the watershed. Soil properties play the important role in hydrological modeling. SWAT model requires different soil Textural and physicochemical properties such as soil texture, available water content, hydraulic conductivity, bulk density, and organic carbon content for different layers of each soil type. The soil data of the study area was gained from the Ministry of Water, Irrigation, and Electricity of Ethiopia. The major aim of soil classification is to convert the user's soils into the SWAT database (or grid properties). Soils in the study watershed are classified based on the FAO 2007classification system. The main soil type in the study area was Chromic luvisols and Eutric vertisols, which covers 75.23% in total (Chromic luvisols 58.34% and Eutric Vertisols 16.89%).whereas the left soil types of the study area covers Chromic combisols 15.21 %, lithic leptosols 6.65%, and Humic nitosols 2.91% respectively.

Table 3. 4 Soil types of Kola River watershed

S NO	Soil Group Name	Name	Soil Group	Area (ha)	% of Coverage
1	Chromic combisols	CM	B	313.09	15.21
2	Chromic luvisols	LV	B	1201.16	58.34
3	Eutric vertisols	VR	C	347.76	16.89
4	Humic nitosols	NT	D	59.92	2.91
5	Lithic leptosols	LP	C	136.83	6.65

IV. Slope

The slope was derived from DEM input so that the model uses this slope for the development of the Hydrological Response unit in addition to landuse and soil input parameters. Based on the FAO slope classification the slope of the study area is classified into a gentle sloping (0-5%), sloping (5-10%), and strongly sloppy (10-15%), moderately steep (15-20%), and steep (>20%).

Table 3. 5 Slope classes and area coverage of kola watershed

Classes	Slope Range (%)	Area	
		ha	%
1	0-5	5781.08	28.09
2	5_10	3353.91	16.3
3	10_15	3084.6	14.99
4	15_20	6336.07	30.79
5	>20	2025.75	9.84

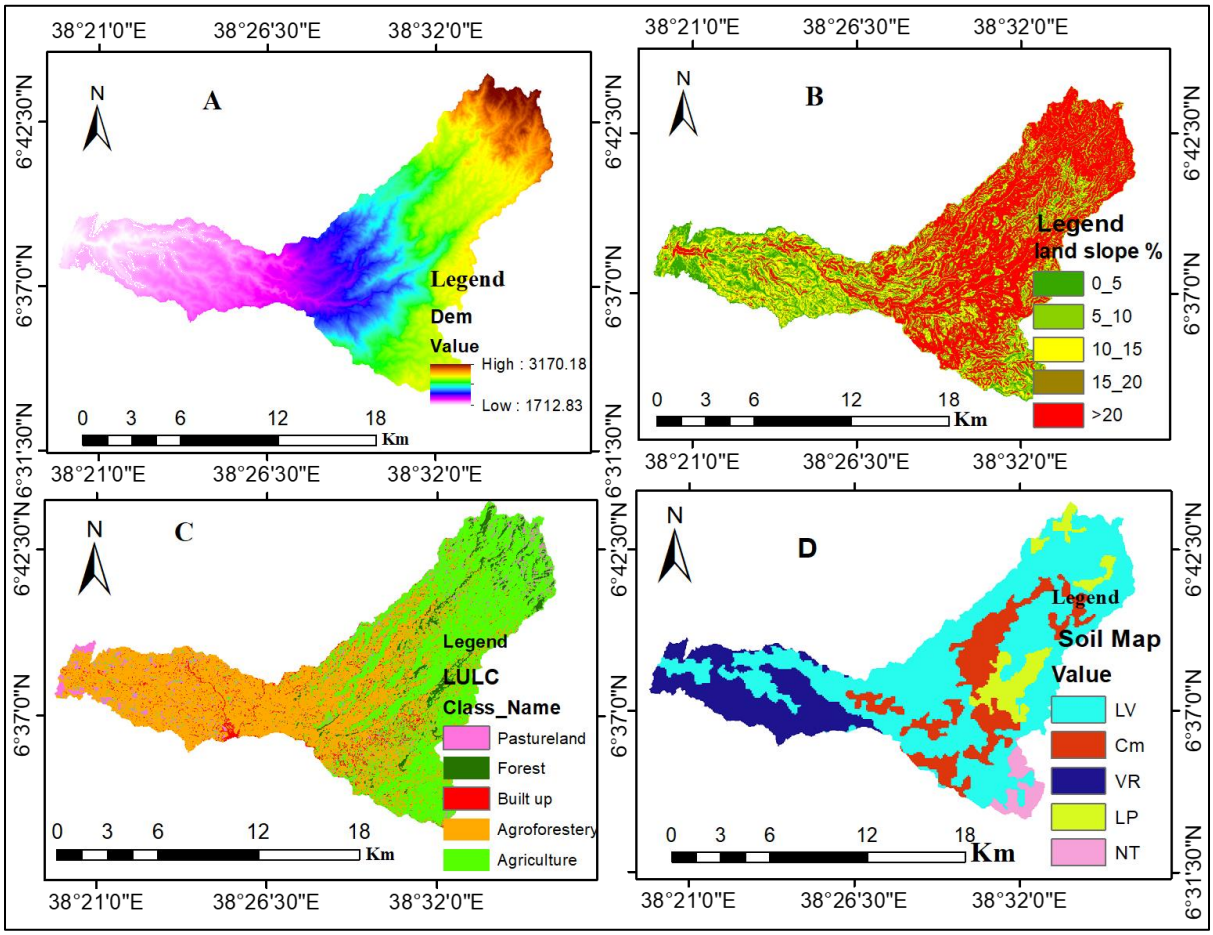

Figure 3. 3 Maps of spatial data of Kola River Watershed: DEM (A), Slope map (B), Landuse map (C) Soil map (D) of 1988.

3.2.4.2. Meteorological data

The meteorological data is among the most required parameter of the SWAT model. The major Meteorological data required during the simulation of SWAT model were rainfall, temperature, solar radiation, relative humidity, and wind speed respectively. For this study, the required metrological data were collected from Ethiopian Metrological Agency. The available climatic data in the kola River watershed for the current study were mentioned in Table 3.6. However, for some stations, the data length varies depending on the availability and gauging station establishment year.

Table 3. 6 Meteorological station locations and length of data series.

						Data type				
S. No.	Station name	Data length	Latitude	Longitude	Elevation	Rainfall	Temperature	R/Humidity	Solar radiation	Wind speed
1	AW	1988-2018	6.6	38.4	1947	√				
2	DL	1988-2018	6.4	38.3	1579	√	√	√	√	√
3	HS	1988-2018	7	38.4	2841	√	√			
4	TK	1988-2018	6	38.38	1870	√	√			
5	YG	1991-2018	6.2	38.7	1786	√	√			

Where: AW= Aletta Wando, DL= Dilla, HS= Hagere selam, TK=Teferekela, YG= Yergalem

1. Rainfall data

The precipitation data of selected stations, used in this study have a data length of 31 years (1988-2018), except yergalem station which starts in 1991. Even though there were different degrees of missing, values in the mentioned data length. This small missing value and equal duration of time of the synoptic stations are important to the next arc SWAT analysis of preparing weather generator data because the weather generator stations generate missing data of other stations.

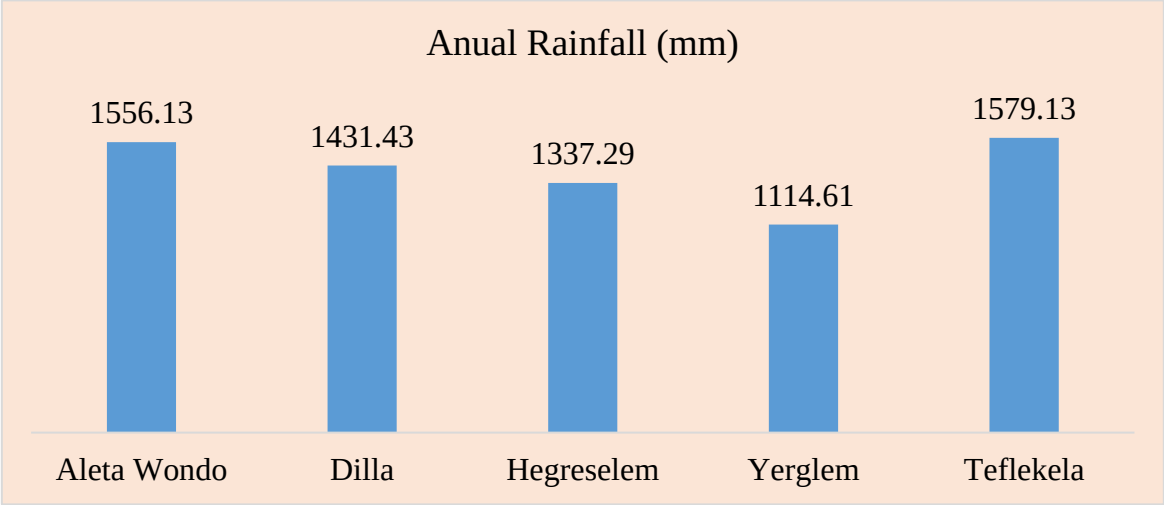

Figure 3. 4 Average Annual Precipitation of the Meteorological Stations (1988-2018).

The precipitation of the Kola River watershed is characterized by a bimodal pattern having maximum precipitation during April, May, September, October, and minimum January, February, and December.

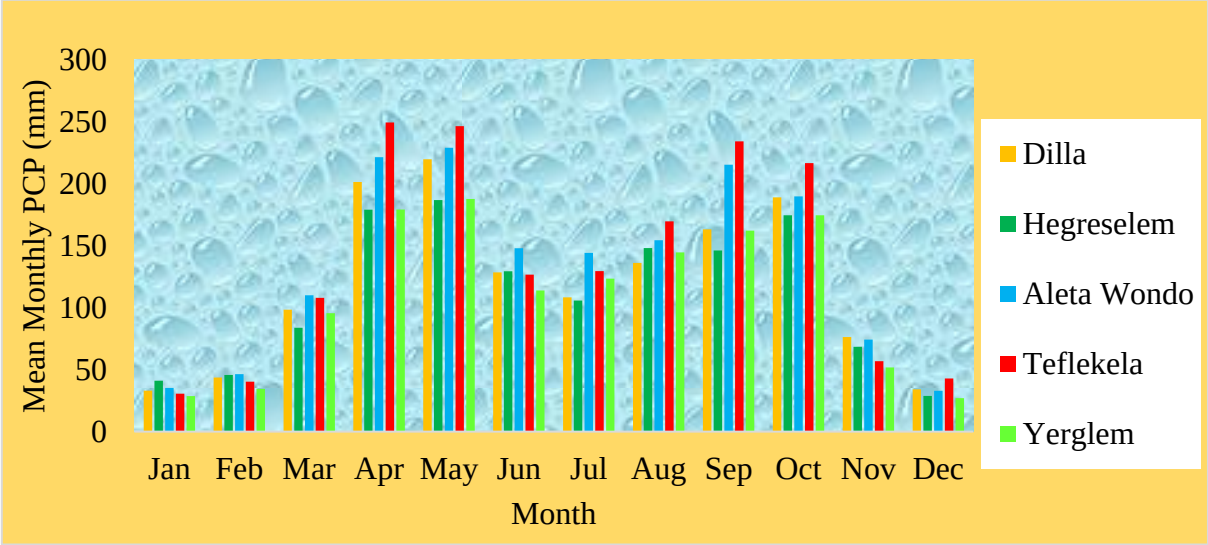

Figure 3. 5 Mean monthly rainfall graph of selected meteorological stations in Kola watershed (1988-2018).

2. Air temperature

The long-term mean annual and monthly, maximum, and minimum temperatures for the selected stations are shown in Figures 3.6 and 3.5. The magnitude of air temperature varies with altitude. The highest and the lowest air temperature exhibited at the lowest altitude and higher altitude respectively.

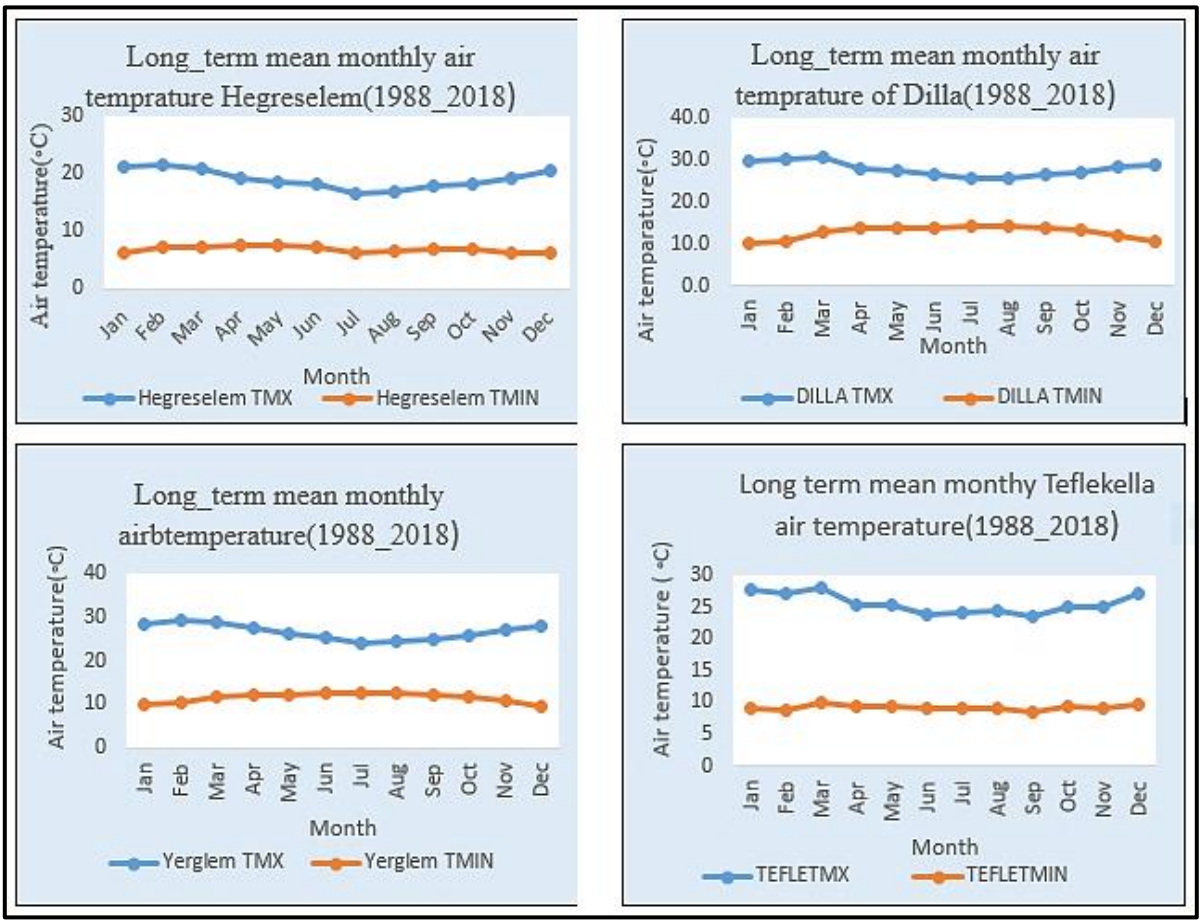

Figure 3. 6 Long-term mean monthly variations of minimum and maximum air temperature (1988-2018)

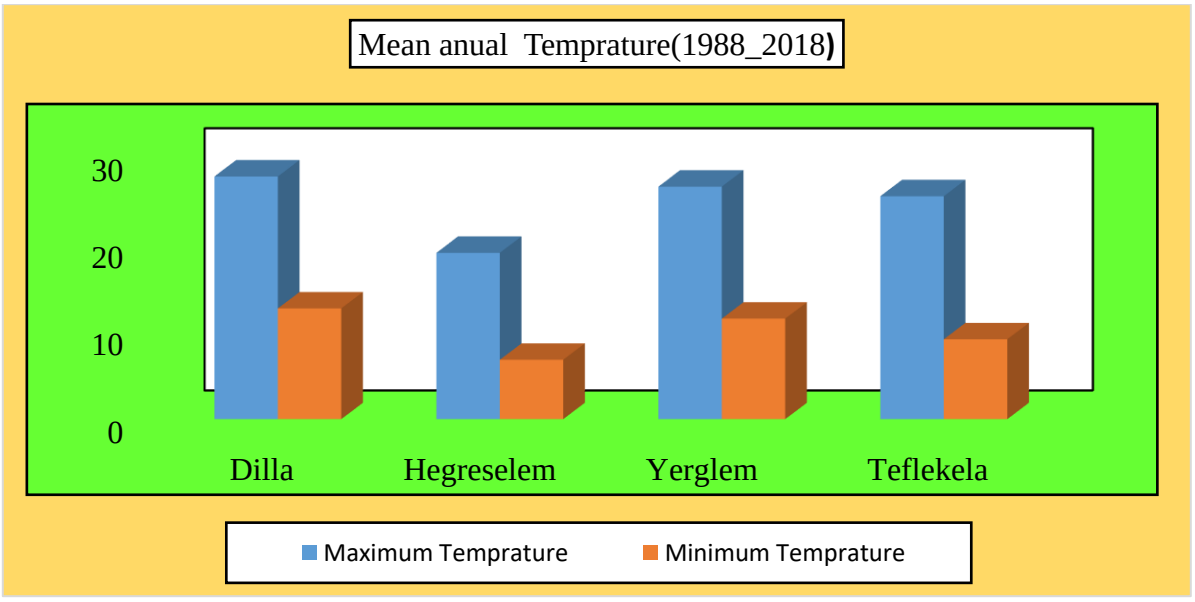

Figure 3. 7 Long-term mean annual air temperature of the study watershed

3. Other climatic data

In addition to precipitation and temperature the other climatic data such as, relative humidity, solar radiation, and wind speed were needed to run the SWAT model, however, this data was not founded in all stations that were considered in the study area. All required climatic data were found at Dilla station which the only synoptic station nearest to this study area. These data were filled from Dilla station for the other stations by using a weather generator.

3.2.4.3. Flow data

Observed flow data was required in the Soil and Water Assessment Tool (SWAT) for sensitivity analyses, calibration, and validation. The observed streamflow data of 1980-2013(GC) yeas, which was recorded at the outlet of the Kola River Watershed was collected from, Ministry of Water Resources, Irrigation and Energy of Ethiopia (MoWIE), Hydrology department, and prepared in the format the SWATmodel required.

3.2.4.4. Metrological data analysis

The precipitation data was checked for inconsistency before it is used for further analysis. The quality control can be done by visual inspection, accumulated plot, and double mass curve. This will help to identify if there are any gaps or unphysical peaks in the data series and correct them before the data is used as input to the model. The First Step in data quality control is a visual inspection. It was done by plotting the time series data against time. The percentage of missing data points for five precipitation stations is shown in Table 3.7 below.

Table 3. 7 Percentage of missing data for precipitation in all stations.

S.No.	Station name	Data points	Missing pt. Data	Data without missing	% of missing
1	Aletta Wando	10950	365	10585	3.3
2	Dilla	11315	3627	7688	3.6
3	Hagere selam	13315	522	12793	3.9
4	Teferekela	10,950	182	10768	1.7
5	Yirgalem	9855	800	9055	8.1

3.2.4.5. Filling missing data for the selected stations.

Some stations have short breaks in the records because of the absence of the observer or because of instrumental failures. It is often necessary to estimate or fill in this missing record. Filling the missing data on a daily scale is implemented in the SWAT model itself. The complete long-term statistical information from the synoptic stations enables us to fill in the missing data based on the Markov-chain model embedded in the SWAT (Schuol and Mikayilov, 2007). However, for representing the climate in the watershed, the missing precipitation of a station was estimated from the observations of precipitation at some other stations as close to and as evenly spaced around the station with the missing record as possible.

There are different methods to fill in missing data, such as arithmetic mean, normal ratio, and inverse distance weighting, and regression method. Among these, the normal ratio method was used in this study depending on watershed characteristics.

$$Px=\frac{1}{N}\sum_{i=1}^{i=n}\frac{Nx}{Ni}Pi \quad \text{(3.1)}$$

Where: Px = the missing precipitation for any storm at the interpolation station x,

Pi = the precipitation for the same period for the same storm at the i^{th} station of a group of index stations.

Nx = the normal annual precipitation for station x,

Ni = the normal annual precipitation value for the i^{th} station.

3.2.4.6. Homogeneity Test of Rainfall Data.

The homogeneity of parameters analysis is important to the variation of the statistical properties of the time series. To select the representative meteorological station for the analysis of rainfall estimation, checking the homogeneity of group stations are important and the homogeneity of the selected stations, were carried out by non-dimensional.

$$Pi=\frac{\bar{P}i}{\bar{P}}*100 \quad \text{(3.2)}$$

Where: Pi is the non-dimensional value of precipitation for the month in the station i

$\bar{Pi}$ is over year's average monthly precipitation for the station i

$\bar{P}$ is over year average yearly precipitation for station i

A time-series observational data is relatively homogenous if the periodic data proportionally behave in a comparable similar pattern. The selected stations were plotted for comparison

purposes as presented in figure 3.8, and the figure indicates that stations have the same trend of distribution pattern, this shows that the group of selected stations are homogeneous.

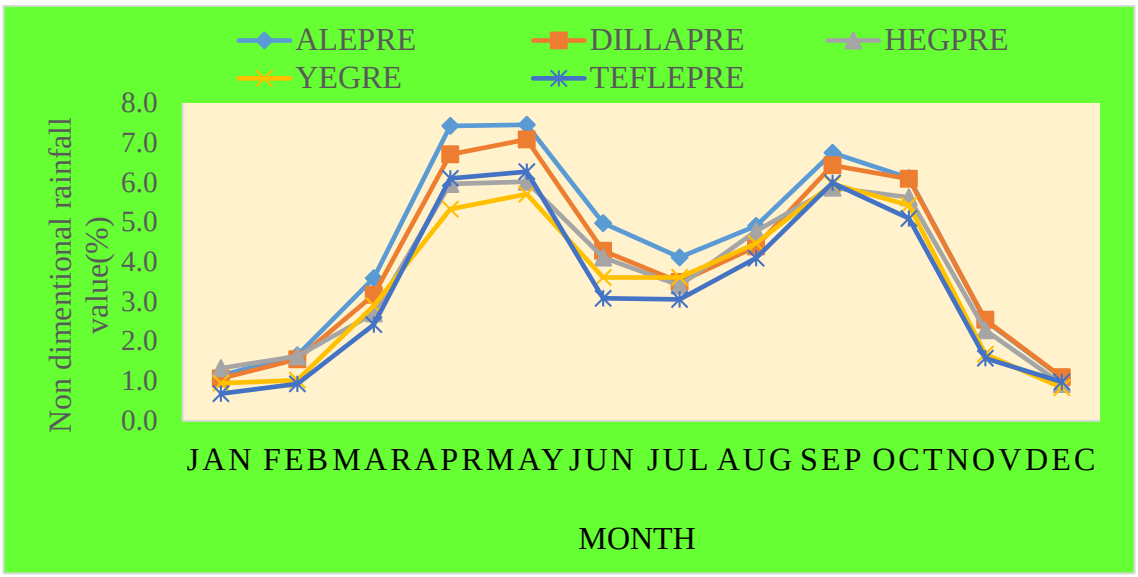

Figure 3. 8 Homogeneity tests for selected weather station at Kola watershed

3.2.4.7. Consistency test of selected stations by using Double mass curve.

A double mass curve analysis has been implemented to check the consistency of the rainfall stations. The principle of double mass curve analysis is to plot accumulated values of the station under investigation against the accumulated value of another station, or accumulated values of the average of other stations, over the same period. Through the double mass curve, inconsistency in the time series data (in particular jumps) was investigated. These indicated in the double mass plot, showing an inflection point in the Straight line. The data series, which were inconsistent, were adjusted to consistent values by proportionality. This method helped in determining the best realistic correlation of different stations located near the watershed. If the cumulative plot of the double mass curve shows a different, gradient it should be corrected as:

$$PCX = Px\left(\frac{Mc}{Ma}\right) \quad \text{..... (3.3)}$$

Where Pcx = correct precipitation at any time $t1$ at station x

Px = original record precipitation at any time $t1$at station x

Mc = correct slope of the double mass curve

Ma = original slope of double mass curve

Some of the results of the consistency check for a group of stations are presented in the figure below.

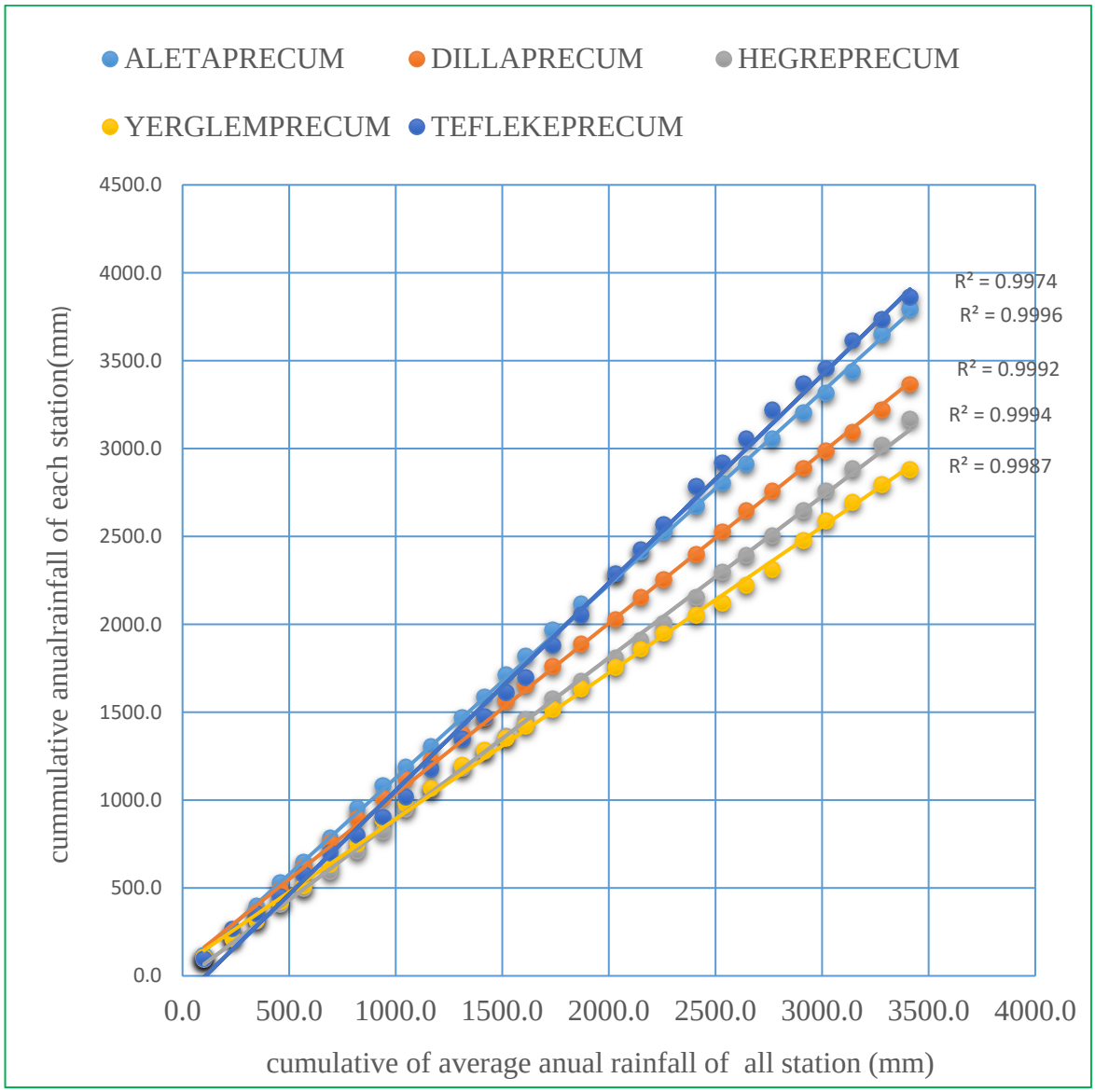

Figure 3. 9 Double mass analysis representing data consistency of stations on the Kola watershed.

3.2.4. 8. SWAT Model set up, and hydrological response analysis.

SWAT operates on a daily time step is designed to predict the impact of landuse and management on water. The model is process-based, computationally efficient, and capable of continuous simulation over long periods. Major model components include weather, hydrology, soil temperature and properties, plant growth, nutrients, pesticides, bacteria and pathogens, and

land management (Arnold, 2012).In SWAT, a watershed is divided into multiple sub-watersheds, which are then further subdivided into hydrologic response units (HRUs) that consist of homogeneous landuse, management, topographical, and soil characteristics. Alternatively, a watershed can be subdivided into only sub-watersheds that are characterized by dominant landuse, soil type, and management.

3.2.4.9. Watershed delineation

The first step in creating the SWAT model input is a delineation of the watershed from DEM and the inputs entered into the SWAT model were organized to have spatial characteristics and the DEM were projected into the same projection called UTM Zone 37N, which is a projection parameter for Ethiopia. Subwatershed and watershed delineation of the area was done using DEM data with the help of the ArcSWAT model on ArcGIS.10.4. By creating a new SWAT project set up, watershed delineation was performed (i.e. DEM project set up, flow direction and accumulation, stream network, outlet, and inlet definition, whole watershed outlet, delineate watershed, and calculation of sub-basin). A watershed was partitioned into several sub-basins, for modeling purposes. For the stream definition, 2000ha used as a threshold-based stream definition option was used to define the minimum size of the sub-basins. Similarly, stream networks sub-watershed and topographic parameters were estimated using the same strategy. The elevation of the area is also generated from DEM when the watershed was delineated. The highest elevation of the area is 1712.83m and the lowest is 3170.22m above sea level.

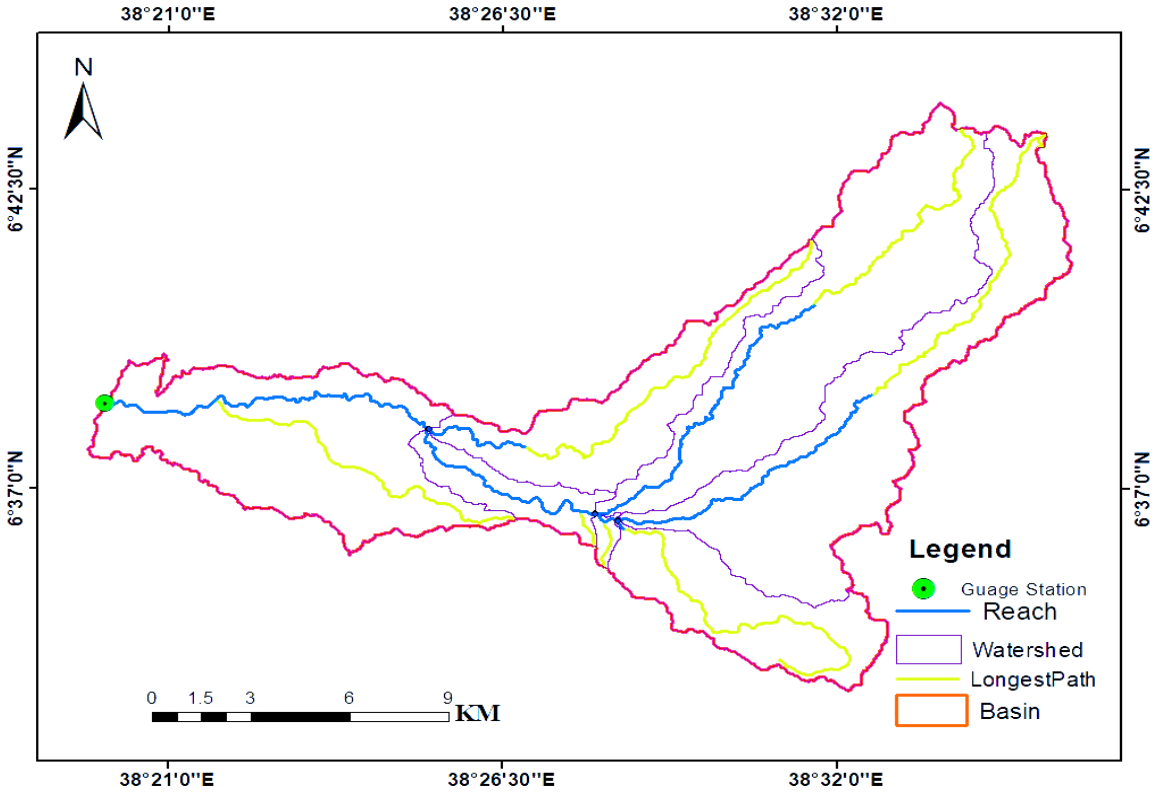

Figure 3. 10 Delineated Watershed of the study area

3.2.4.10. Hydrological response units (HRU)

For simulation, a watershed is subdivided into many homogenous sub-basins (hydrologic response units or HRUs) having unique soil, slope, and landuse properties. The input information for each sub-basin will be grouped into categories of weather; unique areas of land cover, soil, and slop within the sub-basin. HRU analysis tool in Arc SWAT helps to load landuse, soil layers, and slope maps to the project. The delineated watershed by Arc SWAT and the prepared landuse and soil layers were overlapped. The multiple slope option (an option that considers different slope classes), were considered in this study. The classification was carried out based on a height range of DEM used during watershed delineation. The slope values of the watershed were reclassified by percent, into five classes (0-5, 5-10, 10-15, 15-20, and >20 respectively). Therefore, for this study, HRU definition with multiple options that accounts for 5% landuse, 10% soil, and 10% slope threshold combination was used. Hence, the sub-basin was divided into 42 HRU, each has unique landuse and soil combinations. The number of HRU varies within the sub-watersheds.

3.2.4.11. Weather Generator`

Another key section of Arc SWAT next to HRU is an analysis of Weather Data. Weather data necessary for running a basic SWAT simulation were precipitation, wind speed, solar radiation relative humidity in addition to the maximum and minimum temperature. In our country, there is a lack of a full long period of climatic data most of the stations have only one or two climatic data types. Therefore, the weather generator solves this problem by generating data from the observed one (Danuso and Agron, 2002).In this study measured data for all climatic variables were founded only one synoptic station (Dilla station). Therefore, the missed values of other stations were filled with the weather generator utility in the Arc SWAT model from the values of weather generator parameters.

After HRU definition was finished in Arc SWAT, the designated weather station locations are added to the Monitoring Point layer created during Watershed Delineation. The finally before a SWAT simulation started, write all of the input files required by SWAT and produced from the preprocessed data from Arc SWAT were carried out. After preprocessing of the required input for the SWAT model, flow simulation was performed for years of recording periods starting from 1988 through 2006 the first two years of which will be used as a warm-up period.

3.2.4.12. Sensitivity analysis

Sensitivity analysis is the process of identifying the sensitive parameter among the parameters that can affect the model outputs. All of the parameters are not equally sensitive depending on the nature of the model outputs and physical conditions of the study area. Identifying and minimizing the number of parameters to be used in the calibration step by making use of the most sensitive parameter that mostly controls the behavior of the simulated values was one of the tasks in the sensitivity analysis process. SWATCUP version 2019 was used for senility analysis, calibration, and validation. There are several sensitivity parameters in SWAT CUP with their maximum and minimum values respectively. A t-test is then used to identify the relative significance of each parameter. The global sensitivities estimates of the average changes in the objective function resulting from changes in each parameter, while all other parameters are changing. This gives relative sensitivities based on linear approximations and, hence, only provides partial information about the sensitivity of the objective function to model parameters (Karim, 2007). T-stat provides a measure of sensitivity (larger in absolute values

are more sensitive) p-values determined the significance of the sensitivity. A value close to zero has more significance.

3.2.4.13. Calibration and Validation

The model was calibrated using a sequential uncertainty fitting (SUFI-2) algorithm which was founded in the SWAT-CUP computer program. Calibration is an alteration of model parameters by checking results against observations to check a similar response over time. This involves comparing the model outcomes, entered with the use of observed stream flows data. During model calibration, manual and automatic calibration methods were applied.

Automated model calibration requires that the uncertain model parameters are systematically changed, the model is run, and the required outputs (corresponding to measured data) are extracted from the model output files. The main function of an interface is to provide a link between the input/output of a calibration program and the model. The simplest way of handling the file exchange is through text file formats (Karim, 2007).

The graphical and statistical approaches were used to evaluate the SWAT model performance many iterations were conducted until the acceptable values were obtained for surface runoff and base flow independently. The flow calibration procedure made by SWAT developers was carefully followed (Santhi, 2006) the observed flow of the Kola River (1988_2013) was used for calibration and validation. From total available flow data (26 years) the two years data were used for a warm-up purpose, two-third of the available flows at gauging stations (15 years) flow data were used in the calibration of the swat model.

The purpose of model validation is to check whether the model can predict flow for another range of periods or conditions than those for which the model was calibrated. Model validation involves rerunning the model using input data independent of data (meteorological data) used in calibration (by the different periods of a simulation) but keeping the calibrated parameters unchanged. Like model calibration, the model performance evaluation parameters were calculated and checked whether the model performed very well or not. In this study one-third of the available streamflow (8year) data, kola gauging station was used for the validation purpose.

3.2.4.14. Model performance evaluation

Checking Model performance is not optional before it can be applied to a specific area. In this study, both graphical and statistical methods of performance evaluation were used to check the compatibility of the model for this study. The graphic method consisted of plotting observed versus simulated hydrographs to compare them visually. The quantitative methods of evaluation were dependent on the three model evaluation methods namely: the Nash-Sutcliffe coefficient of efficiency (NSE), Coefficient of determination (R^2), and percent bias (PBIAS). These three objective functions are widely used in evaluating the performance of the hydrological model (Gassman, 2007).

Coefficient of determination (R^2) describes the proportion of the total variance in the observed data that can be explained by the model. The closer the value of R^2 to 1, the higher is the agreement between the simulated and the measured flow and is calculated as follow:

$$R^2 = \frac{(\sum[Xi-Xav][Yi-Yav])^2}{\sum [Xi-Xav]^2 [Yi-Yav]^2} \quad \text{(3.4)}$$

Where: Xi is measured value, Xav is average measured value, Yi is simulated value, Yav is average simulated value.

Nash and Sutcliffe simulation efficiency (ENS) indicates the degree of fitness of observed and simulated data and given by the following formula

$$NSE = 1 - \frac{\sum(Xi - Yi)2}{\sum(Xi - Xav)2} \quad \text{(3.7)}$$

The value of ENS ranges from 1 (best) to negative infinity. If the measured value is the same as all predictions, ENS is 1. If the ENS is between 0 and 1, it indicates deviations between measured and predicted values. If ENS is negative, predictions are very poor, and the average value of output is a better estimate than the model prediction (Nash and Sutcliff, 1970).

Percent bias (PBIAS) measures the average tendency of the simulated data to be larger or smaller than their observed counterparts (Lu, 2015).

$$PBIAS = \left(\frac{\sum(Xi - Yi)}{\sum(Xi)}\right) * 100 \quad \text{(3.8)}$$

Where: Xi is measured, and value, Yi is simulated value.

The calibration and validation performance for the SWAT model was considered acceptable when NSE was greater than 0.5. The SWAT model performance is satisfactory when NSE is larger than 0.5, adequate when NSE ranges from 0.54 to 0.65, and very good when NSE is

larger than 0.65. The SWAT model is rated as satisfactory, when the absolute value of PBIAS ranges from 15 to 25, rated well when from 10 to 15, and very good when smaller than 10 (Moriasi et al., 2007).

Table 3. 8 General performance ratings for recommended statistics for a monthly time step

Performance rating	ENS	PBIAS	R2
Very god	.75 < NSE < 1.00	PBIAS < ±10	R2>0.8
Good	0.65 < NSE < 0.75	±10 < PBIAS < ±15	0.7<R2<0.8
Satisfactory	0.50 < NSE < 0.65	±15 < PBIAS < ±25	0.6<R2<0.7
Unsatisfactory	NSE < 0.50	PBIAS > ±25	<0.6

3.2.4.15. Analyzing the effects of LULCC on the hydrological response of the study watershed

Modeling of the effects of landuse land cover on the hydrological response of the study watershed was conducted by using the soil water assessment tools (SWAT) model. In this model, spatial data such as landuse land cover, soil, and digital elevation model were required besides the time serious data such as climatic data and hydrological data as the major inputs of the SWAT model. The study was carried out for four different years (1988, 1998, 2008, and 2018) landuse land covers independently while other additional factors such as soil, digital elevation model (dem), climate, and flow data were taken as constant. Then the calibrated and validated SWAT Model has been run for each LULC map (1988, 1998, 2008, 2018, and predicted 2048) respectively. Then using the output of the model respective to the landuse/land cover at each investigation year the impact of landuse/land cover on the hydrological response of the study watershed was investigated. Generally, the figure below indicates the major steps and process that carried out by SWAT model during the investigation of the impact of the landuse/land cover change on the hydrological response of the study watershed

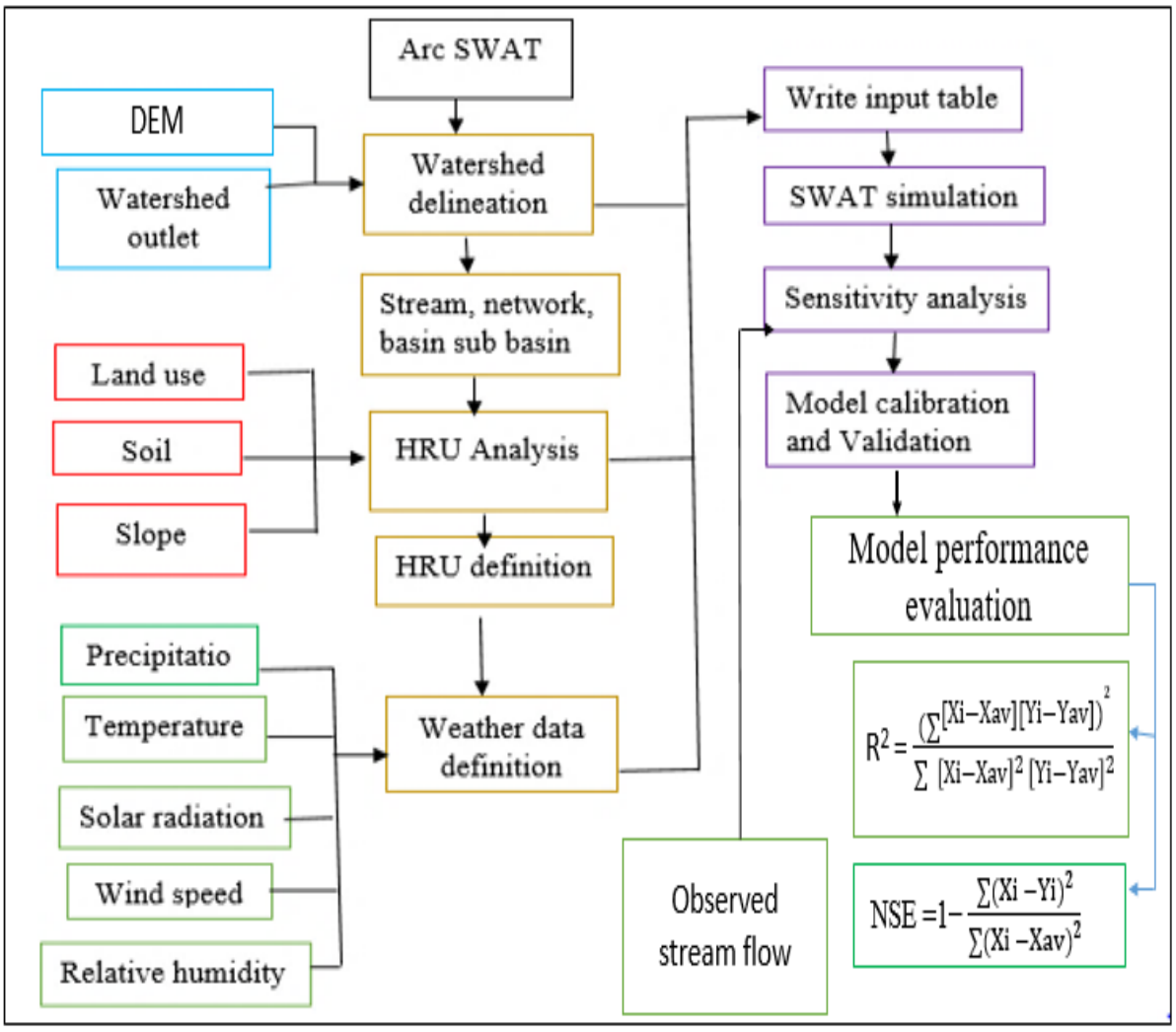

Figure 3. 11 Arc SWAT processing procedures flowchart.

The general conceptual framework which summarizes the major workflow and procedures followed to obtain the assigned objective in the study of impacts of landuse/land cover change on the hydrological response of Kola River Watershed was expressed in the figure below (Figure 3.12).

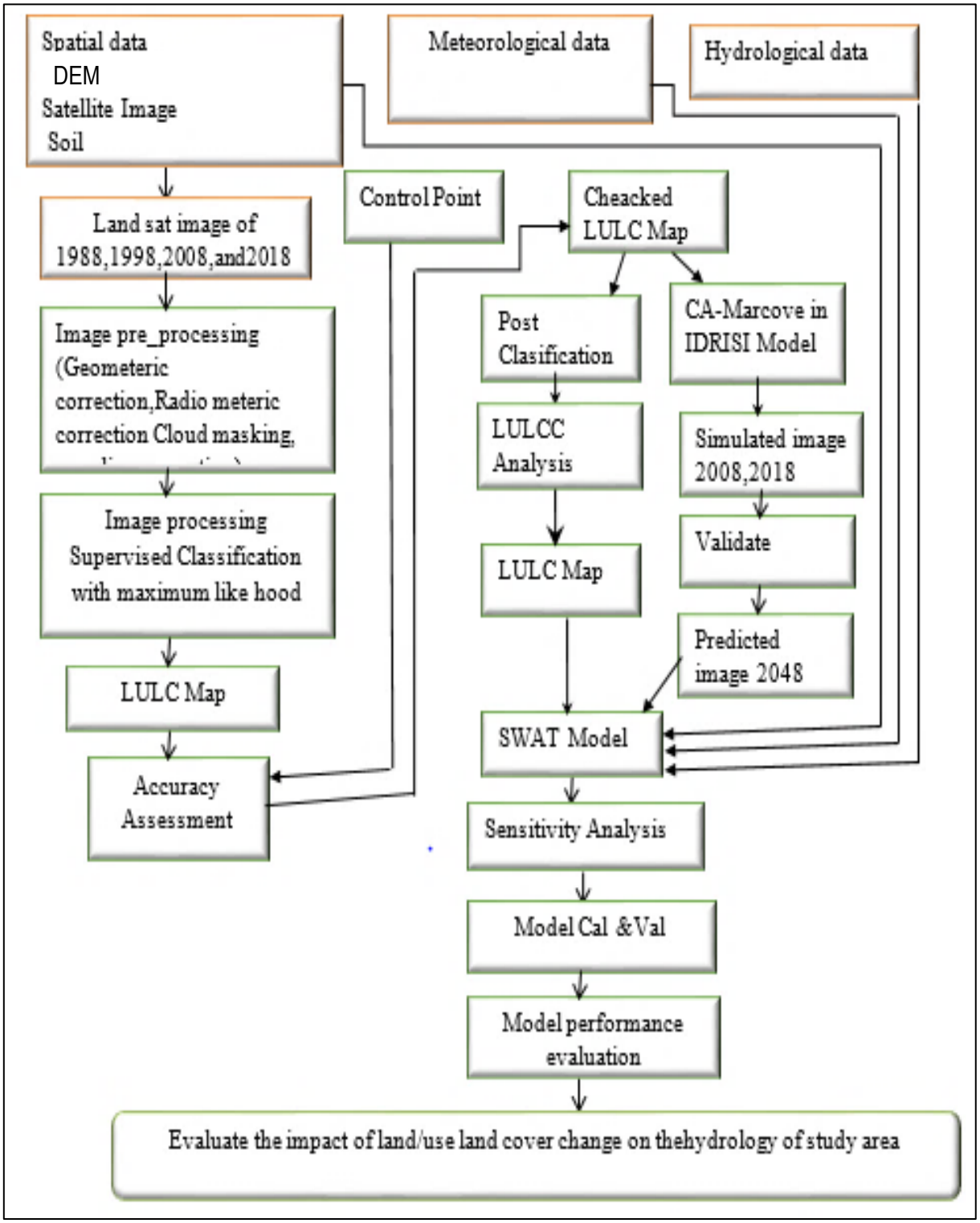

Figure 3. 12 Methodological flow chart

4 RESULTS AND DISCUSSION

4.1. Landuse/Land cover change detection and accuracy assessment

The satellite images of 1988, 1998, 2008, and 2018 years were downloaded from USGS and used to investigate the changes of LULC and its effects on the hydrological response of the study watershed. During image classification, five landuse/land cover classes were identified based on the historical knowledge about the study area and band reflectance of the remote sensing data. The landuse types of the study area include Agriculture, Agroforestry, Built-up, Pastureland, and Forest respectively. Agriculture and Agroforestry are well distinguished in Landsat imagery. The result of the landuse/land cover analyses of the study area showed that agroforestry and agriculture were the dominant landuse classes that cover more than 80% of the watershed. Though before change detection and investigation of its impact on the hydrological response of the study watershed, the accuracy assessment was done for each classified image. The classification results and their accuracy assessments were discussed in the following paragraph. Generally to check the time series landuse/land cover change in the kola River watershed satellite images of the different years were downloaded and classified, starting from 1988 and by taking ten years interval so 1998, 2008, and 2018 were classified as their results were summarized in Table 4.5, by their area and percentage coverage of a total watershed area.

4.1.1 Landuse/Land cover map for 1988.

After the Landsat image of the 1988 year was downloaded, image preprocessing, image classification, and post-classification process were conducted, the 1988 landuse/land cover map was prepared. The obtained result of satellite image classification of the1988 indicated that agroforestry covered the largest portion of the Watershed which covers an area of 9556.68ha (46.47%), followed by agriculture 8828.87ha (42.93%), pastureland 762.82ha (3.71%), forest 739.74ha (3.6%), and built up area677.15ha (3.29%) respectively. The figure below figure 4.1 indicates the 1988 landuse/land cove map.

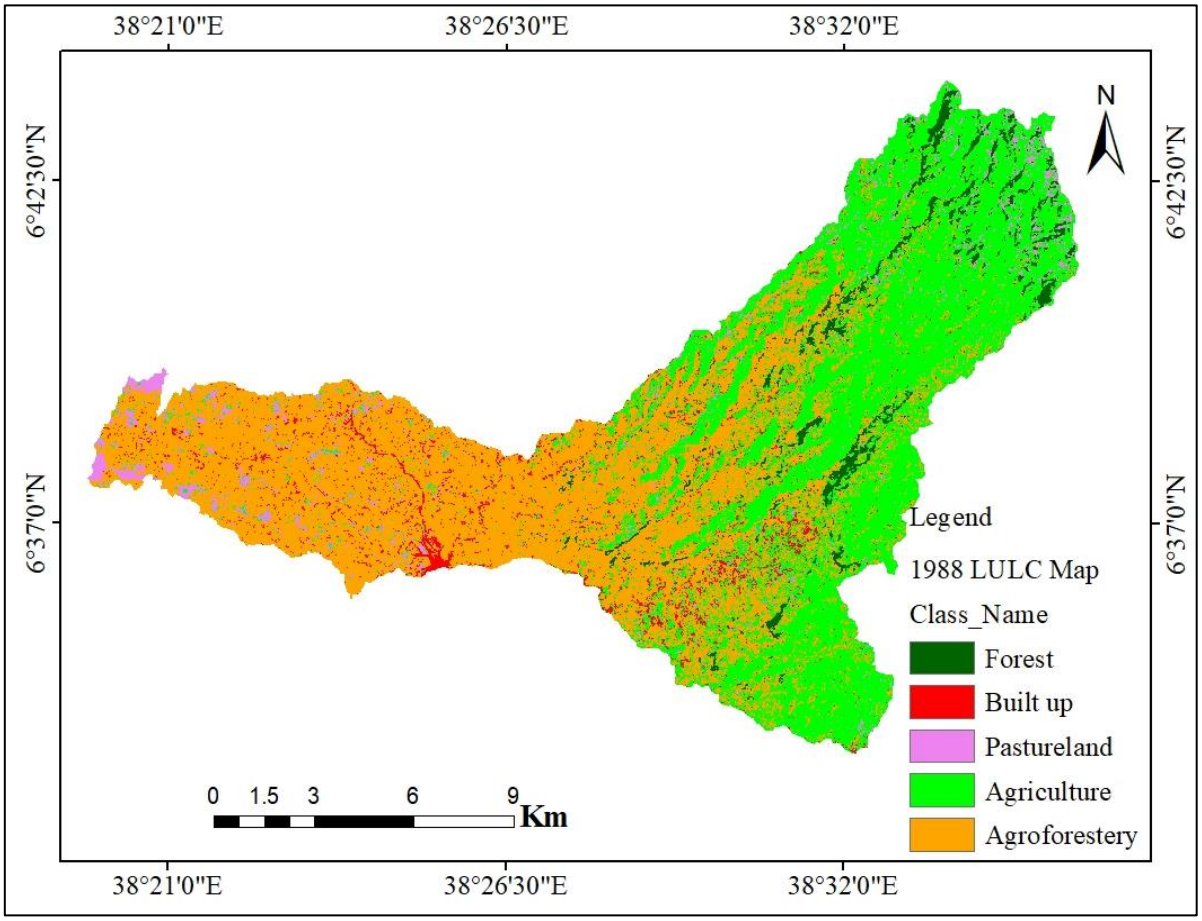

Figure 4. 1 LULC map of the study area in 1988.

After the satellite image of 1988 classified to pre-defined landuse types, the accuracy assessment of the classified image was performed by taking a total of 304 reference points from Google earth from the total collected reference, 51, 56 52, 71, and 74 points were allocated for the forest built up, pastureland, agricultural and agroforestry respectively to prepare confusion matrix. Table 4.1 indicates the detail of the confusion matrix of 1988 and the result of accuracy assessments. The overall accuracy of 87.83% and overall kappa statics of 0.846 were achieved for the 1988 LULC map, as recommended by (Badura et al., 2011), the founded accuracy assessment result showed an acceptable value.

Table 4. 1 Accuracy assessment of LULC Map of 1988

		Reference Data								
Classified Data		FR	BU	PAS	AG	AGF	Row Total	EC	UA	CK
	FR	42	2	0	2	0	46	8.70%	91.30 %	0.8955
	BU	0	46	0	0	0	46	0.00%	100.00 %	1
	PAS	0	2	45	0	1	48	6.25%	93.75 %	0.9246
	AG	4	2	1	64	3	74	13.51%	86.49 %	0.8237
	AGF	5	4	6	5	70	90	22.22%	77.78 %	0.7063
	Column Total	51	56	52	71	74	304	Diagonal total		OK
	EO	17.65 %	17.86 %	13.46 %	9.86%	5.41%		267	OA	0.8461
	PA	82.35 %	82.14 %	86.54 %	90.14 %	94.59 %			87.83 %	

Where, AG=Agricultural, AGF=Agroforestry, BU=Built up, FR=Forest, PAS=Pastureland, EO=Error of omission, EC=Error of commotion, CK=Conditional kappa statics, OA=Overall accuracy, OK=Overall kappa statics, PA=Procedural accuracy, UA=User accuracy

4.1.2 Landuse/land Cover for 1998.

The landuse land cover types of 1998 in the study area were founded as similar to 1988 but their coverage areas were changed. Agriculture and built-up areas increased as agroforestry, pastureland and forest decreased. As the result depicted in (Table 4.5) the land-use/land cove coverage proportion to the total area of the study area respecting to each landuse/land cover were, Built-up 722.01ha (3.51%), Pastureland 528.49ha (2.57%), Forest 688.47ha (3.34%), Agriculture 9266.05ha, (45.07%), and agroforestry 9359.56ha (45.51%). The founded result emphasizes there was a change of landuse/land cover between 1988 and 1998. Figure 4.2 indicates the 1998 landuse/land cover map of the study Watershed.

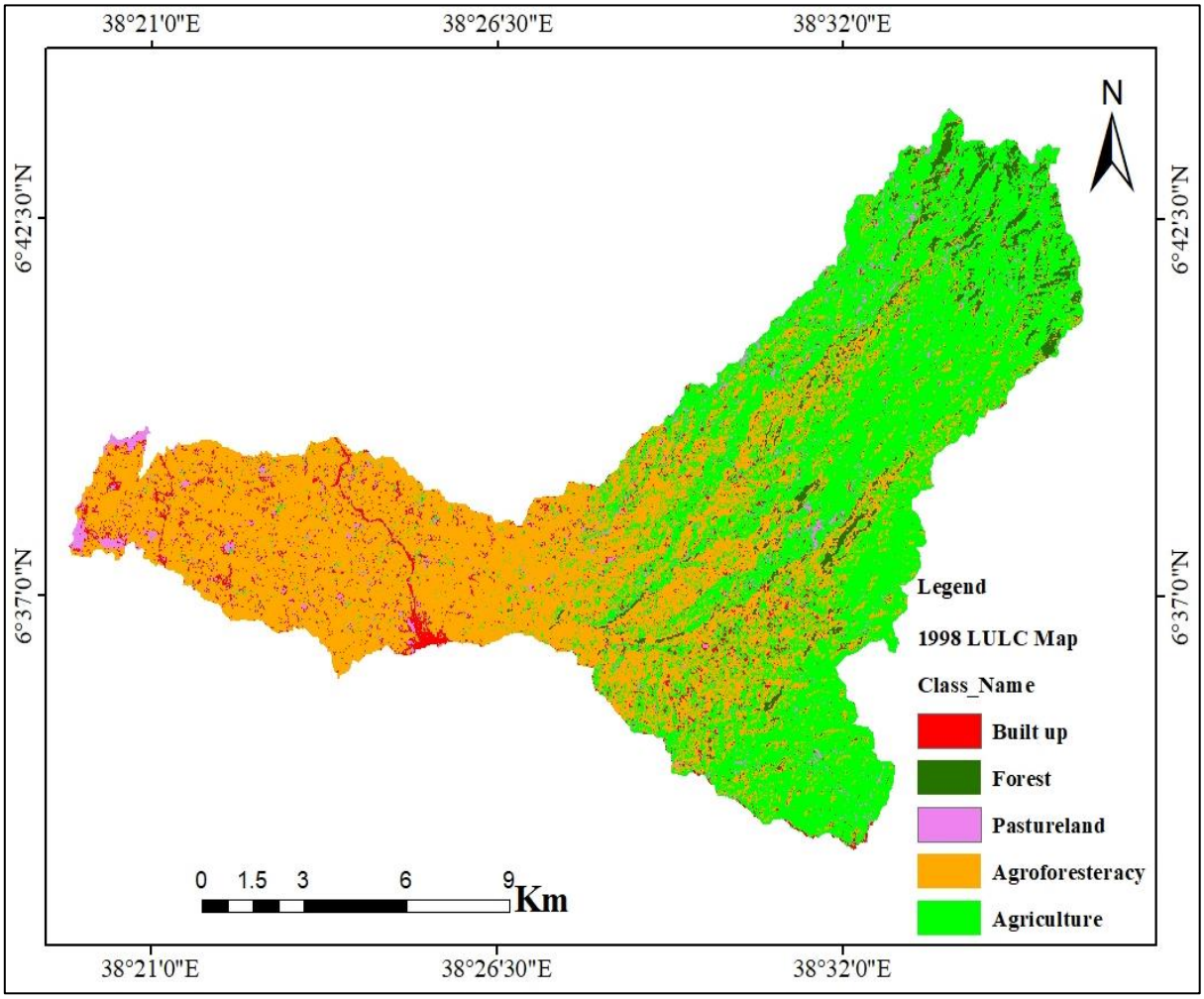

Figure 4. 2 LULC map of the study area in 1998.

For the sake of checking the accuracy of the 1998 landuse/land cover map, the accuracy assessment was performed by taking a total of 328 reference points from Google earth. The reference points taken concerning the LULC classes were, 51, 52 53, 85, and 87 for the forest, built up, pastureland, agricultural, and agroforestry. The accuracy assessment was carried out and the founded results were mentioned in the table below (Table 4.2). The accuracy assessment result shows acceptable outputs of the overall accuracy of 87.83% and overall kappa statics of 0.846. The kappa statics founded for this year is greater than 0.81 founded in the acceptable range as indicated in Table 3.2.

Table 4. 2 Accuracy assessment of LULC Map of 1998

		Reference Data								
Classified Data		BU	FR	PAS	AGF	AG	Row Total	EC	UA	CK
	BU	45	1	0	0	0	46	2.17%	97.83 %	0.97 42
	FR	1	44	0	1	2	48	8.33%	91.67 %	0.90 13
	PAS	1	1	48	1	2	53	9.43%	90.57 %	0.88 75
	AGF	2	3	2	80	10	97	17.53%	82.47 %	0.76 34
	AG	3	2	3	3	73	84	13.10%	86.90 %	0.82 18
	Column Total	52	51	53	85	87	328	Diagonal total		OK
	EO	13.46 %	13.73 %	9.43 %	5.88 %	16.09 %		290	OA	0.85 23
	PA	86.54 %	86.27 %	90.57 %	94.12 %	83.91 %			88.41 %	

Where, AG=Agricultural, AGF=Agroforestry, BU=Built up, FR=Forest, PAS=Pastureland, EO=Error of omission, EC=Error of commotion, CK=Conditional kappa statics, OA=Overall accuracy, OK=Overall kappa statics, PA=Procedural accuracy, UA=User accuracy.

4.1.3 Landuse/Land Cover for 2008.

As the classification results summarized in Table 4.5 showed, in 2008 large areas of Kola River Watershed were occupied by agricultural and agroforestry. Whereas the agriculture and built up increased the left land-use types such as agroforestry, pastureland, and forest decreased, by following the same trends to the previous change conditions. As the result indicated in the Table below the proportions of each land-use/land cover type were mentioned as follow Agriculture 9742.98ha (47.73%), Agroforestry 9173.81ha (44.61%), Built-up areas 783.71ha (3.81%), Forest 480.75ha (2.34%) and Pastureland 384.02ha (1.87%) respectively.in 2008year agricultural land accounts for the largest landuse of the study area than the former study years as Figure 4.3 indicated

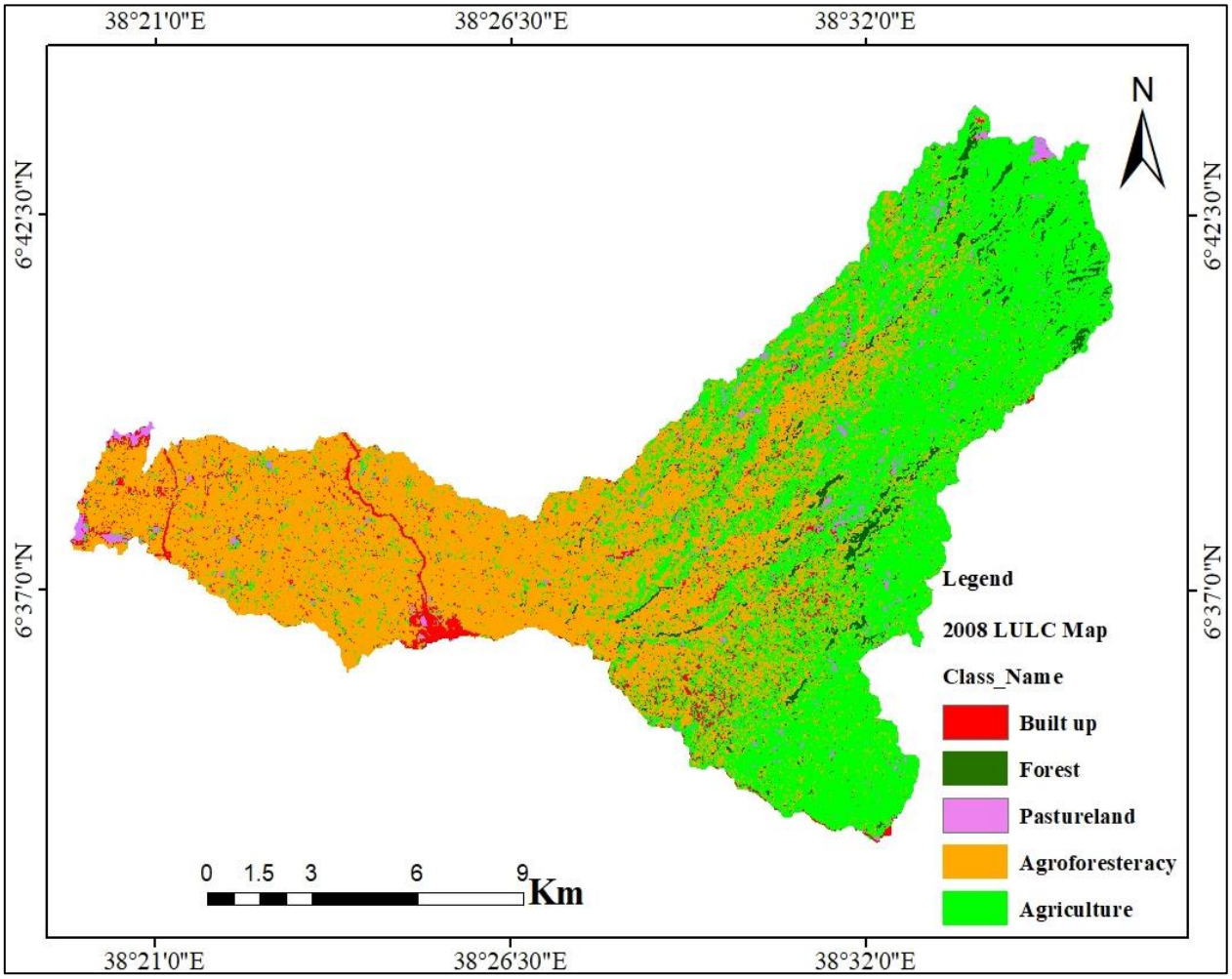

Figure 4. 3 LULC map of the study area in 2008

The Landsat ETM+ sensor was used to obtain a satellite image of 2008, then after through image processing, the 2008 landuse/land cover map was prepared by supervised image classification technique. to have confidence in the image classification the accuracy assessment was done. The obtained results of user's accuracy showed that in 2008 the maximum class accuracy was 100%, which was built up where correctly classified and the minimum was Agroforestry class with an accuracy of 77.78 % as presented in Table 4.3 below. In 2008, the class accuracies range from 73.3% to 90%. The overall accuracy and overall kappa statics of the 2008 classified image were 89.15% and 0.86 respectively, the founded value indicates strong agreements with the recommended value by (Badura et al.,2011) so the classification results were acceptable to use during the investigation of the impact of LULCC on the hydrology of the study watershed.

Table 4. 3 Accuracy assessment of LULC Map of 2008.

	Reference Data							EC	UA	CK
Classified Data		PAS	FR	BU	AGF	AG	Row Total			
	PAS	40	1	0	0	0	41	2.44%	97.56 %	0.97 13
	FR	1	44	1	0	1	47	6.38%	93.62 %	0.92 42
	BU	2	0	49	0	1	52	5.77%	94.23 %	0.93 15
	AGF	3	6	2	107	7	125	14.40%	85.60 %	0.78 83
	AG	5	3	2	2	64	76	15.79%	84.21 %	0.79 91
	Column Total	51	54	54	109	73	341	Diagonal total		OK
	EO	21.57 %	18.52 %	9.26 %	1.83 %	12.33 %		313	OA	0.85 93
	PA	78.43 %	81.48 %	90.74 %	98.17 %	87.67 %			89.15 %	

Where, AG=Agricultural, AGF=Agroforestry, BU=Built up, FR=Forest, PAS=Pastureland, EO=Error of omission, EC=Error of commission, CK=Conditional kappa statics, OA=Overall accuracy, OK=Overall kappa statics, PA=Procedural accuracy, UA=User accuracy

4.1.4 Landuse/Land cover for 2018.

For image classification and preparing land-use/land cover map of 2018, Landsat 8 Operational Land Imager (OLI) and Thermal Infrared Sensor (TIRS) are available on the board of Landsat 8. These two sensors provide global landmass at a spatial resolution of 30m (visible, NIR, SWIR); 100m (thermal), and15m (panchromatic) (Vanhellemont, 2015).in this study Landsat 8/OLI sensor was used to download the satellite image of 2018 from USGS. The classification landuse/land cover types of 2018 and their respective areas were listed in Table (4.5). Though as the achieved result of the 2018 landuse/land cover map, indicated that agriculture was the largest share of the landuse/ land cover of the study area, which occupied an area of 11007.11ha (53.52%) followed by agroforestry 8049 ha (39.14 %), Built-up areas account for 839.01ha (4.08%), Forest 437.49 ha (2.13 %), and Pastureland 232.28 ha (1.13 %)), from the total extent

of the study area, respectively. As figure 4.4 indicates the agricultural lands showed a higher expiation rate while pasture land and forest decreased.

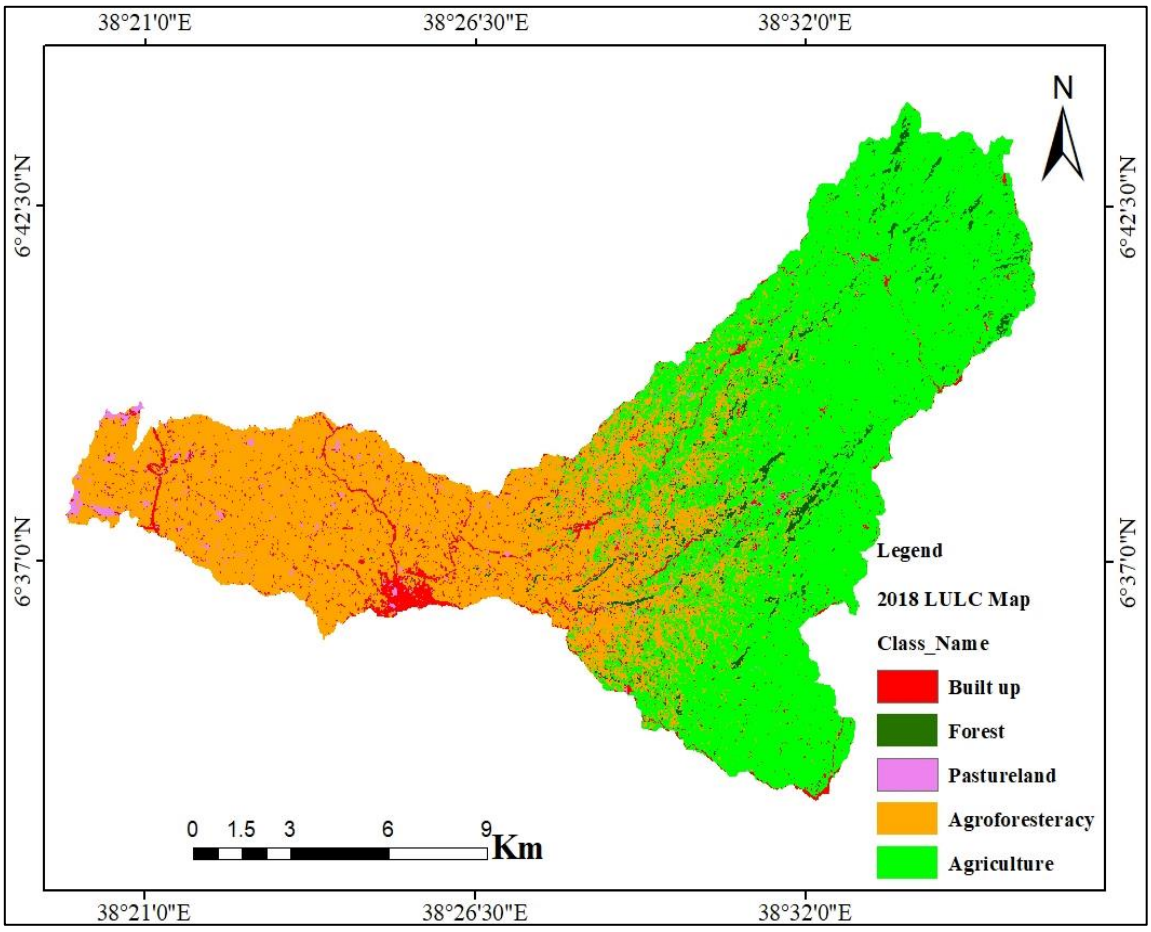

Figure 4. 4 LULC map of the study area in 2018

After the classification of satellite images of 2018, the accuracy assessment was done to check where the classified map was accurately classified or not. the accuracy of the 2018 classified map was done by taking a total of 364 reference points from Google earth. The results of user's accuracy in this study showed that in 2018 the maximum class accuracy was achieved for forest while, the minimum was obtained for agroforestry class as the result presented in table 4.4 below indicated. The overall accuracy and kappa statics of the 2018 landuse/land cover was 91.76, 0.893 respectively. The founded result indicated that the classification was almost perfect according to (Badura et al., 2011) kappa statistics recommended range.

Table 4. 4 Accuracy assessment of LULC Map of 2018

		Reference Data								
		AGF	PAS	FR	BU	AG	Row Total	EC	UA	CK
Classified Data	AGF	110	5	4	1	1	121	9.09%	90.91%	0.8692
	PAS	0	41	1	1	0	43	4.65%	95.35%	0.9454
	FR	0	2	44	0	0	46	4.35%	95.65%	0.9494
	BU	0	2	0	51	2	55	7.27%	92.73%	0.9138
	AGF	1	4	2	4	88	99	11.11%	88.89%	0.8519
	Column Total	111	54	51	57	91	364	Diagonal total		OK
	EO	0.90%	24.07%	13.73%	10.53%	3.30%		334	OA	0.8932
	PA	99.10%	75.93%	86.27%	89.47%	96.70%			91.76%	

Where, AG=Agricultural, AGF=Agroforestry, BU=Built up, FR=Forest, PAS=Pastureland, EO=Error of omission, EC=Error of commission, CK=Conditional kappa statics, OA=Overall accuracy, OK=Overall kappa statics, PA=Procedural accuracy, UA=User accuracy.

Table 4. 5 Areal coverage of LULC of the study area 1988_2018

	1988LULC		1998LULC		2008LULC		2018LULC	
Class name	ha	%	ha	%	ha	%	ha	%
Agriculture	8828.87	42.93	9269.05	45.07	9742.98	47.38	11007.11	53.52
Agroforestry	9556.68	46.47	9359.56	45.51	9173.81	44.61	8049.29	39.14
Built up	677.15	3.29	722.01	3.51	783.71	3.81	839.10	4.08
Forest	739.74	3.60	686.47	3.34	480.75	2.34	437.49	2.13
Pastureland	762.82	3.71	528.49	2.57	384.02	1.87	232.28	1.13
Total	20565	100	20565	100	20565	100	20565	100

Figure 4.5 shows the summary of landuse/land cover types of the Kola watershed from 1988 to 2018.

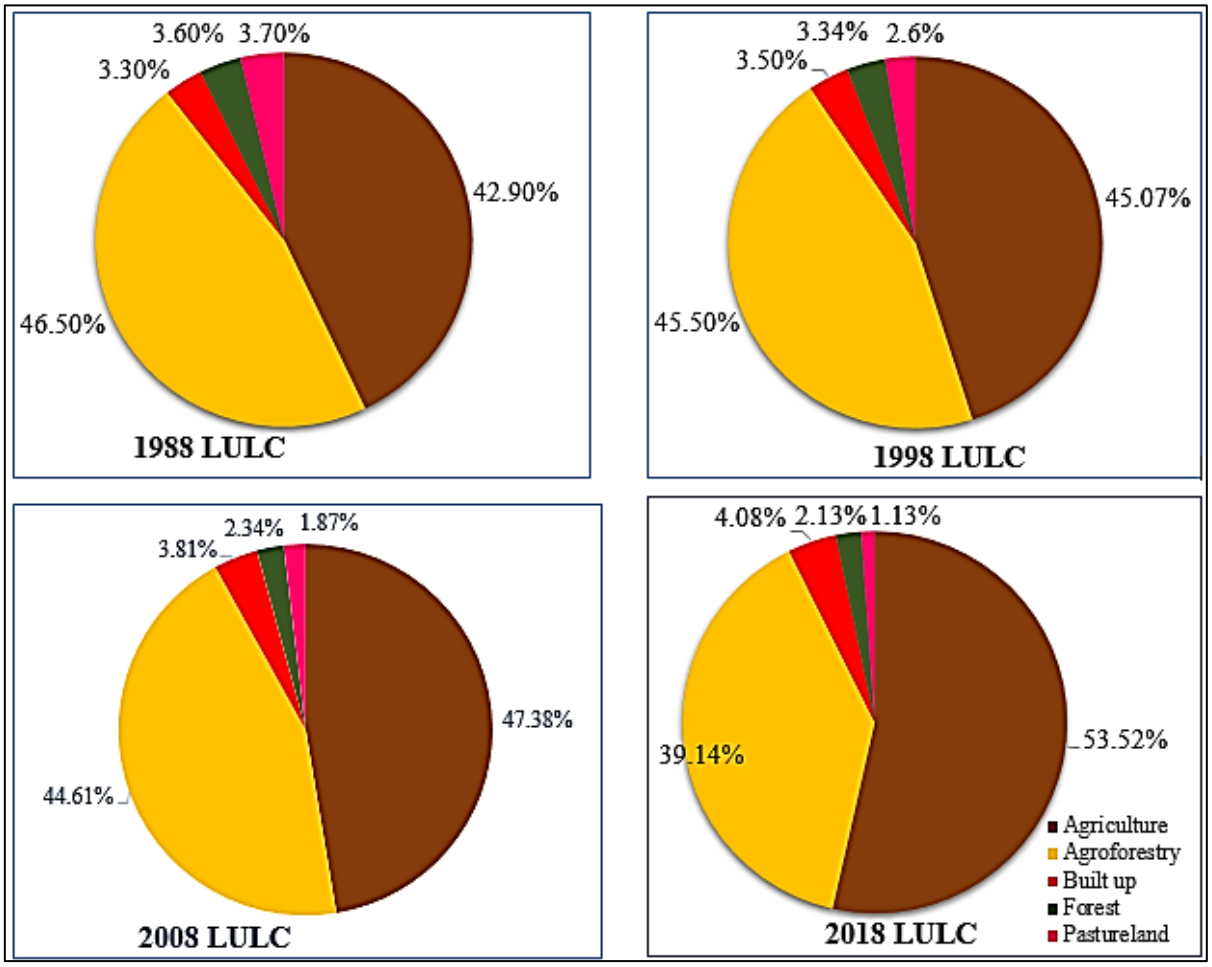

Figure 4. 5 Summary of LULC change in the Kola watershed (1988_2018)

The use of remote sensing products relating to changes for scientific, management, or policy support activities all requires quantitative accuracy statements to increase the confidence in the information generated and in any subsequent reporting or interpretations made. A variety of probability sampling designs apply to accuracy assessment and training area estimation, with the most commonly used designs being simply random, stratified random, and systematic (Stehman, 2009).

In this study stratified random sampling was used to satisfy the accuracy assessment and area of interest estimation. The sampling scheme has been fixed, the exact number of samples to be taken decided. As a rule of thumb recommends at least 50 samples per class. If the area exceeds 500 km^2or the number of categories is more than 12, then at least 75–100 samples should be taken per class (Congalton, 1988a).based on the above criteria since this study area was less than 500m^2 and the number of the class was five depending on the rule of thumb 50 and above

sample size were taken, the allocation of the sample was depended on the size of landuse classes. The accuracy assessment of the classified data of 1988, 1998, 2008, and 2018 confirmed that the results are reasonable and satisfactory for any applications. As specified by the USGS classification scheme, the minimum acceptable standard for the overall accuracy is ≥ 85%. The accuracy computed in this study satisfies the minimum requirement for all classified images so it is acceptable to use the prepared landuse/land cover maps for the investigation of the effect of landuse/land cover change on the hydrological response of the study area.

4.1.5. Analysis of landuse/land cover change.

In the conversion matrix (Table 4.6), the values of the row show the initial year and the column values represent the final year landuse/land cover. As the achieved result indicated in from a total of 11005.84ha agricultural in 2018, 7865.51ha remained as an agricultural 2213.13ha agroforestry; 221.81ha buildup, 370.23ha forest, and 335.16ha from pastureland were gained respectively. In the same way, as seen clearly in the matrix, from the total of 8049.05ha Built up in 2018, 137.81ha remain as built up, 423.27ha agroforestry, 229.28ha agricultural, 47.39, ha pastureland and 1.02ha forest were contributed to built-up. In contrast to the above the other landuse land covers, such as pastureland, forest, and agroforestry were decreased. The post-classification conversion matrix of 1988_1998, 1998_2008, 2008_2018, and 1988_2018, were computed and their consecutive values were mentioned in (Appendix Table 1).

Table 4. 6 Transition Matrix of Landuse land cover between 1988and 2018.

		2018 LULC					
		Agricultural	Agroforestry	Built-up	Forest	Pastureland	Grand Total
1988 LULC	Agriculture	**7865.51**	633.47	229.28	42.99	57.34	8828.59
	Agroforestry	2213.13	**6760.11**	423.27	98.16	60.66	9555.32
	Built up	221.81	303.02	**137.81**	0.31	14.23	677.18
	Forest	370.23	76.51	1.02	**291.97**	0	739.74
	Pastureland	335.16	275.94	47.39	4.05	**99.98**	762.53
	Grand Total	11005.84	8049.05	838.78	437.48	232.21	20563.35
Change difference		3140.33	1288.94	700.96	145.51	132.23	
Net change		2177.25	-1506.27	161.6	-302.26	-530.32	

i Temporary landuse/land cover change.

The temporary change of the landuse/land cover of the study area was analyzed between the consecutive study period, as well as the first and last year respectively, and the results were presented in Table 4.7. As the output obtained indicated, pastureland, forest, and agroforestry were decreased by, (69.55%, 40.86%, and 15.77) while, built-up and agricultural increased by (23.92%, 24.67%) respectively from 1988 to 2018 in the study area

Table 4. 7 Landuse land cover change in the study area.

	1988_1998LULC		1998_2008LULC		2008_2018LULC		1988_2018LULC	
Class name	ha	%	ha	%	ha	%	ha	%
Agriculture	+440.18	+4.99	+473.93	+5.11	+1264.13	+12.97	+2178.24	+24.67
Agroforestry	-197.12	-2.06	-185.75	-1.98	-1124.52	-12.26	-1507.39	-15.77
Built up	+44.86	+6.62	+61.70	+8.54	+55.39	+7.07	+161.95	+23.92
Forest	-53.27	-7.20	-205.72	-29.97	-43.26	-9.00	-302.25	-40.86
Pastureland	-234.32	-30.72	-144.47	-27.34	-151.74	-39.51	-530.53	-69.55

The minus sign indicates the decreases of the LULC types and the positive sign shows increases in LULC in consecutive years.

Loss, gain, and net change of the landuse/land covers in each decade and three decades (between the first and last year), were analyzed. The result shows that Agriculture and built-up were gained, while agroforestry, forest, and pastureland were lost throughout the investigation period in the study area.

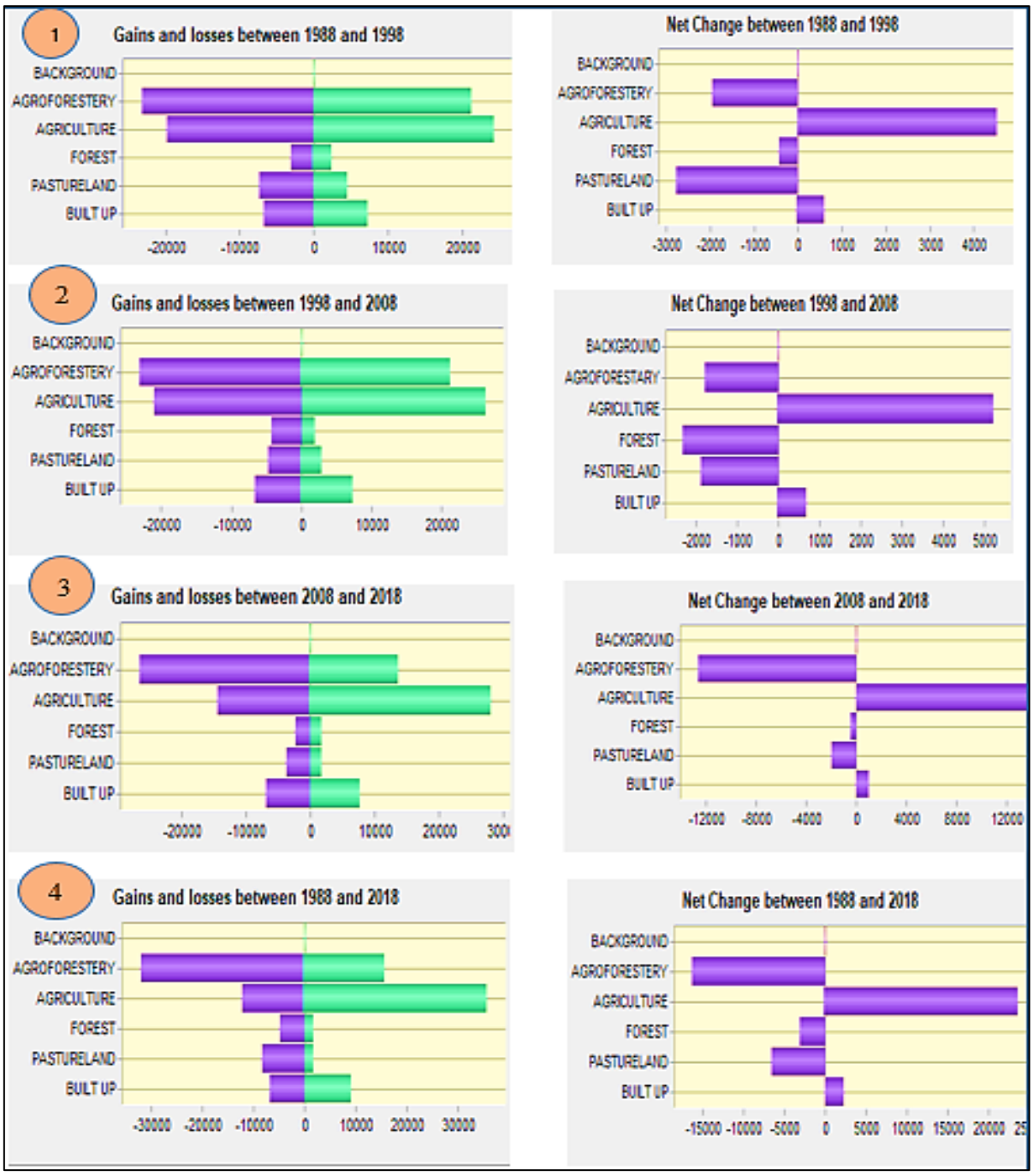

Figure 4. 6 Gains and losses, and net change for 1988-1998, 1998-2008, 2008-2018, and 1988 –2018.

ii Rate of Landuse/Land Cover Change

The annual rate of change for individual landuse classes was calculated for 1988-1998, 1998-2008, 2008-2018 (10 years), and 1988-2018 (30 years) respectively. Analysis of the annual LULC change revealed that agriculture and built-up experienced an increasing trend whereas agroforestry, forest, and pastureland show a continuous decline throughout the entire study period (Table 4.8).

Table 4. 8 Annual changes between each consecutive and the begging and last year.

	1988 -1998LULC		1998-2008LULC		2008 -2018LULC		1988 -2018LULC	
Class name	ha	%	ha	%	ha	%	ha	%
Agriculture	+44.02	+0.50	+47.39	+0.51	+126.41	+1.30	+72.61	+0.82
Agroforestry	-19.71	-0.21	-18.57	-0.20	-112.45	-1.23	-50.25	-0.53
Built up	+4.49	+0.66	+6.17	+0.85	+5.54	+0.71	+5.40	+0.80
Forest	-5.33	-0.72	-20.57	-3.00	-4.33	-0.90	-10.07	-1.36
Pastureland	-23.43	-3.07	-14.45	-2.73	-15.17	-3.95	-17.68	-2.32

The minus sign indicates the annual decreases of the LULC types and the positive sign shows annual increases of LULC in consecutive years.

After the classification of satellite data, and checking the reliability of the result depends on the overall accuracies of the classified images landuse/land cover change rate analysis was conducted. The results insights the landscape of the study area has experienced significant LULC change over the last 30 years (1988-2018). The LULC changes analysis results of the LULC category achieved through classification are presented in Table 4.7, which shows that there is a change in landuse/land cover over time. The LULC change of the area showed that the expansion of agriculture, and built-up, while the decrease in agroforestry, forest, and pastureland, was observed. The reduction of different LULC types happens as a result of agricultural expansion, fuelwood, and charcoal production. The study conducted near the kola watershed by Mamuye et al. (2020) from 1985 to 2018 indicated the same trends of LULCC, with different magnitude.

4.2 Predicting of the Future LULCC with IDRISI (CA- Markov Method)

The Markov chain and cellular automata models are used to predict the future landuse/land cover of the study area. Before, the model used to predict the future LULC the model performance was checked by predicting the 2018 image using 1988 1998, and 2008LULC images. The transition probabilities statistics were generated using classified LULC images of 1988 as the first (earlier) image and LULC image of 1998 as later (second) image by using Markov transition estimator to predict LULC of 2018. The number of time intervals (periods) between the first and second images is 10 years and the first and the third image is 20 years. The numbers of time steps (iterations) to project forward from the second image and third image are 20 years, and 10 years respectively to predict LULC in 2018. The table below indicates the actual classified and projected landuse/land cover of 2018.

Table 4. 9 Actual and predicted LULC (2018)

	Predicted 2018LULC		
LULC types	Classified 2018 LULC(ha)	predicted based on1988and1998 LULC(ha)	predicted based on1988and 2008 LULC(ha)
Agriculture	11007.11	10997.01	9958.41
Agroforestry	8049.29	8947.17	9103.5
Built up	839.1	869.46	905.67
Forest	437.49	472.86	406.17
Pastureland	232.28	271.53	405.54

I Validation of CA Markov model

For the model validation, the simulated LULC of 2018 by CA-Markov was compared to the actual classified LULC map of 2018. The model evaluation performed investigating the correlation of the actual classified map and a projected map of 2018 as indicated in the figure below. Figure 4.7 indicated that the actual and classified maps have high relationships.

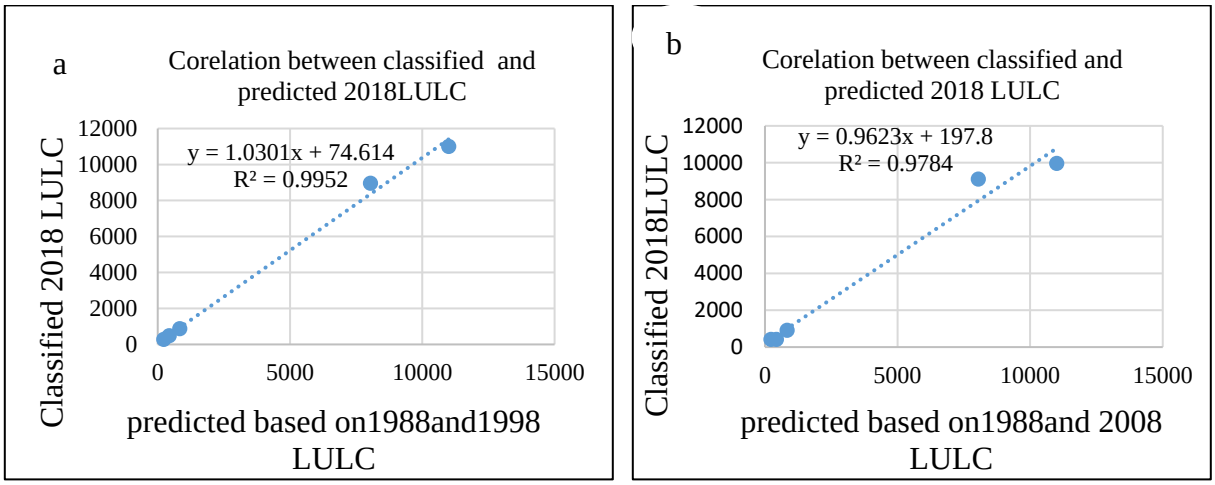

Figure 4. 7 Relationships between area statistics of predicted LULC of 2018 using 1988 and 1998LULC image (a), 1988 and 2008 (b).

Analysis of the agreement/disagreement components of the simulated 2018 image and the actual classified image was given the following results (Table 4.10), 0.0066 (error due to quantity/Disagree Quantity) and 0.0801 (error due to allocation/Disagree Grid cell). Therefore, the data label indicated that the main disagreement between the two maps was due to an allocation error rather than quantity error, of the simulated and actual image.

Table 4. 10 Results of validation analysis of 2018 simulated and actual classified image.

Agreement/disagreement	Value
Agreement Chance	0.1667
Agreement Quantity	0.3093
Agreement Grid cell	0.4374
Disagree Grid cell	0.0801
Disagree Quantity	0.0066

Validations through different statistics have been also done. All the Kappa statistics such as Kno this kappa index stands for standard kappa index for agreement (89.6%), Klocation (84.53%), KlocationStrata (84.53%), and Kstandard (83.46%) were also computed. The values of each kappa statics were above 80%, which indicates the better performance of the model in simulating future LULC (Singh., 2015).

Table 4. 11 Results of validation kappa index for 2018 simulated and actual classified image

Kappa index	value	Value (%)
Kno	0.896	89.6
Klocation	0.8453	84.53
KlocationStrata	0.8453	84.53
Kstandard	0.8346	83.46

II future landuse/land cover analysis

To predict the next 30 years' land cover (2048) using a landuse map, the 1988-2018 transition area matrix, and the 2018 transition potential map were used. The CA-Markov model integrates both cellular automata (CA) and Markov models. The prediction of the land cover for 2048 was performed using the key inputs which are a land cover map for the years 1988 and 2018 and the transition areas matrix (table 4.11).

Table 4. 12 Comparison of actual (2018) and projected LULC (2048)

					Temporary Change		Annual change	
	2018		2048		2018_2048LULC		2018_2048LULC	
Class name	ha	%	ha	%	ha	%	ha	%
Agriculture	11007	53.52	12448	60.53	1441.01	13.09	48.03	0.44
Agroforestry	8049.3	39.1	6749.2	32.82	-1300.13	-16.15	-43.34	-0.54
Built up	839.10	4.08	900.82	4.38	61.72	7.36	2.06	0.25
Forest	437.49	2.13	296.54	1.44	-140.95	-32.22	-4.70	-1.07
Pastureland	232.28	1.13	170.23	0.83	-62.06	-26.72	-2.07	-0.89
Total	**20565**	**100**	**20565**	**100**				

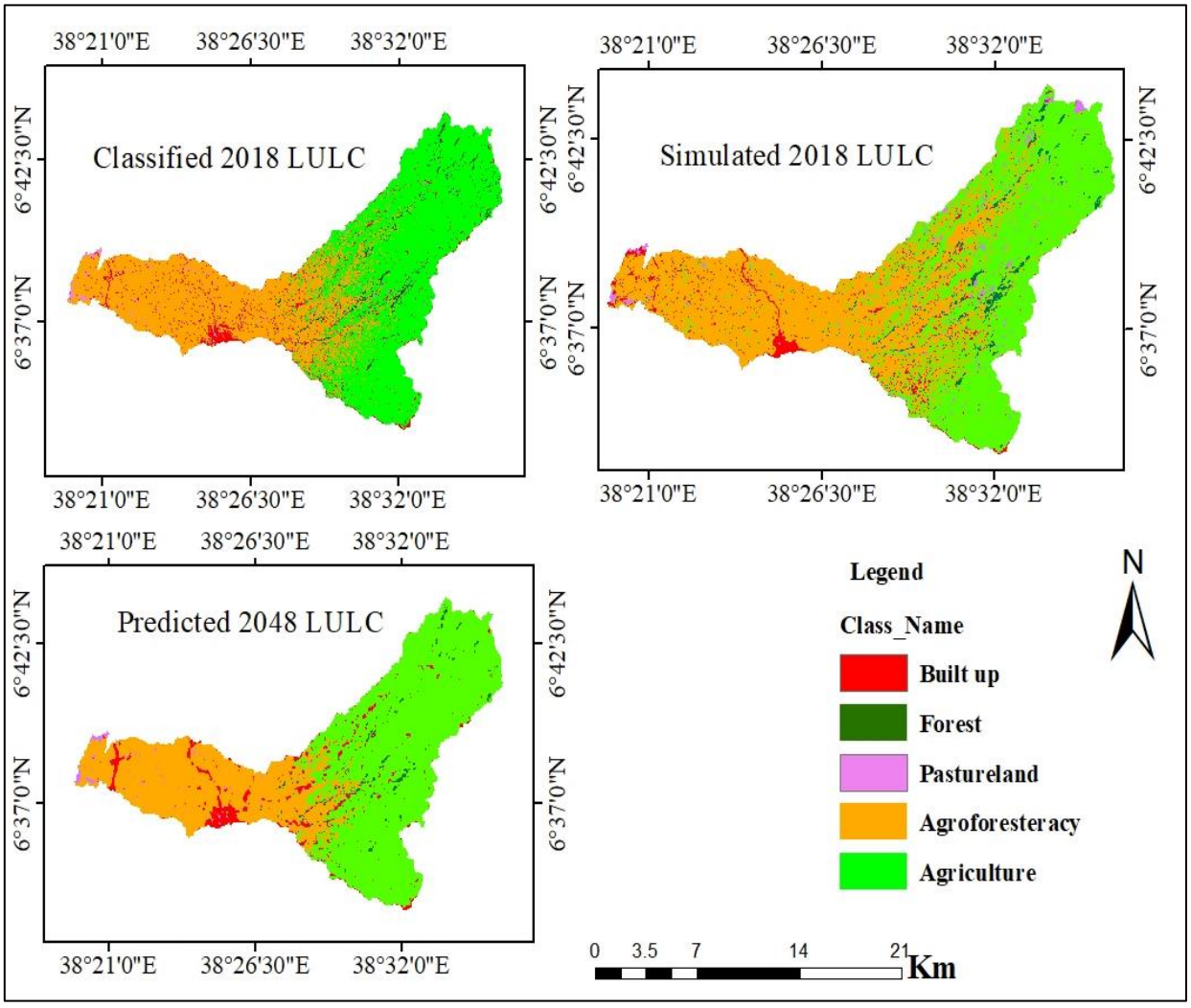

Figure 4. 8 Actual, simulated, and projected map of the study area

After the 2048 LULC map was predicted by using the LULC map of 2018, the result shows land-use change was likely to continue in the future, however, if the green legacy launched by the country in 2019 GC is cautioned and incorporates all the watershed the changes of forest will be not continued as it predicted. The result of this study also tells the same history, meaning that the past trend continued. Agricultural in the study area is predicted to notably increased in 2048 with nearly 13.09 %, followed by Built-up, which 7.36 %. On the contrary, a decreasing trend can be observed for, Agroforestry by16.15% pastureland at 26.72%, and forest at 32.22% (Table 4.12). The findings of this study suggest that the continued expansion of agricultural and built-up were continued at a higher rate as the cost of this other landuse land cover types such forest pastureland and agroforestry were shown higher decline rate. On the other hand, the

reduction of forest agroforestry and pastureland have great impacts on the hydrology of the watershed, because of reduction of an infiltration rate increase of surface runoff and evapotranspiration, so the area needs to be controlled and well managed, and land-use plan should be developed in harmonization way with natural resources conservation.

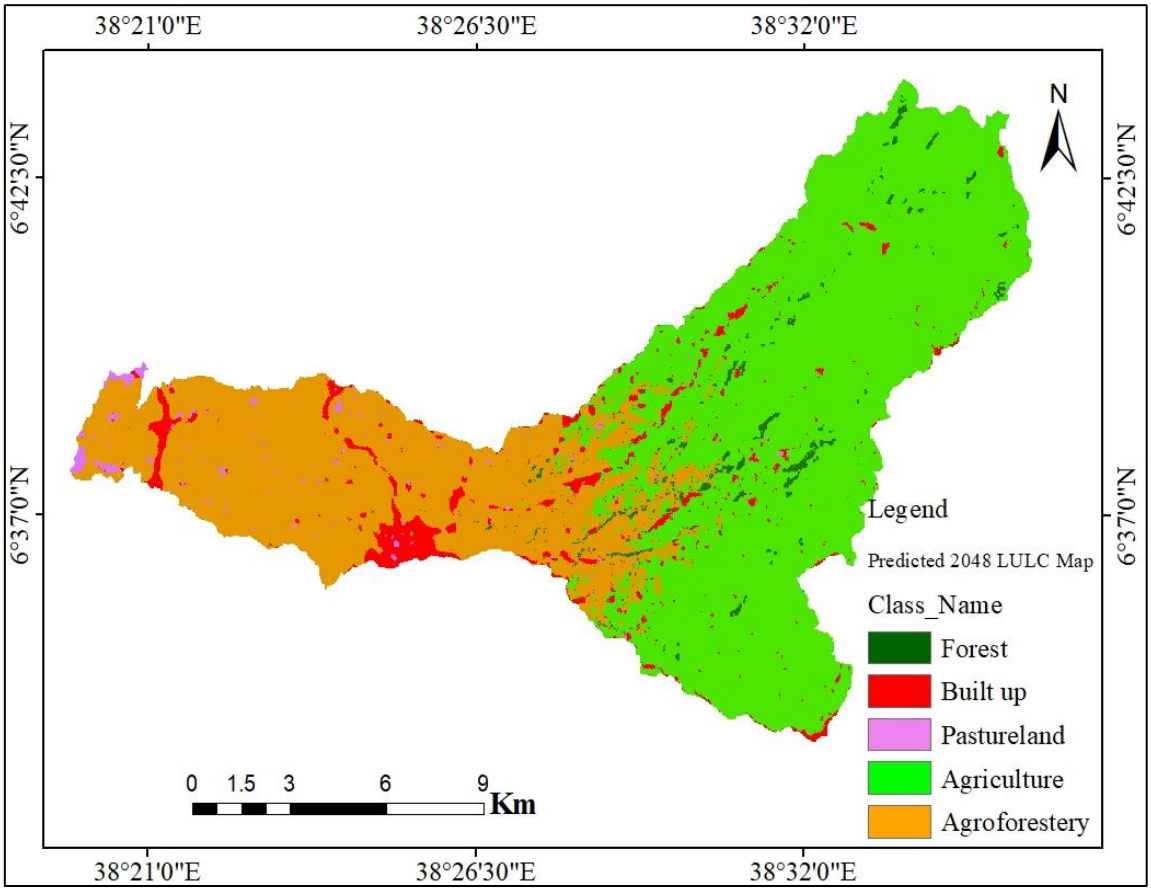

Figure 4. 9 Predicted 2048 LULC map of kola watershed.

4.3 Modeling of the hydrological response of kola River watershed

4.3.1 SWAT model sensitivity analysis

Modeling of the impact of landuse/land cover change on the hydrological response of the study watershed was conducted by using the soil water assessment tools (SWAT) model. Sensitivity analysis was carried out using 13 flow parameters (Appendix 7) and identifies the 8 most sensitive parameters controlling the output variable (Table 4.12). The three most sensitive parameters identified during sensitivity are saturated hydraulic conductivity (R_SOL_K), soil conservation curve number (R_CN2), and Average slope steepness (R_HRU_SLP). Using the above parameters, flow simulation was performed for fifteen years of recording periods starting

from 1990 to 2005.The result of sensitivity analysis of hydrologic parameters, used for calibration of the model. The sensitive parameters are identified based on the value of P-value and t-stat. the P-value having less than 0.05 is the more sensitive model parameter the analysis was performed at the outlet of the catchment for calibration and validation.

Table 4. 13 Sensitivity parameters

Parameter Name	Fitted Value	Min_value	Max_value	Rank
1:R_CN2.mgt	-0.0968	-0.16	0.16	2
2:V_ALPHA_BF.gw	0.1225	0	0.2	7
3:V_GW_DELAY.gw	54.8125	30	55	6
4:R_SOL_AWC (...).sol	0.106175	-0.09	0.5	8
5:R_OV_N.hru	0.008355	-0.01533	0.01533	4
6:R_SOL_K (...).sol	24.35	22	210	1
7:V_CH_K2.rte	53.125	40	70	5
8:R_HRU_SLP.hru	4.585	1	7	3

4.3.2 Calibration and validation

The model calibration was conducted after the sensitive parameters were identified. The monthly flow of the Kola watershed from 1988 to 2005 was used for calibration purposes, from these observed flows the two years (1988 and1989) data were used as a model warm-up purpose. Then by using the sensitive parameter the calibration and validation were done for (1990_2005) and (2006_2013) monthly flows respectively. Graphical comparison of the observed and simulated flow for the calibration (1990_2005) and validation (2006_2013) periods are shown in Figures 4.10a and 4.10b. The results showed simulation has a good relation with the observed flow. Statistical performance evaluation, such as coefficient of determination (R^2), Nash and Sutcliffe efficiency (ENS), and percent of bias (PBIAS) are also determined (Table 13), and The following results were obtained. R^2 (0.87 for calibration and 0.85 for validation) and ENS (0.77, 0.74 for calibration and validation respectively) in addition to these percent of bias 8.5and10.5 were obtained during calibration and validation respectively values show very good consistency between the observed and simulated data. In general, the performance evaluation result obtained during the calibration and validation periods indicated

a very good performance, since the determined value was greater than the recommended Values of $R^2 > 0.6$, NSE > 0.5, and < ±25 for the calibration of the monthly simulated streamflow are usually considered as adequate for an acceptable calibration (Santhi, 2001).

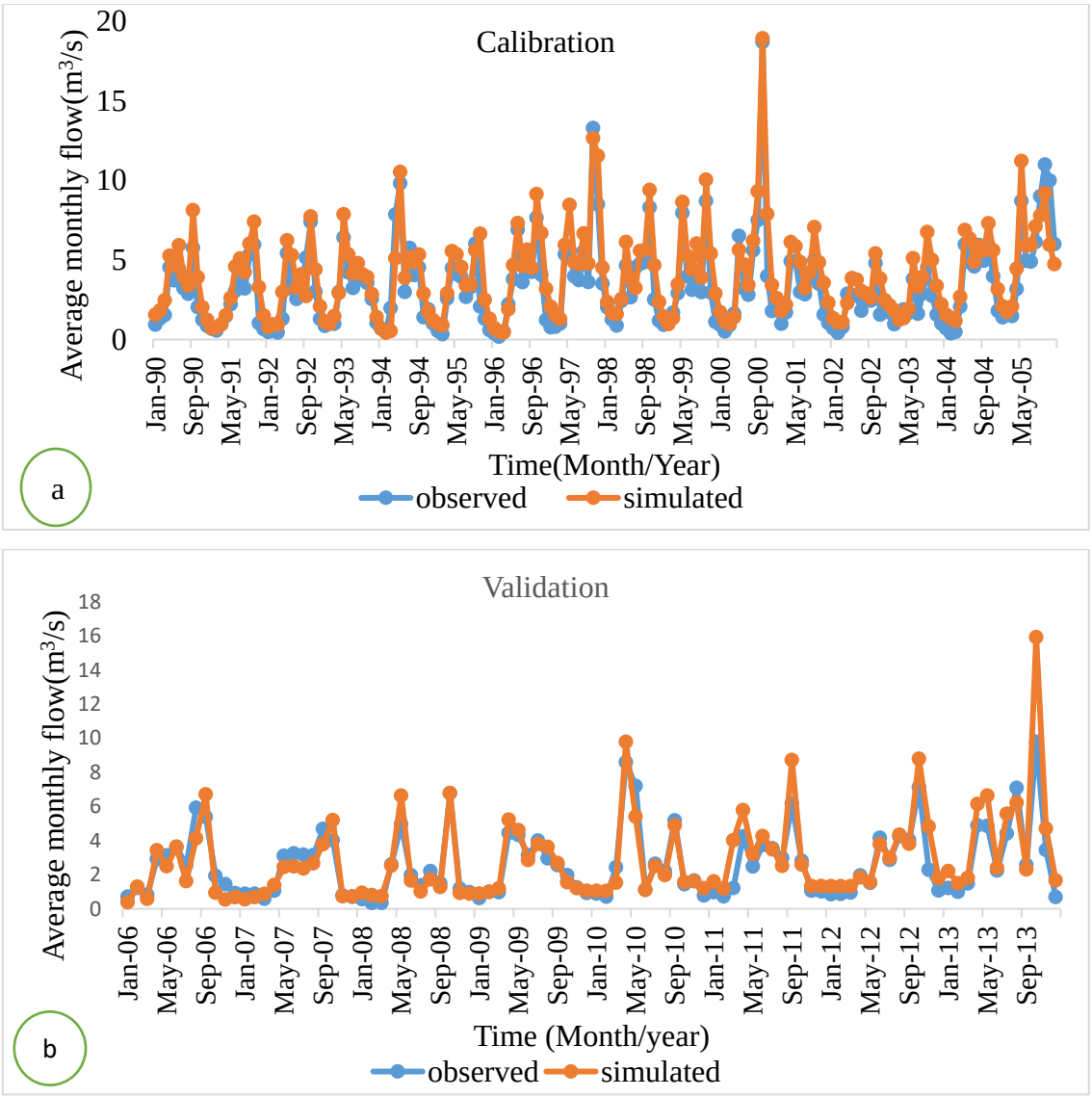

Figure 4. 10 Monthly calibrations (a) and validation (b) of the SWAT model.

The figure below indicates the scatter plot of the simulated and observed flow of the study area for calibration and validation as the result shows the simulated and observed data have good distributions this indicates the observed and simulated value have a strong correlation for calibration and validation respectively.

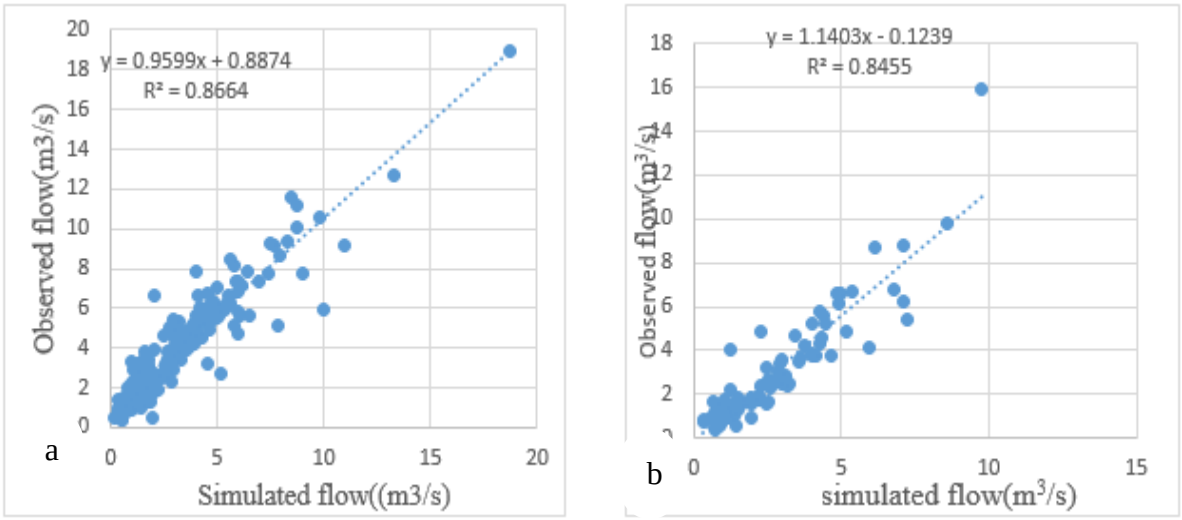

Figure 4. 11 Scatter plot of the observed and simulated monthly average flow (m3 /s) in the calibration (a) and validation (b) period.

The table below shows the summary of the SWAT model performance evaluations for calibration and validation.

Table 4. 14 Model performance statistics for the calibration and validation period.

period	Evaluation statistics		
	R^2	NSE	PBAIS
Calibration	0.87	0.77	8.5
Validation	0.85	0.74	10.5

4.3.3 Evaluation the effect of landuse/land Cover Change on hydrological components

After calibration for (1990_2005) and validation by using observed flow data of (2006_2013), the SWAT model was run by using 1988, 1998, 2008, and 2018 classified landuse/land covers independently and taking the other required data as constant. The investigation of the impact of landuse/land cover change on the hydrological components was also extended to future assessments by using the predicted landuse land cover of 2048. The result found during the investigation of the impacts of LULC changes on hydrological response in the kola River Watershed were summarized in Table 4.15. Corresponding to the increase of Agricultural, and built-up areas and the reduction of forest, pastureland, and agroforestry. Mean monthly value, and their spatial distribution of the hydrological components, such as streamflow (Q), surface

runoff (SURQ), Lateral flow (LATQ), water yield (WY), evapotranspiration (ET), and groundwater shallow aquifer (GW_AQ) were shown in the figure below (Figure 4.12). The graphs were drawn by mean monthly values of hydrological components simulated respected to the landuse/land cover map of 1988,1998,2008,2018 and2048 respectively. As indicated in the figures below over a long time mean monthly changes of the hydrological components was observed. So the obtained results during investigation imply the hydrological response of the study Watershed affected either positively or negatively depending on their response to the landuse/land cover changes that occurred over the investigation periods.

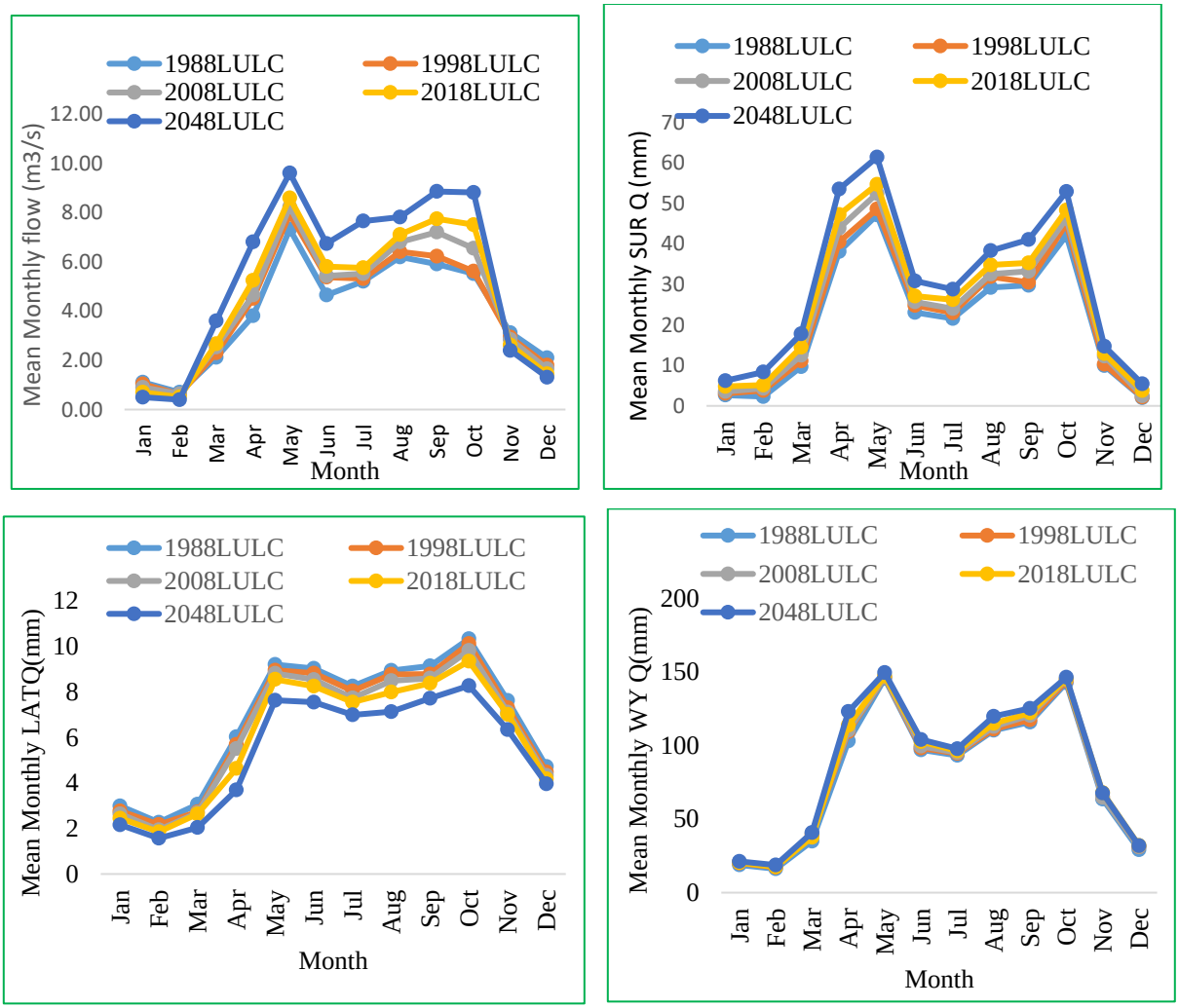

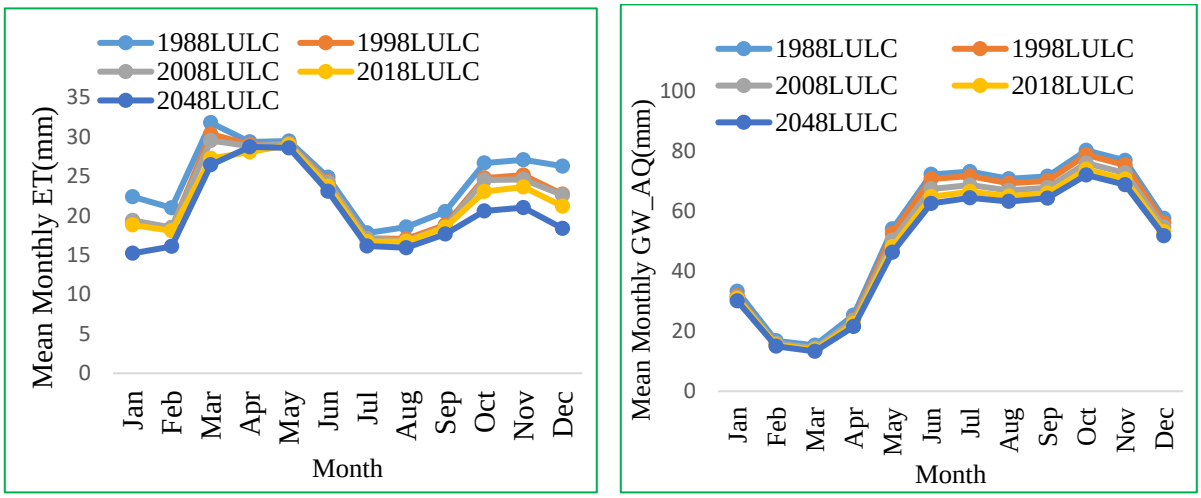

Figure 4. 12 Monthly average (1988-2048) streamflow, surface runoff, lateral flow, water yield, and ET response to the LULC changes in the Kola watershed.

The effect of landuse/land cover change on hydrological components was investigated at different seasons in this study area. In our country (Ethiopia) the season classification is based on rainfall patterns. According to NMSA, (1996), there are three major seasons, Kiremt (main rainy season from June to September), Belg (small rainy season from February to May), and Bega (dry season from October to January). However, this is not true for overall the country. The study area has different spatial and temporal characteristics with bimodal rainfall patterns have four seasons (Belihu et al., 2017). The first rainy season was (March-May) throughout the season mean monthly of discharge 1988 to 2048 periods (6.65m3 /s, 7.07m3 /s, 7.57m3 /s, 8.36m3 /s and 10.79m3 /s in 1988, 1998, 2008, 2018, and 2048, respectively), in addition to the first rainy season, the second rainy season covered (August_October) (6.21m3 /s, 6.59m3 /s, 7.02m3 /s, 7.69m3 /s and 9.85 m3 /s in 1988, 1998, 2008, 2018 and 2048, respectively), the short rainy season (June _July)(4.91m3 /s, 5.11m3 /s, 5.89m3 /s, 6.75m3 /s and 1.66m3 /s) on the other hand, the continuous landuse land cover change in the study area causes' the reduction of dry season flow (November _February) (1.94m3 /s, 1.81m3 /s, 1.68m3 /s, 1.51m3 /s and 1.22m3 /s in 1988, 1998, 2008, 2018 and 2048 period, respectively). The values of other hydrological components such as SURQ, LATQ, WY, and ET at different study years were presented in Table 4.15

Table 4. 15 Seasonal variability Hydrological component due to LULCC 1988_2048

Year	Seasons	Stream flow(m3/s)	SURQ(mm)	LATQ(mm)	WY(mm)	ET(mm)
1988	First rainy season	6.65	42.21	9.74	124.16	29.4
	Second rainy season	6.21	33.68	9.12	122.86	22.57
	Short rainy season	4.91	22.81	8.60	95.08	21.37
	Dry season	1.94	5.81	4.45	32.52	24.9
1998	First rainy season	7.07	44.52	9.45	127.72	29.09
	Second rainy season	6.59	35.79	8.885	124.07	20.2
	Short rainy season	5.11	23.88	8.405	96.35	20.71
	Dry season	1.81	6.08	4.19	34.56	23.18
2008	First rainy season	7.57	48.13	9.21	128.33	28.8
	Second rainy season	7.02	37.32	8.68	125.94	19.97
	Short rainy season	5.47	24.83	8.11	97.29	20.64
	Dry season	1.68	6.33	4.04	34.95	22.8
2018	First rainy season	8.36	50.94	8.865	130.42	28.21
	Second rainy season	7.69	39.47	8.4	127.37	19.42
	Short rainy season	5.89	26.1	7.77	99.4	20.19
	Dry season	1.51	6.61	3.80	35.65	21.79
2048	First rainy season	10.79	57.45	8.00	136.2	28.65
	Second rainy season	9.85	44.08	7.59	130.36	18.05
	Short rainy season	6.75	28.8	6.86	102.84	19.61
	Dry season	1.22	7.2	3.29	38.06	19.46

To investigate the effect of landuse/land cover change on the hydrology of the study watershed, the variation of selected hydrological components between predefined study periods were conducted, and the founded results presented in table 4.16 As the founded result indicated the streamflow more increase in the first and second rainy season by(25.71% and 23.73% respectively between 1988 and 2018) in the same way streamflow increase by (29.03% and 28.08% in the first and second rainy season respectively in the future between 2018 and 2048).

However from change detection between consecutive study periods, the stream flows are more affected during the dry season, as the percentage of change indicated in (Table 4.16), the mean monthly stream flows decrease at a higher rate in the dry season in each investigation period due to the landuse land cover change. The other studies which were conducted by (Mamuye et al., 2020) near this study area founded that there was a decrease in stream flows in the dry season due to the expansion of cultivated land. The dry season was the worst case season in water resource projects, due to water scarcity, so the finding of this study insight the requirement of great consideration and attention on integrated water resource management. In addition to streamflow, the other elements change analysis was conducted and the founded results are put in the table below.

Table 4.16 shows that surface runoff increased by 16.34%, 14.67%, 14.4%, and 13.7% from 1988 to 2018 and 11.34%,10.47%,10.33%, and 8.93% from 2018 to 2048 in the frit rainy season, second rainy season short rainy season, and dry season respectively. This is mainly due to the decrease in agroforestry, forest, and pastureland, while agricultural land and built-up increased. As agriculture increased the soil structure and organic contents affected by a plough during long-term tillage, this condition increases the surface runoff as the infiltration decreased. The same surface runoff water yield also increased through the investigation period in the four seasons (Table 4.16). However, the left hydrological component such as evapotranspiration, groundwater shallow aquifer, and lateral flow, were decreased in the investigation period as indicated in the table below.

Table 4. 16 Seasonal change of hydrological components from 1988 to 2048

Change of seasonal hydrologic components											
		Streamflow		SURQ		LATQ		WYQ		ET	
year	Season	m3/s	%	mm	%	mm	%	mm	%	mm	%
1988_1998	1	0.42	6.32	2.31	5.47	-0.29	-2.93	3.56	2.78	-0.31	-1.05
	2	0.37	5.96	2.11	5.9	-0.23	-2.52	1.2	0.97	-2.37	-11.7
	3	0.2	4.06	1.07	4.7	-0.19	-2.21	1.27	1.32	-0.66	-3.19
	4	-0.13	-6.73	0.26	4.5	-0.26	-5.77	2.03	5.89	-1.72	-7.41
1998_2008	1	0.5	6.61	3.61	7.49	-0.24	-2.54	0.61	0.48	-0.29	-1.01
	2	0.44	6.23	1.54	4.12	-0.21	-2.36	1.87	1.48	-0.22	-1.12
	3	0.36	6.6	0.96	3.81	-0.295	-3.51	0.94	0.97	-0.07	-0.34
	4	-0.14	-8.07	0.25	4.11	-0.155	-3.70	0.39	1.12	-0.38	-1.66
2008 _2018	1	0.79	7.32	2.81	5.52	-0.35	-3.75	2.09	1.6	-0.59	-2.09
	2	0.67	6.77	2.14	5.43	-0.28	-3.17	1.43	1.12	-0.55	-2.85
	3	0.42	6.22	1.27	5.11	-0.34	-4.19	2.12	2.13	-0.45	-2.23
	4	-0.16	-13.51	0.28	4.42	-0.24	-5.99	0.1	0.28	-1.01	-4.64
1988 _2018	1	1.71	25.71	8.33	16.34	-0.86	-8.94	6.26	4.8	-1.19	-4.2
	2	1.48	23.73	5.79	14.67	-0.71	-7.84	4.5	3.54	-3.15	-16.2
	3	0.98	19.96	3.29	14.4	-0.82	-9.60	4.33	4.35	-1.18	-5.84
	4	-0.43	-22.18	0.8	13.7	-0.65	-14.69	3.12	8.76	-3.11	-14.2
2018 _2048	1	2.43	29.03	6.52	11.34	-0.87	-9.81	5.78	4.24	0.44	1.54
	2	2.16	28.08	4.61	10.47	-0.81	-9.64	2.99	2.29	-1.37	-7.59
	3	0.86	14.6	2.7	10.33	-0.91	-11.71	3.43	3.34	-0.58	-2.96
	4	-0.29	-19.3	0.59	8.93	-0.50	-13.22	2.41	6.34	-2.33	-11.96

Where: 1=First rainy season, 2=second rainy season, 3=short rainy season, 4= Dry season

The average annual streamflow of the study watershed has been computed for each investigation period and the founded results were mentioned in Table 4.17. The annual streamflow indicated that there was a variation of flows during the investigation period due to landuse/land cover change from 4.04m^3 /s in 1988 to 4.22m^3 /s in 1998, and 4.45m^3 /s in 2008, and 4.72 m^3 /s in2018 respectively. The trends of increasing agricultural and built-up areas and

reduction of the forest, pastureland, and Agroforestry are predictable to further increase the annual streamflow in 2048 (5.38m^3/s). the annual streamflow change detection between consecutive study years was computed as indicated in the table below. The founded result shows that the annual stream of the Kola watershed increased by 16.83% in the past from 1988 to 2018 and 12.3% in the future from 2018 to 204, due to landuse land cover change from time to time.

Table 4. 17 Mean annual streamflow changes from 1988 to 2048

Year	mean annual streamflow m3/s	Interval	Change	
			m3/s	%
1988	4.04	1988_1998	0.18	(0.19/4.04)*100 = 4.46
1998	4.22	1998_2008	0.23	(0.23/4.22)*100 = 5.45
2008	4.45	2008_2018	0.27	(0.27/4.45)*100 = 6.1
2018	4.72	1988_2018	0.68	(0.68/4.04)*100 = 16.83
2048	5.38	2018_2048	0.66	(0.73/4.72)*100 = 12.3

The annual values of evapotranspiration (ET), soil water(SW), percolation (PERC), surface runoff (SUR), groundwater (GW), and water yield (WY), obtained from simulated of each LULC map from 1998 to 2018 and predicted 2048 were shown in (Table 4.18). Depending on the LULC change from 1988 to 2018, the average annual WY of the watershed was increased by 3% 2.5% from 1988 to 2018, and 2018 to 2048 respectively. In the same way, the average annual ET, LAT, PERC, GW_AQ, and SW decreased by 6.21%, 14.69%, 12.13%, 8.75%, and 3.44% respectively. On the other hand, SUR and WY increased by 22.21% and 3% respectively from 1988 to 2018. The change of the hydrological component seen in this study was due to the expansion of agricultural land and the built-up area in the cost of decreasing forest and agroforestry from time to time during the investigation period. Similar to the historical impact of LULC change on the hydrology of the study watershed continued in the future. the impact of future LULC change on the hydrological response of the study Watershed was analyzed by using the predicted 2048LULC map and the achieved results presented in (Table 4.16). the finding of the investigation of the impact of landuse/land cover on the hydrological response of the study area on an annual base indicated that the annual value of the hydrological components affected by the change of landuse/land cover change occurred in the study area from 1988

to2018 in the past, as well as 2018 to 2048 in the future. The annual change of the hydrological component such as ET, GW, PERC, SW, WY, and SUR was computed and presented in Table 4.18. As the other factors are taken as constant except landuse/land cover, during analyzing the hydrological response of the Watershed, the founded variations of the hydrological components overall pre-defined investigation period have occurred, due to the change of landuse/land cover of the study area.

Table 4. 18 Annual hydrological component values for different LULC from 1988 to 2048 in the study area.

Year	ET (mm)	SW (mm)	PERC (mm)	SURQ (mm)	LATQ (mm)	GW_AQ (mm)	WYLD (mm)
1988	282.12	241.89	530.31	257.4	81.58	647.39	982.67
1998	276.04	239.29	528.02	274.55	78.63	629.39	993.1
2008	273.1	236.51	491.59	292.97	76.11	609.81	1003.77
2018	264.61	233.58	465.98	314.58	69.14	590.77	1011.96
2048	247.98	228.35	423.84	359.2	61.15	553.40	1039.42
Annual hydrological component change by %							
1988 -1998	-2.16	-1.07	-0.43	6.66	-3.62	-2.78	1.03
1998 -2008	-1.07	-1.16	-6.9	6.71	-3.20	-3.11	1.07
2008-2018	-3.11	-1.24	-5.21	7.38	-9.16	-3.12	1.31
1988-2018	-6.21	-3.44	-12.13	22.21	-15.25	-8.75	3
2018-2048	-6.28	-2.24	-9.04	14.18	-11.56	-6.33	2.75

The minus sign indicates the decrease of the values

5. SUMMARY AND CONCLUSIONS

5.1. Summary

This study investigated the impact of landuse land cover change on the hydrological response of the kola River watershed. To accomplish the research different data, such as climatic, hydrological, and spatial data were collected and analyzed. The satellite image of 1988, 1998, 2008, and 2018 provided by Landsat 5 TM, Landsat 7 EMT+, and Landsat 8 OLI sensor were downloaded from USGS, to investigate the landuse land cover change in the kola River watershed. Then ERDAS imagine 2014software used during landuse/land cover classification and mapping. After satellite images were classified to the pre-defined landuse/land cover type, the accuracy assessment was done to check the quality of the classified image. The overall accuracy values of 87.83%, 88.41%, 89.15%, and 91.76%, and Kappa coefficients of 0.8461, 0.8523, 0.8559, and 0.8993 for 1988, 1998, 2008, and 2018 were founded respectively. So the founded kappa coefficient indicated the image classification performed in the perfect range of kappa coefficients as recommended by (Badura et al., 2011).

The annual rate of changes in landuse/land cover of the Kola River Watershed resulted, considerable changes within 30 years. Forest, pastureland, and agroforestry decreased by 2.32%, 1.36%, and 0.53%, respectively; While the rest classes namely agriculture, and built-up, increased by 0.82%, and 0.83%, respectively. AS the finding of the landuse land cover change analysis indicated there was a continuous expansion of agricultural land and built-up areas in the study area, as an increase of population in the watershed from time to time so the farmland dependent family spatially in ruler area increases their agricultural land from time to time. The same to agricultural land built up also shows the continuous expansion through the investigation period, this is due to the study area is mostly productive spatially by cash crops such as coffee and chat, this causes the expansion of coffee processing site, construction of new gravel road and settlements from time to time. However, in contrast to agricultural and built-up, the other LULC types such as agroforestry, pastureland, and forest decreased in all investigation time. The forest was mostly consumed for agricultural expansion and firewood consumption, whereas the pastureland is mostly converted to build up and agriculture.

The future landuse land cover was also projected based on the historical landuse land cover conditions of the study area. For the investigation of the future landuse land cover, the 2018

classified map was taken as a base map and the 30 years (2048) landuse land cover was projected by using the IDRISI (Cellular-Automata Markov (CA-Markov) method). The result of 2048 LULC indicates a continuous increase of agriculture and built-up areas as the other landuse land cover such as forest, pastureland and agroforestry decreased. The result of the change analysis between 2018 and 2048 indicates there were the same trends in future LULCC as historical landuse land cover change.

Soil and Water Assessment Tool was used for hydrological modeling purposes in this study during the investigation of the impact of landuse/land cover change on the hydrological response of the study area. Model sensitivity analysis was made and eight sensitive parameters were selected from the parameter considered during sensitivity analysis. Then, the model calibration and validation were performed, and the following result was obtained: R^2 0.87 for calibration, 0.85 for validation, and Nash Sutcliff efficiency (NSE) values of 0.77and 0.74 for calibration and validation respectively. Because of LULCC, the seasonal flow increased by 25.71%, 23.73%, and 19.96% in the first, second rainy seasons, and short rainy seasons respectively. However, streamflow of the study area decreased by 22.18% in the dry season from1988 to 2018. The annual surface runoff increased by 22.21%, whereas ET, lateral flow, and groundwater shallow aquifer decreased by, 6.21%, 15.25%, and 8.75% respectively. The impact of LULCC on the hydrology of the study watershed also continued in the future, as the result of prediction (2018_2048) showed that seasonal streamflow increased by 29.03%, 28.08%, and 14.6% in the first and second rainy season and short rainy season, respectively and decreased by 19.3% dry seasons. In addition to this, the annual surface runoff and water yield increased, while lateral flow, groundwater shallow aquifer, and evapotranspiration decreased by respectively in the future 2018 to 2048 due to landuse/land cover changes in the study area.

5.2. Conclusion

Based on the finding of the landuse land cover change analysis and its impacts on the hydrological response of the study watershed, the following conclusions were reached. There was a continuous expansion of agricultural land and built-up in the study area, this was due to the increase of population in the watershed from time to time so the farmland-dependent families spatially in ruler area increase their agricultural land from time to time, in contrast to agricultural and built up, there was a continuous decrease of pastureland and forest in all investigation time.

The result of LULC the change prediction between 2018 and 2048 presented a significant change in landuse/land cover in the same trends as the historical landuse land cover change.

The landuse/land cover change has a great impact on the hydrological components such as streamflow, surface runoff, lateral flow, and evapotranspiration of the watershed. The annual streamflow 1988 to 2048 shows the increasing condition due to the expansion of agricultural and built up, as the cost of decreasing agroforestry, forest, and pastureland. On the other hand, the seasonal stream flows indicate highly decreasing from 1988 to 2048 in the dry season due to the landuse land cover change in the study area.

This study shows that the impact of LULCC on the hydrology response of the Kola River Watershed will be continued in the future unless interventions such as soil and water conservation, integrated Water Resource management, and greening legacy are initiated in this study area. This condition requires great consideration because decreasing streamflow in the worst case was the major problem in planning and running the existing water resource project.

Recommendation:

Based on the result obtained during landuse/land cover change analyses, its impacts on the hydrological response of the study watershed, and the conclusion reached, the following recommendations are suggested.

The study was done by considering the impacts of the landuse/land cover change on the hydrology of the Kola River Watershed due to time and budget constraints, the effect of climate change did not consider during the investigation of the effect of landuse/land cover on the hydrological response of Kola River Watershed. From this point of view, it can be

recommended that research have a better result if the effect of climate change is included for further study.

The reference point used in this study was taken from the google earth .due to time and budget constraints, however it is better if the GPS points to cheek the accuracy assessment of the classified satellite image.

As the future predicted landuse/land cover of the study area indicated the change will continued in the future unless any conservation intervention is practice in the study area. So i would like to recommend the soil and water conservation, and the green legacy launched in 2019 in the country should be initiated in the study watershed to reduce the impact of landuse/land cover changes in the future.

Landuse/land covers of the study watershed indicated the expansion of Agricultural land and built-up area as the other landuse/land covers such as Agroforestry, Forest, and Pastureland decreased from time to time, this condition causes the increase of surface runoff by reducing the infiltration rate in the wet season and decreasing base flow in the dry season, so the concerned stakeholder of the study area should be practiced the idea of integrated water resource management

The hydro metrological data available in this study was not good enough, for their availability and quality. So it is better if more investigation is conducted about the availability and the efficiency of the gauging stations founded in the study area, as well as establish the additional modernized gauging stations. This task helps to have reasonable hydro metrological data for longer temporal and spatial scales, which reduce the uncertainties and increase the performance of the modeling in the study area.

6. **REFERENCES**

Abdrhman, B. (2011). The effect of Landuse change on the hydrology of akaki catchment.

Ahmed, B. a. (2012). Modeling Urban Land Cover Growth Dynamics Using Multitemporal Satellite Images: A Case Study of Dhaka, Bangladesh. ISPRS International Journal of Geoinformation, 1, 3-31. doi:10.3390/ijgi1010003.

Alamirew, D. (2006). Modeling of Hydrology and Soil Erosion of Upper Awash River Basin. Ph.D. Thesis, University of Bonn, 233.

Amsalu, A. S. (2007). Long-term dynamics in land resource use and the driving forces in the Beressa watershed, highlands of Ethiopia. J. Environ. Manage, 448_459.

Andreassian, V. (2004). Waters and forests: from historical controversy to scientific debate. J HYDROL, 127.

Ariti, A. T, van Vliet J, and Verburg P. H. (2015). Land-use and land-cover changes in the Central Rift Valley of Ethiopia assessment of perception and adaptation of stakeholders. Applied Geography, 65, 28–37.

Arnold, J. G. (2012). Swat model calibration and validation. American Society of Agricultural and Biological Engineers. 55(4), 1491-1508.

Arnold, JG, Srinivasan R, Muttiah RR, Williams JR. (1998). Large Area Hydrologic Modeling and Assessment Part I: Model Development. Journal of the American Water Resources Association; 34(1):, 73-89.

Badura, Victoria, Read, Aaron, Briggs, Robert, de Vreede, Gert-Jan. (2011). Coding for Unique Ideas and Ambiguity: A Method for Measuring the Effect of Convergence on the Artifact of an Ideation Activity. IJSODIT, 17.

Bajwa, H, Tim, U. (2002). Toward immersive virtual environments for GIS-based Floodplain. In Proceedings of 22nd ESRI User Conference. San Diego.

Bastidas, L. H. (2002). Emerging paradigms in the calibration of hydrologic models. Water Resources Publications, LULC, Englewood, CO, USA, 25_56.

Beven, K. (1997). Distributed Modelling in Hydrology: Application of the TOPMODEL concpt,Wiley, Chichester,360.

Birhanu, A, Masih I,van der Zaag P,. Nyssen J, Cai, X. (2019). Impacts of landuse and land cover changes on hydrology of the Gumara catchment, Ethiopia," Physics and Chemistry of the Earth. Parts A/B/C, 112, 165–174.

Biswajit, Nath, Zhihua Wang,Yong Ge, Kamrul Islam,Ramesh P. Singhand Zheng Niu. (2020). Landuse and Land Cover Change Modeling and Future Potential Landscape Risk Assessment Using Markov-CA Model and Analytical Hierarchy Process. Geo_Information, 2.

BoARD. (2016). (Bureau of Agriculture and Rural Development)Unpublished organizational documents.

Breuer, L. H. (2009). Assessing the impact of landuse change on hydrology by ensemble modeling (LUCHEM). I: Model intercomparison with current landuse. ADV WATER RESOUR 32(2), 129-146.

Brown, D.G., Pijanowski, B.C., Duh, J.D. (2000). Modeling the Upper Midwest, USA", Journal of Environmental Management, 59, 247-263.

Chimdessa K, Quraishi S, Kebede A, Alamirew T. (2018). "Effect of landuse land cover and climate change on river flow and soil loss in Didessa River Basin, South West Blue Nile, Ethiopia. Hydrology, 6.

Choto M, and Fetene A. (2019). Impacts of landuse/land cover change on streamflow and sediment yield of Gojeb watershed, Omo-Gibe basin, Ethiopia. Remote Sensing Applications: Society and Environment, 14, 84-99.

Congalton, R. (1988a). A comparison of sampling schemes used in generating error matrices for assessing the accuracy of maps generated from remotely sensed data. Photogrammetric Engineering and Remote Sensing. 54(5):593–600.

Costanza, R. (1989). Model goodness of fit: a multiple resolution procedure. Ecol. Model, 47, 199-215.

Cuo, L. (2016). Landuse/land cover change impacts on hydrology in large river basins. Terrestrial water cycle and climate change: natural and human-induced impacts. John Wiley and Sons, Inc, 103_134.

Danuso, Francesco , Agron, Ital . (2002). Climak: A stochastic model for weather data generation. Italian Journal of Agronomy.

Dareje, D. H. (2010). Impact of land-use change on reservoir sedimentation (case study of karadobi). msc theises.

de Sherbinin, A. (2004, April ,15). Land-Use and Land-Cover Change, A CIESIN Thematic Guide. http://sedac.ciesin.columbia.edu/tg/guide_main.jsp.

Defries, RS, Eshleman KN. (2004). Land-use change and hydrologic processes: A major focus for the future. Hydrologic Process, 18, 2183–2186.

Eastman, R. J. (2006). IDRISI Andes, Guide to GIS and Image Processing Clark University. 87-131.

Esayas, Y. (2010). Evaluating the impact of landuse land cover change on soil erosion and runoff using swat model at tikur wuha watershed. MSc.

Eyasu, Elias, Weldemariam ,Seifu, Bereket Tesfaye and Wondwosen Girmay. (2019). Impact of landuse/cover changes on lake ecosystem of Ethiopia central rift valley. Elias et al., Cogent Food & Agriculture (2019), 5: 1595876

Fan, F, Weng, Q, Wang, Y. (2007). Landuse land cover change in Guangzhou, China, from 1998 to 2003, based on Landsat TM/ETM+ imagery. 7, 1323-1342.

FAO. (2011). The state of the world's land and water resources for food and agriculture (SOLAW) – Managing systems at risk. London: Food and Agriculture Organization of the United Nations, Rome, and Earthscan.

Feldman, A. (2000). Hydrologic Modeling System HEC-HMS technical reference manual. US Army Corps of Engineers. Hydrologic Engineering Center: Second St., Davis, CA 95616.

Food, G. (2002). Status of land classification Accuracy Assessment Remote sensing 80. 185-201.

Fufa D, Abbulu Y. (2015). Hydrological impacts due to land-use and land-cover changes of Ketar watershed, Lake Ziway catchment, Ethiopia. International Journal of Civil Engineering and Technology (IJCIET), 6, 34-45.

Gaohong, Yin, Gregoire, Mariethoz, and Matthew F. McCabe. (2016). Gap-Filling of Landsat 7 Imagery Using the Direct.

Gashaw T, Tulu T,Argaw M. (2018). Modeling the hydrological impacts of landuse/land cover changes in the Andassa watershed, Blue Nile Basin, Ethiopia. Science of the Total Environment, 619-620, 1394–1408.

Gassman, P. W. (2007). The Soil and Water Assessment Tool: Histological development. applications, and future research directions. T ASABE 50(4), 1211-1240.

Gebrehewet, K. B. (2004). Landuse and land cover changes in the central highlands of Ethiopia: The case of yerer mountain and its surroundings. Dissertation, 25.

Gebresamuel, G. B. (2010). Land-use changes and their impacts on soil degradation and surface runoff of two catchments of Northern Ethiopia. Acta Agriculturae Scandinavica Section B – Soil and Plant Science, 60, 211_226.

Genene T, Abiy G. (2014). Review on Overall Status of Soil and Water Conservation System and Its Constraints in Different Agro Ecologies of Southern Ethiopia. Journal of Natural Sciences Research, 4, 65-68.

Gericke, O. P. (2004). Hydrological modeling of river basins Using HSPF model. Proceedings. Biennial Conference, (pp. 1-920). Cape Town: ISBN.

Giri, Chandra; Long, Jordan. (2014). Land Cover Characterization and Mapping of South America for the Year 2010 Using Landsat 30 m Satellite Data. Remote Sense, 10, 9494-9510.

Giriraj, A., Irfan-Ullah, M., Murthy, M. S., & Beierkuhnlein, C. (2008). Modeling Spatial and Temporal Forest Cover Change Patterns (1973-2020): A Case Study from South Western Ghats (India). Sensors (Basel, Switzerland), 8(10), 6132–6153.

Girmay, G., Singh, B. R., Dick, Y. (2010). Land-use changes and their impacts on soil degradation and surface runoff of two catchments of northern Ethiopia. Acta Agriculturae Scandinavica, Section B –Plant Soil Science, 211-226.

Guo, H., Hu, Q., Jiang, T. (2008). Annual and seasonal streamflow responses to climate and land-cover changes in the Poyang Lake basin, China. Journal of Hydrology, 355, 106_122.

Haregeweyn. N, Tesfaye.S, Tsunekawa.A. (2015). Dynamics of use and land cover and its effects on hydrologic responses: a case study of the Gilgel Tekeze catchment in the highlands of Northern Ethiopia. Environmental Monitoring and Assessment, 187, 4090.

Hashemian, M. A. (2004). Study of sampling methods for accuracy assessment of classified remotely sensed data.

Hatem M and Prasanna D. (2017). Modeling Future Landuse and Land-Cover Change in the Asyut Region Using Markov Chains and Cellular Automata.

Ike, S. (2017). Impact of landuse land cover change on runoff and water quality. dissertation.

Islam, K, Rahman M.F and Jashimuddin M. M. (2018). Modeling landuse change using Cellular Automata and Artificial Neural Network: The case of Chunati Wildlife Sanctuary, Bangladesh. Ecol. Indic, 88, 439–453.

Jensen, J. (1996). Introductory Digital Image Processing: A Remote Sensing Perspective. (2nd, Ed.)

Jensen, J. (2007). Remote Sensing of the Environment: An Earth Resource Perspective Prentice-Hal.

Jin, H. L. (2015). Flood-runoff in semi-arid and sub-humid regions, a case study: A simulation.

Kabba, V. T. S, Li, J. (2011). Analysis of landuse and land cover changes, and their ecological implications in Wuhan, China. Journal of Geography and Geology, 3, 104, 3, 104.

Kahsay, B. (2004). Landuse/land cover changes in the central highlands of Ethiopia: the case of yerer mountain and its surroundings, MSc Addis Ababa university. 147.

Karim, A. (2007). Use manual for SWAT_CUP, SWAT calibration, and uncertainty analysis program. Swiss Federal Institute of Aquatic Science and Technology, Eawag, Duebendorf, Switzerland.

Kassa, T. M. (2009). Watershed Hydrological Responses to Changes in Landuse and Land Cover, and Management Practices at Hare Watershed, Ethiopia. Dissertation, 37.

Kumar, M., Bhatt, G., and Duffy, C.J. (2008). An efficient domain decomposition framework for an accurate representation of geodata in distributed hydrologic models. International Journal of Geographical Information Science, 23(12):1569-1596.

Lambin, E. F. (2003). Dynamics of land-use and land-cover change in tropical regions. Annual Review of Environment and Resources, 28, 205–241. doi:10.1146/annual.

Lambin, E.F. and Geist, H.J. (2006). Landuse and Land Cover Change-Local Processes and Global Impacts. Springer, 18.

Lu, Z. Z. (2015). Hydrologic Responses to Landuse Change in the Loess Plateau: Case Study in the Upper Fenhe River Watershed. 2015, 676030.

Lyons, M.B., Phinn, S.R. and Roelfsema, C.M.. (2012). Long-term land cover and seagrass mapping using Landsat and object-based image analysis from 1972 to 2010 in the coastal environment of South East Queensland, Australia. ISPRS Journal of Photogrammetry and Remote Sensing.

Mamuye Belihu, S. T. (2020). Hydrologic response to landuse land cover change in the Upper Gidabo Watershed, Rift Valley Lakes Basin, Ethiopia. HydroResearch, 3, 85_94.

Mechael, A. (2016). Characterizing regional groundwater flow in the Ethiopian Rift: A multimodel approach applied to Gidabo River Basin. Austrian Journal of Earth Sciences.

Melese, A. M. (2012). The Impact of Landuse Change on the Hydrology of the Angereb Watershed, Ethiopia. International Journal of Water.

Melone, F., Barbetta, S., Diomede, T., Peruccacci, S., Rossi, M., Tessarolo, A. and Verdecchia, M. (2005). Review and selection of hydrological models–Integration of hydrological models and meteorological inputs. Resulting from WP1, Action. 13.

Mori M, Hirose Y,Akamatsu Y,Li, Y. (2004). Object-based classification of IKONOS data for rural landuse mapping.

Moriasi, D. N, Arnold, J. G, Van Liew, M. W, Bingner, R. L, Harmel, R. D, Veith T. L. (2007). Model evaluation guidelines for systematic quantification of accuracy in watershed simulations. Transactions of the ASABE, 50, 885–900.

Narayan, K. S. (2011). Calibration and Validation of SWAT Model for Low Lying Watersheds: A Case Study on the Kleine Nete Watershed, Belgium. In Hydro Nepal Journal of Water Energy and Environment.

Nash, J.E, Sutcliffe, J.V. (1970). River flow forecasting through conceptual models, partI-a discussion of principles, J.Hydrology., 282_290.

Neitsch, S. A. (2005). Soil and Water Assessment Tool, Theoretical Documentation: Version. Temple, TX.USDA Agricultural Research Service and Texas A & M Black land Research Centre.

Neitsch, S. A. (2009). Soil and water assessment tool theoretical documentation. version2009.Texas, USA.

NMSA. (1996). Climatic and Agro_Clamatic Resources of Ethiopia. 1.

Oliver, T.H. Morecroft, M.D. (2014). Interactions between climate change and landuse change on biodiversity: Attribution problems, risks, and opportunities. Wiley Interdiscip. Rev. Clim. Chang. 317–335.

Paul, D. G. (2015). The impact of coffee-based agroforestry on the hydrology of the upper Genale River basin, Sidama Zone, Ethiopia.

Pontius, J. (2000). Quantification error versus location error in comparison of categorical maps. Photogrammetric Engineering and Remote Sensing, 66(5), 1011-1016.

Pontius, J.R.G.,and Schneider, L.C.,. (2001). Land-cover change model validation by a ROC method for the Ipswich watershed, Massachusetts, USA. Agriculture, Ecosystems and Environment, 85, 239-248.

Prakasam, C. (2010). Landuse and land cover change detection through remote sensing approach: A case study of.

Praveen, Subedi, Kabiraj Subedi, Bina Thapa. (2013). Application of a Hybrid Cellular Automaton – Markov (CA-Markov) Model in Land-Use Change Prediction: A Case Study of Saddle Creek Drainage Basin, Florida." Applied Ecology and Environmental Sciences 1, no. 6: 126-132. doi: 10.12691/aees-1 -6-5.

Rawat, J.S, Kumer, M. (2015). Monitoring landuse/cover change using remote sensing and GIS techniques: A case study of Hawalbagh block, district Almora, Uttarakhand, India. The Egyptian Journal of Remote sensing and space science Vo 18. 77-84.

Reid, R.S., Kruska, R.L., Muthui, N., Taye, A., Wotton, S., Wilson, C.J., and Woudyalew. (2000). Land-use and land-cover dynamics in response to changes in climatic. Landscape Ecology 15, 339-355.

Rohshare R, A. J. (2008). Application of a SWAT model for estimating runoff and sediment in two mountainous basins in central Iran. Hydrological Sciences Journal, 53(5), 977-988. doi:10.1623/hysj.53.5.977

Sang, L., Zhang, C., Yang, J., Zhu, D, and Yun, W. (2011). Simulation of landuse spatial pattern of towns and villages based on CA-Markov model", Mathematical and Computer Modelling, 54, 938-.

Santhi, C. S. (2006). Modeling approach to evaluate the impacts of water quality management plans implemented in a watershed in Texas. Environmental Modeling and Software, 21, 1141-1157.

Schuol, Juergen, Mikayilov, Fariz. (2007). Using Monthly Weather Statistics to Generate Daily Data in a SWAT Model Application to West Africa. Ecological Modelling.

Sertel, E,Imamoglu, M.Z, Cuceloglu, G, Erturk, A. (2019). Impacts of Land Cover/Use Changes on Hydrological Processes in a Rapidly Urbanizing Mid-latitude Water Supply Catchment. Water, 11, 1075.

Silberstein, R. (2006). Hydrological models are so good, do we still need data? Environmental Modeling & Software. 1340e_1352.

Singh, V. (2002). Mathematical modeling of watershed hydrology. J. Hydrol. Eng., 7(4):, 270-292.

Singh., S. M. (2015). Predicting spatial and decadal LULC changes through Cellular Automata Markov Chain models using earth observation datasets and geo-information. Enviro process, 2, 61-78.

Skaggs, R. W., D. M. Amatya, G. M. Chescheir, C. D. Blanton, and J. W. Gilliam. (2006). Effects of drainage and management practices on hydrology of pine plantation. In Proc. Intl. Conf. on Hydrology and Management of Forested Wetlands, St. Joseph, Mich.: ASABE.

Stehman, S. V. (2009). Sampling designs for accuracy assessment of land cover. International journal of remote sensing, 30_5243_5272.

Taye, A. (2009). Impact of landuse/land cover change on catchment hydrology and water quality of legedadi-dire catchments, Ethiopia. aau/ MSC Thesis, 7.

Thakkar, A.K., Desai, V.R., Patel, A. and Potdar, M.B. (2016). Impact Assessment of Watershed Management Programmes on Landuse/Land Cover Dynamics using Remote Sensing and GIS. Remote Sensing Applications: Society and Environment.

Tran, D.X., Pla, F., Latorre-Carmona, P., Myint, S.W., Caetano, M. and Kieu, H. (2017). Characterizing the relationship between landuse land cover change and land surface temperature. ISPRS Journal of Photogrammetry and Remote Sensing, 124.

Vanhellemont, Q. R. (2015). Advantages of high-quality SWIR bands for ocean color processing: Examples from Landsat-8. Remote Sensing of Environment, 18.

Verburg, P. H., K. Kok, R. G. Pontius, and A. Vledkamp. (2006). Modeling Land-Use and Land Cover Change.in E. F. Lambin and H. Geist, editors. Landuse and Land Cover Change; Local Process and Global Impacts. Springer, Berlin.

Verburg, P.H. and Overmars, K.P. (2009). Combining top-down and bottom-up dynamics in landuse modeling: exploring the future of abandoned farmlands in Europe with the Dyna-CLUE model. Landscape Ecology, 24, 1167–1181.

Woldeamlak Bewket and Solomon Abebe. (2013). Land-use and land-cover change and its environmental implications in a tropical highland watershed, Ethiopia, International Journal of Environmental Studies. 70, 126-139.

Yang, L., Feng, Q., Yin, Z., Wen, X., Si, J., Li, C. and Deo, R. C. (2017). Identifying separate impacts of climate and landuse/cover change on hydrological processes in the upper stream of Heihe River, Northwest China. Hydrological Processes, 31, 1100-1112.

Yesuph A, Y and Dagnew A, B. (2019). Landuse/cover spatiotemporal dynamics, driving forces, and implications at the Beshillo catchment of the Blue Nile Basin, North Eastern Highlands of Ethiopia. Environmental Systems Research, 1.

7. APPENDIXES

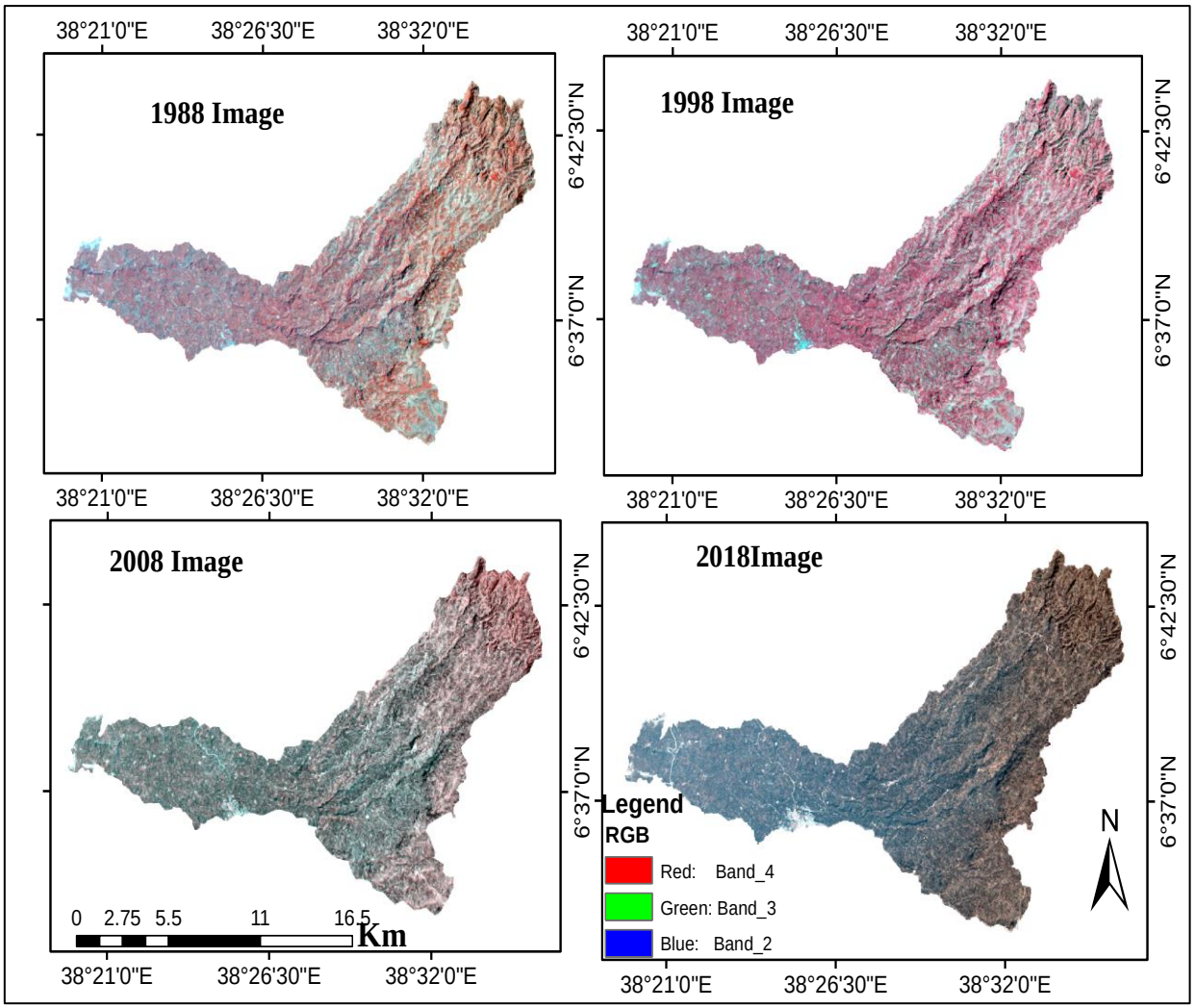

Appendix Figure 1: Satellite Data for 1988, 1998, 2008, and 2018.

Appendix Table 1 LULCC matrix of 1988-1998(a), 1998-2008(b), 2008-2018(c), and 1988-2018(d)

a)

		1998 LULC					
		Agriculture	Agroforestry	Built-up	Forest	Pastureland	Grand Total
1988 LULC	Agriculture	**7194.16**	1070.71	186.94	120.71	256.35	8828.87
	Agroforestry	1563.82	**7568.53**	284.81	75.74	63.77	9556.68
	Built up	206.85	279.68	**152.43**	0.05	38.14	677.15
	Forest	49.10	235.99	2.63	**451.62**	0.40	739.74
	Pastureland	255.27	205.23	94.43	38.32	**169.57**	762.82
	Grand Total	9269.20	9360.15	721.23	686.45	528.23	20565.25

b)

		2008LULC					
1998 LULC		Agriculture	Agroforestry	Built-up	Forest	Pastureland	Grand Total
	Agriculture	**7537.91**	1323.38	196.30	17.84	193.62	9269.05
	Agroforestry	1472.96	**7405.38**	316.68	153.10	11.45	9359.56
	Built up	232.87	263.64	**204.60**	0.71	20.19	722.01
	Forest	240.66	121.92	5.65	**308.41**	9.82	686.47
	Pastureland	257.31	61.01	60.22	0.66	**149.30**	528.49
	Grand Total	9741.72	9175.33	783.45	480.71	384.37	20565.58

c)

	2018 LULC						
2008LUC		Agriculture	Agroforestry	built-up	Forest	Pastureland	Grand Total
	Agriculture	**8597.86**	798.73	230.90	43.87	71.62	9742.98
	Agroforestry	1781.92	**6922.68**	320.61	112.45	36.16	9173.81
	Built up	240.08	255.32	**257.96**	1.86	28.48	783.71
	Forest	155.58	46.45	0.27	**278.45**		480.75
	Pastureland	231.66	26.12	29.36	0.85	**96.02**	384.02
	Grand Total	11007.11	8049.29	839.10	437.49	232.28	20565.27

d)

	2018LULC						
1988LULC		Agriculture	Agroforestry	Built-up	Forest	Pastureland	Grand Total
	Agriculture	**7865.51**	633.47	229.28	42.99	57.34	8828.59
	Agroforestry	2213.13	**6760.11**	423.27	98.16	60.66	9555.32
	Built up	221.81	303.02	**137.81**	0.31	14.23	677.18
	Forest	370.23	76.51	1.02	**291.97**	0.00	739.74
	Pastureland	335.16	275.94	47.39	4.05	**99.98**	762.53
	Grand Total	11005.84	8049.05	838.78	437.48	232.21	20563.35

e)

	2048LULC						
2018LULC		Agriculture	Agroforestry	Built-up	Forest	Pastureland	Grand Total
	Agriculture	**10871.69**	39.68	88.08	11.94	2.79	11014.18
	Agroforestry	1348.59	**6473.17**	163.89	60.92	8.57	8055.14
	Built up	98.92	43.46	**650.11**	0.11	49.29	841.88
	Forest	171.05	2.45	0.46	**263.52**		437.48
	Pastureland	32.32	3.08	8.71		**188.48**	232.60
	Grand Total	12522.57	6561.83	911.24	336.49	249.14	20581.28

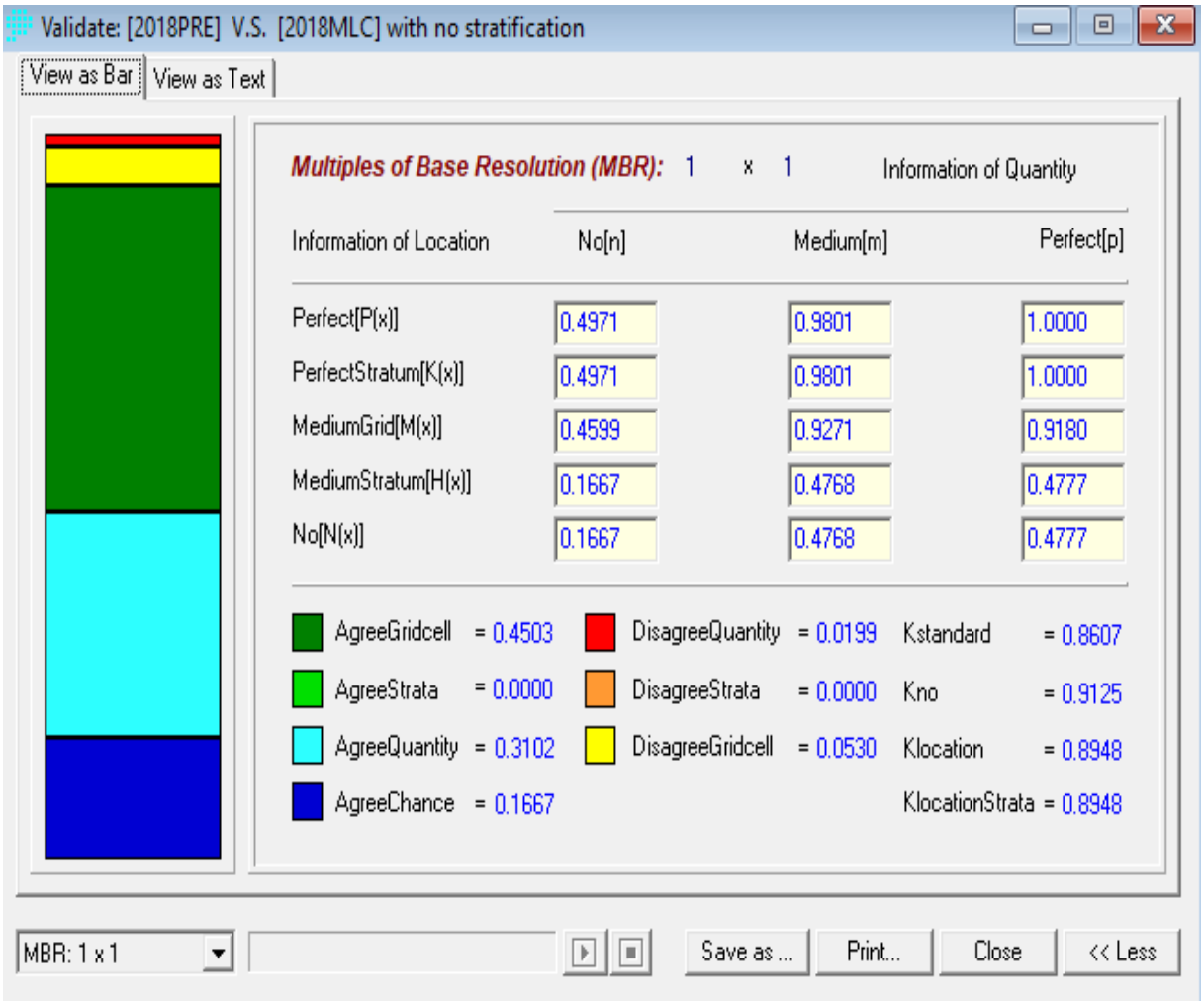

Appendix Figure 2: Validation of simulated 2018LULC by 2018clasified image.

Appendix Table 2: Transition matrix of Markov prediction to 2048 based on LULC 2018 map.

Transition Probabilities Grid

Given : Probability of changing to :

	BUILT UP	PASTURELA	FOREST	AGRICULTU	AGROFORE
BUILT UP	0.2117	0.0229	0.0003	0.3139	0.4512
PASTURELAND	0.0689	0.1353	0.0055	0.4581	0.3322
FOREST	0.0017	0.0000	0.4231	0.4673	0.1079
AGRICULTURE	0.0320	0.0078	0.0049	0.8764	0.0789
AGROFORESTERY	0.0504	0.0071	0.0110	0.2353	0.6962

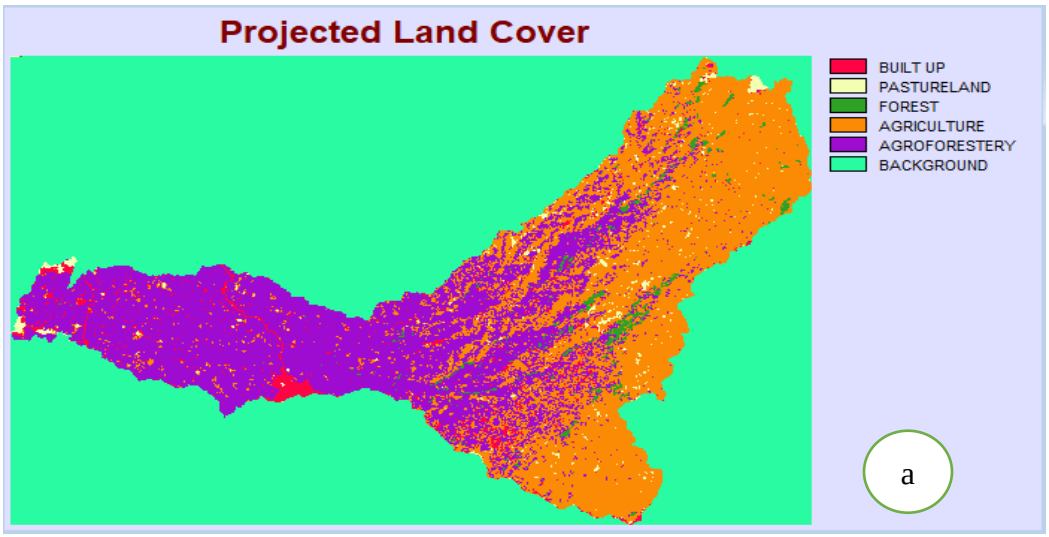

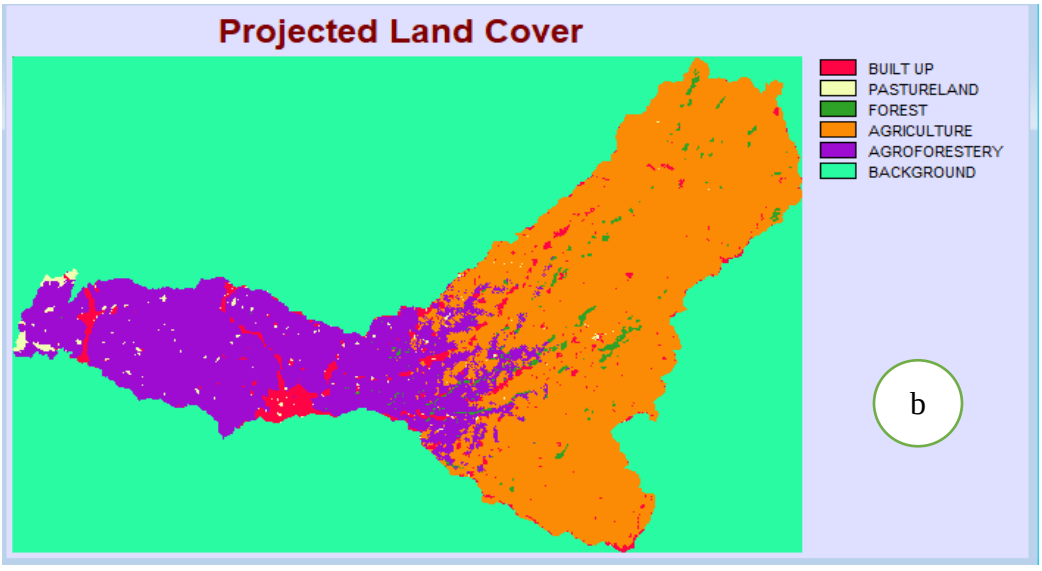

Appendix Figure 3: projected 2018(a) 2048(b) LULC by CA_ Marcove

Appendix Table 3: Annual rainfall of stations around kola watershed in (mm)

year	Dilla Pre	Hegre pre	AletwonPre	TeflePre	YerglemPre
1988	1540.17	1187.90	1469.76	1681.20	1469.76
1989	1146.38	1153.50	1373.20	1311.70	1270.30
1990	1316.15	1135.00	1348.70	1174.90	1216.68
1991	1230.22	1117.40	1374.80	1143.60	1232.70
1992	1541.61	1444.80	1651.11	2045.30	1305.30
1993	1630.00	1154.56	1722.70	1053.60	1281.80
1994	1471.71	1169.93	1571.70	1132.40	1343.00
1995	1478.69	1036.30	1428.90	1537.60	1136.40
1996	1729.15	1208.29	1649.90	1422.60	1472.20
1997	1660.15	1372.70	2014.70	1186.00	1400.70
1998	1385.47	1343.60	1582.60	1240.50	1740.50
1999	1287.25	1517.40	1234.20	1353.30	1075.70
2000	1299.40	1407.30	1425.30	1846.70	1102.72
2001	1785.64	1370.40	1957.18	2022.40	1576.20
2002	1101.50	1169.20	1438.30	1536.00	942.10
2003	1156.30	1017.60	1496.00	1615.90	852.50
2004	1102.80	1156.00	1289.00	1062.50	947.62
2005	1270.30	1429.20	1755.50	2133.30	1239.00
2006	1493.40	1192.59	1778.50	2076.40	1538.59
2007	1698.90	1583.05	2079.10	2834.10	1574.30
2008	1498.10	1231.60	1460.80	1652.00	1381.70
2009	1203.87	1153.30	1356.60	1693.83	1211.50
2010	1718.32	1756.60	1811.67	2587.50	1377.00
2011	1578.80	1731.11	1546.13	1645.18	1082.70
2012	1439.50	1125.70	1319.70	1597.18	1267.90
2013	1314.97	1347.17	1688.60	1977.48	1499.51
2014	1575.40	1728.69	1811.20	1785.44	2046.27

2015	1155.50	1350.50	1346.87	1061.18	1256.57
2016	1293.50	1477.60	1466.63	1909.29	1567.50
2017	1541.30	1641.02	2425.41	1424.08	1403.40
2018	1730.05	1755.20	1737.20	2435.04	1203.27
Average	1431.43	1337.59	1600.39	1650.91	1323.08

Appendix Table 4: Mean monthly rainfall (mm) data for stations around the study area

Month	DillaPre	HegrePre	ALEwonPre	TeflekePre	YerglemPre
Jan	33.07	41.07	35.23	30.57	28.71
Feb	43.62	45.75	46.30	40.26	34.47
Mar	98.32	83.85	109.96	107.99	95.57
Apr	201.37	179.05	221.35	249.38	179.21
May	219.73	186.72	228.96	246.42	187.71
Jun	128.46	129.39	147.99	126.64	113.90
Jul	108.31	105.74	144.13	129.50	123.40
Aug	136.09	148.05	154.36	169.67	144.60
Sep	163.13	146.17	215.25	234.12	162.14
Oct	188.96	174.51	189.76	216.64	174.53
Nov	76.33	68.43	74.18	56.88	51.84
Dec	34.05	28.84	32.90	42.85	26.99

Appendix Table 5: Maximum, minimum and mean monthly temperature (^{o}C) records of the stations in and around the study area.

MONTH	DILLA		HEGRESELEM		YERGLEM		TEFLEKELLA	
	TMX	TMIN	TMX	TMIN	TMX	TMIN	TMX	TMIN
Jan	29.85	10.09	21.15	6.31	28.44	10.00	27.77	9.02
Feb	30.12	10.76	21.46	7.07	29.15	10.37	27.00	8.85
Mar	30.73	12.64	20.80	7.18	28.97	11.51	27.95	9.98
Apr	28.04	13.94	19.18	7.51	27.54	12.25	25.36	9.20
May	27.19	13.81	18.52	7.44	26.05	12.11	25.20	9.31
Jun	26.36	13.72	18.28	7.27	25.26	12.40	23.87	9.06

Jul	25.41	14.29	16.68	6.37	24.13	12.71	24.14	9.17
Aug	25.58	14.17	16.81	6.51	24.55	12.62	24.28	8.95
Sep	26.28	13.63	17.78	6.80	24.96	12.04	23.57	8.43
Oct	26.99	13.33	18.29	6.82	25.84	11.82	24.95	9.34
Nov	28.09	11.68	19.32	6.34	26.88	10.88	25.06	9.03
Dec	28.72	10.39	20.52	6.12	27.72	9.68	27.24	9.61
Average	27.8	12.7	19.1	6.8	26.6	11.5	25.5	9.2

Appendix Table 6: Long term mean monthly discharge of Kola River (1988_2013)

Year	Jan	Feb	Mar	Apr	May	Jun	Jul	Aug	Sep	Oct	Nov	Dec
1988	0.73	0.53	0.48	0.91	1.92	3.40	10.06	12.18	5.01	8.22	2.58	1.10
1989	0.70	0.56	0.57	1.37	1.78	2.59	3.83	2.48	5.08	5.47	2.26	2.01
1990	0.92	1.32	1.53	2.54	3.42	3.45	2.21	2.87	2.76	2.03	1.24	0.85
1991	0.67	0.57	0.74	1.17	1.21	1.06	3.46	1.81	4.34	1.96	1.02	0.65
1992	0.47	0.58	0.44	1.30	1.42	2.21	2.54	9.09	5.14	11.40	3.01	1.29
1993	0.86	1.03	0.69	1.38	7.42	5.22	2.84	2.36	2.76	5.05	2.55	1.05
1994	0.67	0.51	0.58	0.86	1.82	1.78	8.75	7.05	3.83	3.40	2.19	0.99
1995	0.34	0.33	0.38	1.49	1.52	0.65	0.95	3.28	6.03	6.08	1.30	0.59
1996	0.38	0.17	0.51	1.21	2.79	10.91	3.60	7.05	7.26	4.65	1.07	0.45
1997	0.26	0.11	0.09	1.16	2.61	1.77	3.73	6.04	1.52	5.70	6.50	2.52
1998	2.03	1.26	0.88	1.41	2.65	3.76	4.53	11.76	4.87	9.31	2.51	0.98
1999	0.62	0.41	0.68	0.90	1.96	1.56	2.96	3.23	2.87	4.70	2.95	1.10
2000	0.51	0.30	0.29	0.63	1.51	1.26	1.81	7.60	3.50	8.71	2.99	1.08
2001	0.68	0.49	0.50	0.92	1.91	2.09	2.84	3.91	2.99	3.51	1.56	1.04
2002	0.70	0.42	0.58	0.87	2.38	2.14	1.32	2.05	2.04	2.00	1.56	0.97
2003	0.70	0.36	0.37	0.89	0.97	0.81	1.62	2.88	2.51	2.75	1.56	1.00
2004	0.70	0.39	0.47	1.07	1.98	2.25	1.30	1.94	2.45	3.90	1.37	0.81
2005	0.59	0.34	0.47	1.17	3.71	3.44	4.69	6.99	10.29	11.23	8.48	5.94
2006	0.71	0.62	1.02	2.10	4.50	3.62	6.54	5.91	4.38	3.92	2.84	2.51
2007	1.27	0.88	0.59	1.06	3.10	5.35	3.86	9.93	4.67	4.01	1.78	0.89
2008	0.56	0.33	0.24	0.39	0.96	1.96	1.37	3.20	3.49	2.77	5.58	1.07
2009	0.62	0.46	0.27	0.43	1.02	2.43	0.89	1.66	1.86	3.97	1.25	1.32
2010	1.19	0.71	2.43	4.59	7.60	3.51	4.63	5.11	5.68	5.14	1.65	0.77
2011	0.57	0.32	0.21	0.24	1.37	2.73	3.84	4.98	5.16	3.80	2.06	1.14
2012	0.55	0.27	0.15	0.46	0.72	1.16	2.86	4.25	4.03	3.13	1.49	0.87
2013	0.51	0.26	0.40	0.79	1.70	2.54	6.41	9.08	11.56	8.78	1.44	0.28

Appendix Table 7: Sensitivity parameters and their definition.

			Range	
SNO	Parameters	Definition	MIN	Max
1	CN2	SCS run off curve number(dimensionless)	-0.2	0.2
2	ALPHA_BF	Base flow alpha factor(days)	0	1
3	GW_DELAY	Groundwater delay (days)	30	450
4	GWQMN	Threshold depth of water in the shallow aquifer required for return flow to occur (mm)	0	2
5	REVAPMN	Threshold depth of water in the shallow aquifer for "revap" to occur (mm)	0	500
6	SOL_AWC	Available water capacity of the soil layer (mm H2O/mm soil)	0	1
7	SLSUBBSN	Average slope length (m)	10	150
8	HRU_SLP	Average slope steepness	1	1
9	ESCO	Soil evaporation compensation factor.	0	8
10	EPCO	Plant uptake compensation factor.	0	1
11	OV_N	Manning's "n" value for overland flow	0.1	30
12	SOL_K	Saturated hydraulic conductivity.	0	2000
13	CH_K2	Effective hydraulic conductivity in main channel alluvium	-0.01	500

Appendix Table 8: Average monthly basin values

		SNOW			WATER		SED	
MON	RAIN (MM)	FALL (MM)	SURF Q (MM)	LAT Q (MM)	YIELD (MM)	ET (MM)	YIELD (T/HA)	PET (MM)
1	30.01	0	3.17	2.87	41.43	15.95	1.49	40.94
2	34.64	0	4.16	2.17	24.76	15.91	3.03	36.93
3	86.23	0	12.59	2.93	32.4	28.27	6.55	38.42
4	176.62	0	43.56	5.79	75.24	28.14	16.65	30.09
5	195.91	0	54.2	9.23	116.96	28.27	15.75	29.74
6	117.64	0	25.98	8.82	106.3	23.07	7.06	25.74
7	113.06	0	22.26	8.04	103.45	16.51	6.43	18.71
8	140.58	0	31.6	8.77	111.36	17.99	8.68	20.56
9	148.35	0	33.18	8.88	113.9	19.74	9.3	22.83
10	167.49	0	49.51	10.12	140.01	23.2	12.03	30.25
11	56.87	0	11.47	7.41	96.28	20.88	3.98	37.41
12	23.17	0	2.14	4.58	65.94	18.38	0.79	41.91